

Wave Propagation in Equal Mass Plasmas

by

Graeme Andrew Stewart B.Sc.

Thesis
submitted to the
University of Glasgow
for the degree
of Ph.D.

Department of Physics and Astronomy,
The University,
Glasgow G12 8QQ

October 1992

ProQuest Number: 11007937

All rights reserved

INFORMATION TO ALL USERS

The quality of this reproduction is dependent upon the quality of the copy submitted.

In the unlikely event that the author did not send a complete manuscript and there are missing pages, these will be noted. Also, if material had to be removed, a note will indicate the deletion.



ProQuest 11007937

Published by ProQuest LLC (2018). Copyright of the Dissertation is held by the Author.

All rights reserved.

This work is protected against unauthorized copying under Title 17, United States Code
Microform Edition © ProQuest LLC.

ProQuest LLC.
789 East Eisenhower Parkway
P.O. Box 1346
Ann Arbor, MI 48106 – 1346

Thesis
9402
copy 1

GLASGOW
UNIVERSITY
LIBRARY

To my Mother, Father and Sister

Summary

This thesis is concerned with wave propagation in equal mass plasmas. Equal mass plasmas have two components, both of the same mass but with opposite charges, and consequently they have a symmetry which is not present in the more usual electron-ion plasmas. This symmetry can be expected to lead both to a modification of results derived for electron-ion plasma, causing some phenomena to change, others to disappear and new phenomena to arise. With respect to the problem of wave propagation this is certainly the case.

Equal mass plasmas are important in the laboratory and in astrophysics. In chapter one we briefly introduce the problem, firstly setting the scene by describing the 'Plasma Universe' and then introducing equal mass plasmas and mentioning a few molecular plasmas of this type. Chapter one is concluded with a review of the work done on electron-positron plasmas in astrophysics.

Chapter two derives the equations needed to undertake the study of wave propagation in plasmas. We start from the most general description of the plasma as one point in Γ Space and go on to derive the standard fluid equations. As we are dealing with an equal mass plasma, where both components are equally important, we derive the equations for a general multi-species plasma.

In chapter three the problem of linear wave propagation in an equal mass plasma is tackled. We show that the special symmetry of equal mass plasmas simplifies the problem immensely, and that the well known phenomena of Faraday rotation and whistler wave modes are absent from the equal mass plasma. Dispersion relations are derived for the plasma in the cold and warm cases and the extension of equal mass symmetry to kinetic theory is discussed.

Chapter four extends the work of chapter three to electron-positron plasmas. We discuss the validity of the models studied, the first of which considers the effect of the plasma being at a relativistic temperature ($kT \geq m_e c^2$). We then extend this model to incorporate, in a simple fashion, the effects of particle annihilation and creation in the plasma. In both cases we find that Faraday rotation is absent.

In chapter five nonlinear plasma physics is introduced and its importance emphasised. We describe the solution of electrostatic plasma oscillations in a plasma of cold electrons and stationary ions. A numerical simulation is undertaken of the same problem for cold equal mass plasmas and, in stark contrast to the electron-ion case, a fundamental instability is found. A quasilinear analytic solution is found for the problem which corresponds well to the numerical results.

Finally, in chapter six, we discuss extensions of the work in this thesis, in particular the generalisation of chapter five to warm plasmas. We also pose some related problems concerning equal mass and electron-positron plasmas.

The original work of this thesis is contained in chapters three to five. Chapter three has been published in *Journal of Plasma Physics*, chapter five has been submitted to *Journal of Plasma Physics* and chapter four is being developed for publication.

I wish I could write you a melody so plain
That could hold you dear lady from going insane
That could ease you and cool you and cease the pain
Of your useless and pointless knowledge

Bob Dylan, *Tombstone Blues*

At the moment of scientific thought when a generalisation turns into a prediction – and that prediction is triumphantly verified through experience – at that moment, human thought is supplied with its proudest and most justified satisfaction!

Leon Trotsky, *Dialectical Materialism and Science*

He gave man speech, and speech created thought,
Which is the measure of the universe;
And Science struck the thrones of earth and heaven.

Percy Bysshe Shelly, *Prometheous Unbound*

Acknowledgements

The work contained in this thesis was carried out while the author was a research student in the Astronomy and Astrophysics Group at the Department of Physics and Astronomy in the University of Glasgow. My thanks go to all the staff and students of the group for their help, tolerance and general good humour throughout the last three years. Thanks also to all those involved with the provision of the group and departmental facilities which have enabled this research to be carried out.

I would like to thank my supervisor, Professor Ernest Laing, for his help and encouragement during my research here. The provision of enough space to research freely, but enough discipline to research productively is due to his experience, and I have benefited enormously. Thanks are also due to Professor John Brown, Saad Abdul-Russak and Dr. Anthony Garrett for many fruitful discussions about equal mass plasmas and their strange symmetries.

A special mention must go to Amarjit, David, Saad and Lyndsay for sharing offices with me at various times, and providing an outlet for my anguish when all was not well. Thanks also to all the Coffee Club members for their wit, wisdom and dangerously strong coffee; to Christine, Daphne and Linda for their organisational skills and for helping me get paid, get help or get Tipp-Ex (as was appropriate); to Amarjit and Andy for elucidating the mysteries of various computer systems and of TeX; to the *Orion* (R.I.P.), for showing me the true meaning of patience.

A 'thank you' to all my friends, family and comrades who have contributed enormously to my psychological well-being during the last three years – particularly to Donatella, Catherine, Aixa, Khalid and Phil for listening, talking and knowing when to tell me to shut up.

Having come to the end of the writing up of this thesis it is perhaps also a place to acknowledge the philosophy which has supported the author over the last three years. In this respect the works of Bob Dylan must be taken as a starting point of the humanity which the author feels. His 'melodies so plain' have certainly eased the 'pain' over the last year, but it is also my hope that the end result is not too 'useless' or 'pointless' (though at times, yes, it did seem that way!) However, when it all works and the answer drops out, that is the moment which we as scientists live for. It seems appropriate to use a quote from Trotsky to illustrate this, as the feeling of the author is, that on the threshold of the 21st Century the classical Marxism of Marx, Engels, Lenin and Trotsky (a true 'social' science) offers the best hope of salvation from the miseries of starvation, poverty and crisis which afflict the world.

Finally I would like to thank Fiona, for introducing me to Dylan, for proofreading above and beyond the call of duty, and for providing support, encouragement and friendship which have been invaluable. It is she who has had to bear the brunt of the 'thesis blues', I hope the experience was not too trying and that any debts can be repaid.

Graeme A. Stewart

Contents

Summary	i
Acknowledgements	iii
Chapter 1 Introduction	1
1.1 Plasma Physics and the Plasma Universe	1
1.2 Equal Mass Plasmas	2
1.3 Electron-Positron Plasmas	3
Chapter 2 Derivation Of Fluid Equations	6
2.1 Γ Space and Liouville's Equation	6
2.2 BBGKY Hierarchy	7
2.3 Truncating The Series - The Vlasov Equation	8
2.4 The Fluid Equations	10
2.5 The Momentum Equation	12
2.6 Maxwell's Equations	13
Chapter 3 Linear Waves In Equal Mass Plasmas	15
3.1 Introduction	15
Notation and Figures	15
3.2 Dispersion Relation For A Magnetised Plasma	16
3.3 The Cold Plasma	17
3.4 The Cold Equal Mass Plasma	18
Parallel Solutions	19
Faraday Rotation and Whistler Waves	20
Perpendicular Solutions	21
General Propagation	22
CMA Diagram For Equal Mass Plasmas	23
3.5 Warm Equal Mass Plasmas	24
Parallel Solutions	26
Perpendicular Solutions	26
General Propagation	27
3.6 Collisional Effects In A Warm Equal Mass Plasma	28
Solutions For Waves Π_y	30
Solutions For Waves Π_{xz}	30
3.7 Equal Mass Symmetry in General Distributions	30
Derivation of Symmetry Conditions	31

Interpretation of Criteria	32
Allowed Distributions	33
Chapter 4 Linear Waves In Electron-Positron Plasmas	42
4.1 Introduction	42
Figures	44
4.2 Relativistic Electron-Positron Plasmas	44
Dispersion Relation	44
Dispersion Relation For Waves Π_y	46
Dispersion Relation For Waves Π_{xz}	48
4.3 Annihilation And Creation In Electron-Positron Plasmas	51
Dispersion Relation	53
Solutions For Waves Π_y	56
Solutions For Waves Π_{xz}	56
Chapter 5 Nonlinear Waves In Equal Mass Plasmas	65
5.1 Nonlinear Physics	65
5.2 Electrostatic Plasma Waves in Electron-Ion Plasmas	66
5.3 Electrostatic Plasma Waves in Equal Mass Plasmas : Numerical Simulation	68
Numerical Integration	69
Numerical Integration of Electron-Ion Plasma	70
Numerical Integration of Equal Mass Plasma	70
Fourier Analysis	72
5.4 Electrostatic Plasma Waves in Equal Mass Plasmas : Quasilinear Analysis	73
Comparison of Quasilinear Theory and Numerical Experiment	77
5.5 Conclusions	78
Chapter 6 Future Work	88
6.1 Normal Wave Modes in Inhomogeneous and Hot Plasmas	88
6.2 Nonlinear Waves	89
References	92

It took me a year to find out it could have been done in a week

William Henry Bragg (*paraphrased*)

In Nature's infinite book of secrecy

A little I can read

William Shakespeare, *Anthony & Cleopatra* I.iii, 10

Chapter 1

Introduction

1.1 Plasma Physics and the Plasma Universe

The study of the nature and properties of ionised gases is a wide ranging and varied field. It encompasses elegant, abstract theories; large scale numerical simulations; wide-ranging extraterrestrial observations (and since 1959 *in-situ* measurements) and both large and small Earth bound experiments. However all these multifarious pursuits fall under the general title of *Plasma Physics*, as does the work of this thesis.

The importance of plasma physics is twofold. Firstly there is the laboratory plasma, the study of which holds the promise of a plentiful energy supply from nuclear fusion. Secondly there is the study of the universe in which we as human beings exist. It is known that 99.9999% (by volume) of the observable universe is in a plasma state. Thus to study the universe is to study plasma physics. This fact is becoming more and more inescapable as we learn more about the structure of the universe – which is inhomogeneous and filled with currents. These new views of the universe have led to a fascinating and powerful challenge to orthodox astronomy and cosmology. The fact that the universe is inhomogeneous is a problem for big bang cosmologies. If the CoBE results are interpreted as the radiation signature of the big bang, then no known mechanism could have caused the observed universe to form since the big bang (Lerner 1992). By contrast a plasma universe (see Alfvén 1990) will automatically produce inhomogeneities. Everywhere that we have sent probes, field aligned ‘Birkeland’ currents have been found. We know that there are magnetic fields on the interstellar, galactic and intergalactic scales (which must be produced by currents of some form) and so it is postulated that Birkeland currents exist on these scales too. Once a current is flowing the double-layer instability produces field aligned electric fields and the strong currents flowing in this region produce an azimuthal magnetic field which compresses the plasma. As Alfvén has stated, the plasma universe is inhomogeneous and filamentary, and this is just what we observe.

Astronomers and cosmologists are also saddled with mysterious ideas of ‘dark matter’. In order to get the big bang to produce sensible results at least ten times more material than we observe has to exist in the universe. This material is also needed (although in varying quantities) to explain the motion of galaxies. As we cannot see it, it has been denoted ‘dark’. However in a plasma universe, there are electromagnetic forces acting between the large currents in galaxies and as such there is no problem with ‘plasma’ galactic dynamics (see Peratt 1986, who also explains much concerning the evolution of radio galaxies.)

In these fields, and many others, plasma physics is playing a key role in a new understanding of the universe. With the continuing evolution of supercomputers, opening up new regimes to simulation study, plasma dynamics are seen to be key to galactic and supergalactic motions. The ‘Plasma Universe’ is definitely expanding.

1.2 Equal Mass Plasmas

The concern of this thesis is the propagation of waves in equal mass plasmas. An equal mass plasma (as the name suggests) is composed of two components with the same mass and opposite charge. This is in contrast to the situation found in most of plasma physics where the plasma is dominated by electrons and much heavier ions. (Even protons are 1836 times heavier than electrons. Thus, an electron scattering off a proton is roughly equivalent to a pedestrian being scattered by an Intercity 125.)

This great difference in mass between the two components of the plasma leads to a distinction between different regimes of wave propagation – normally only one component plays a significant role, i.e. high frequency electromagnetic waves where the electron motion is important or low frequency sound waves where the ion motion is important. Even if the dynamics of both components are included, usually one component yields the dominant behaviour and the other contributes only secondary effects. In an equal mass plasma the situation is fundamentally different. Both components have the same mass so that the dynamics of both are equally important to the whole plasma. However, equal mass plasmas have a symmetry associated with them which is not present in the electron-ion plasma, and this might be exploited to make the understanding of these plasmas easier – in fact we shall demonstrate (particularly in chapters three and four) that this happens.

It might seem that equal mass plasmas are an abstract area of study. This is not so. The most obvious plasma which might be equal mass is that of a particle–anti-particle plasma. This would obviously fulfill the criterion of being equal mass, and indeed electron-positron plasmas have received considerable attention from the astrophysical community (see the short review below). However, this is not the only occurrence of equal mass plasmas. Certain molecular plasmas can be equal mass as well.

If a plasma is formed from positive and negative ions then a nearly equal mass plasma can be formed, differing in mass by only twice the weight of the electron, i.e. the H^+H^- plasma formed at Kyoto University (Itatani 1992). The plasma formed when a laser beam ablates the surface of a Uranium target is also nearly equal mass, being formed not of U^+ and e^- , but of UO_2^+ and UO_3^- . This plasma is of particular interest as it has been proposed that high intensity lasers might be used to stimulate fission in a Uranium target (Boyer *et al.* 1988, Murnane *et al.* 1989).

Even if a molecular plasma is not exactly equal mass then the study of equal mass plasmas will give some clues as to the behaviour of the plasma, providing in a sense another view point on the problem. One view point is that of the electron-ion plasma with no symmetry, but simplified by the fact that one plasma species can be ignored. The other will be the equal mass plasma, where no species can be ignored but there is a simplifying symmetry. If the real plasma is almost equal mass then both species must be considered but the symmetry is broken. Clearly this is a harder problem so the intuition gained from the equal mass plasma will be important.

1.3 Electron-Positron Plasmas

As was mentioned above, electron-positron plasmas have received considerable attention from the astrophysical community. This has generated a considerable number of papers aimed principally at understanding the *particle* nature of such plasmas, not at elucidating their plasma properties. However, they do provide a framework in which to set the present work (particularly chapter four) so a brief review is in order.

The positron was first detected by Carl Anderson in 1932, but the era of astrophysical electron-positron physics was opened up only in 1970 with the detection of a $511keV$ annihilation line from the galactic centre by MacCallum & Leventhal (1983) (electrons and positrons have a rest mass of $511keV$ and form two gamma rays at this energy when they annihilate). This gave indications of large numbers of pairs – large enough to have a significant effect upon the plasma in which they were generated.

Although this was the first observational evidence for electron-positron plasmas, there were theoretical arguments that pointed to the existence, and importance, of these plasmas. Sturrock (1971) showed that the electric fields formed around pulsars were strong enough to accelerate particles to MeV energies and that these particles would produce cascades of electron-positron pairs. The importance of these pairs was underlined by Cordes (1983) who pointed out that the radio emission of pulsars cannot be understood without pair production in the pulsar atmosphere. It was therefore thought that the annihilation line detected at the galactic centre might be formed from intense radiation produced by material infalling upon a black hole (Lingenfelter & Ramaty 1983), although there is now some doubt as to whether a black hole does indeed lie at the galactic centre

(Phinney 1988). (The fact that positrons are there is undisputed.)

From the 1970's it was noted that compact nonthermal radio sources had very low linear polarization (Jones & O'Dell 1977). Wardle (1977) observed that Faraday rotation was virtually absent in such sources. Jones & O'Dell argued that this put a severe limit on the number of cold (non-relativistic) electrons in such sources (Faraday rotation varies as $1/\gamma$). However, it was realised, from symmetry considerations, that an electron-positron plasma would produce the same effect (Nordelinger 1978). Nordelinger and Kundt & Gopal-Krishna (1980) showed that such plasmas could exist without immediately annihilating.

The fact that electron-positron plasmas might exist in compact radio sources prompted theorists to examine the properties of such a system. Burns & Lovelace (1982) considered a beam of pairs produced by the accretion disk dynamo formed around a supermassive black hole ($\sim 3 \times 10^8 M_\odot$). This dynamo generates a current of 10^{18}A and the relativistic electron beam which forms it can produce copious quantities of pairs by scattering from low energy photons. These pairs emerge in a vortex funnel which could be the source of the extragalactic jets observed in certain galaxies (see review by Begelman *et al.* 1984), which can also exhibit the low Faraday rotation found in compact radio sources. (There are problems though with using this mechanism to explain the annihilation line in the galactic centre (Lightman *et al.* 1987).)

Further work on this problem was done by Zdziarski (1988) who considered, in some detail, the electron-positron cascade produced by the impact of high energy electrons and gamma-rays upon low energy background photons. It was realised that the pair creation and annihilation which would occur would modify the gamma-ray spectrum, softening it by absorbing high energy gamma-rays through pair production.

Although a lot of work was now being done on pair production by particle and photon sources, a more abstract interest in relativistic plasmas had been shown before this time. Bisnovatyi-Kogan *et al.* (1971) considered the equilibria of a 'thin' electron-positron plasma, i.e. one which was less than one optical depth thick to gamma-rays.† They found that the 'thin' plasma had a maximum temperature, $T_* = kT/m_e c^2 = 41$. Beyond this point, pair creation would runaway, denying the plasma an equilibrium. This work was extended by a number of authors: Laing (1979); Lightman & Band (1981); Lightman (1982); Takahara & Kusunose (1983). In particular, Lightman extended the work of Bisnovatyi-Kogan *et al.* to a finite sized plasma and showed that electron-positron

† Although the calculation could be done for an optically thick system quite easily using statistical mechanics (indeed Chapman (1936) had done so) it was felt that this calculation would not be appropriate to astrophysics as the objects under consideration did not radiate like blackbodies and could not therefore be in thermal equilibrium.

plasmas develop a negative specific heat above a critical temperature; after this point further heating produces more pairs and the net energy per particle drops. If this process continues, so many pairs are produced that the plasma becomes optically thick to radiation and a thermal equilibrium is formed. Takahara & Kusunose considered the effect of magnetic fields on the plasma and found that critical maximum temperature decreases when a field is present.

There is an important point to be made about the above papers. Exclusively they concentrate upon the particle effects of the addition of e^-e^+ pairs. This in itself is a very difficult and highly nonlinear problem, so perhaps it is not surprising that none of them consider the plasma which is formed as a *plasma*, i.e. being able to sustain waves and other collective phenomena. Indeed the absence of Faraday rotation in electron-positron plasmas, though intuitively realised in by Nordelinger (1978) was not proven for equal mass plasmas until Stewart & Laing (1992) with the result being extended to electron-positron plasmas in this thesis (see chapter four).

Holcomb & Tajima (1989) were the the first to start to consider the actual plasma which is formed by electron and positrons. In doing so they considered the electron-positron plasma which is formed in the early big bang universe (assuming the big bang took place, see §1.1) and for a short time dominates the matter component of the universe (from $t \approx 0.1s \rightarrow \approx 1s$). They studied linear wave propagation in such plasmas to see how primordial magnetic fields might be generated. Tajima & Taniuti (1990) went on to study nonlinear waves in the same context and in this case the untapped potential of the subject was immediately revealed. When they considered the nonlinear interaction of the plasma with photons they discovered new soliton solutions for acoustic waves which are not present in electron-ion plasmas.

We are still at the beginning of the study of electron-positron plasmas as plasmas, and it is noticeable that in the above papers which did consider the plasma physics of electron-positron plasmas, very simple situations were envisaged – uniform plasmas where annihilation could be ignored. This is in contrast to the complexities of the equilibria found when considering all the processes which go to actually forming such plasmas, but it is necessary, as the problem of plasma physics in such complex situations is very hard indeed.

In this thesis we shall adopt similar assumptions to those of Holcomb, Tajima & Taniuti in order to simplify the problem, though in chapter four we shall relax some of these criteria. In addition, we shall consider only equal mass plasmas in chapters three and five (ignoring relativity and annihilation), but it is still hoped that this will be a useful contribution to the continuing studies of electron-positron plasmas.

Chapter 2

Derivation Of Fluid Equations

2.1 Γ Space and Liouville's Equation

The starting point for the derivation of any of the equations of plasma physics must be an exact description of the plasma. Therefore, we begin with a plasma of N particles distributed among S species, each species s containing $N(s)$ particles. The *exact* state of the plasma at time t is described by $F[X_1^1, X_1^2, \dots, X_1^{N(1)}, X_2^1, \dots, X_2^{N(2)}, \dots, X_S^{N(S)}, t]$, i.e. one point in $6N$ dimensional phase space (or Γ space). Each X_j^i is the set of position and velocity coordinates of the i th particle of species j , i.e. $X_j^i = (\mathbf{r}_j^i, \mathbf{v}_j^i)$.

To attempt to solve the equations for a plasma in such microscopic detail is impossible (involving $3N$ equations of motion for velocity in $6N$ other variables) so we instead start from a distribution of state probabilities, ρ , such that

$$\rho(X_1^1, X_1^2, \dots, X_1^{N(1)}, X_2^1, \dots, X_2^{N(2)}, \dots, X_S^{N(S)}, t) dX_1^1 \dots dX_S^{N(S)} \quad (2.1)$$

is the probability that the plasma is in state $[(X_1^1, X_1^1 + dX_1^1), \dots, (X_S^{N(S)}, X_S^{N(S)} + dX_S^{N(S)})]$ at time t . As we shall at no time require to identify individual particles then we shall consider only distributions which are symmetric with respect to particle exchange within each species.

Normalisation requires that

$$\int \int \dots \int \rho dX_1^1 \dots dX_S^{N(S)} = 1. \quad (2.2)$$

Now according to Liouville's equation, the system conserves volume in Γ space, i.e.

$$\frac{\partial \rho}{\partial t} + \sum_{s=1}^S \sum_{i=1}^{N(s)} \frac{\partial}{\partial \mathbf{r}_s^i} (\rho \mathbf{v}_s^i) + \sum_{s=1}^S \sum_{i=1}^{N(s)} \frac{\partial}{\partial \mathbf{v}_s^i} (\rho \mathbf{a}_s^i) = 0. \quad (2.3)$$

As we are dealing with forces such that the acceleration \mathbf{a} only depends on velocity through $\mathbf{v} \times \mathbf{B}$ we can rewrite Liouville's equation as

$$\frac{\partial \rho}{\partial t} + \sum_{s=1}^S \sum_{i=1}^N \mathbf{v}_s^i \cdot \frac{\partial \rho}{\partial \mathbf{r}_s^i} + \sum_{s=1}^S \sum_{i=1}^N \mathbf{a}_s^i \cdot \frac{\partial \rho}{\partial \mathbf{v}_s^i} = 0. \quad (2.4)$$

Ensemble averages are defined in the usual way,

$$\langle Q(X_1^1, \dots, X_S^{N(S)}) \rangle = \int \int \dots \int \rho Q(X_1^1, \dots, X_S^{N(S)}) dX_1^1 \dots dX_S^{N(S)}. \quad (2.5)$$

Given that the exact n particle distribution function of species s is

$$F_s^n(X^{(1)}, X^{(2)}, \dots, X^{(n)}) = \sum_{s'=1}^S \sum_{i=1}^n \delta[X_{s'} - X^{(i)}] \delta(s' - s) \quad (2.6)$$

then the average n particle distribution function is

$$f_s^n(X^{(1)}, \dots, X^{(n)}) = \frac{N(s)!}{(N(s) - n)!} \int \int \dots \int \rho(X_1^1, \dots, X_{s-1}^{N(s-1)}, X^{(1)}, \dots, X^{(n)}, X_s^{n+1}, \dots, X_S^{N(S)}) dX_1^1 \dots dX_{s-1}^{N(s-1)} dX_s^{n+1} \dots dX_S^{N(S)}. \quad (2.7)$$

We have of course used the symmetry of ρ and we have also assumed that the values of $X^{(1)}$ to $X^{(n)}$ do not overlap.

Similarly we define the combined distribution functions for $n(s)$ particles of species s , $n(s')$ particles of species s' as

$$C(f_s^{n(s)}, f_{s'}^{n(s')}) = \frac{N(s)!}{(N(s) - n)!} \frac{N(s')!}{(N(s') - n')!} \int \int \dots \int \rho dX_1^1 \dots dX_{s-1}^{N(s-1)} dX_s^{n(s)+1} \dots dX_{s'-1}^{N(s'-1)} dX_{s'}^{n(s')+1} \dots dX_S^{N(S)} \quad (2.8)$$

2.2 BBGKY Hierarchy

The Liouville equation governed the evolution of ρ . To find the equivalent equation for f_s^n we multiply the Liouville equation by $N(s)!/(N(s) - n)!$ and then integrate with respect to all dX 's except $dX_s^1 \dots dX_s^n$. Assuming that the acceleration of each particle \mathbf{a}_s^i can be written

$$\mathbf{a}_s^i = \sum_{s'=1}^S \sum_{j=0}^{N(s')} \mathbf{a}_{s,s'}^{ij}, \quad (2.9)$$

where $\mathbf{a}_{s,s'}^{ij}$ is the acceleration of particle i of species s produced by particle j species s' (0 if $s = s'$ and $j = i$). $\mathbf{a}_{s,s'}^{i0}$ is taken to be the acceleration caused by external fields and $\mathbf{a}_{s,s'}^{i0}$, where $s' \neq s$ is 0.

After integration we have

$$\frac{\partial f_s^n}{\partial t} + \sum_{i=1}^n \mathbf{v}_s^i \cdot \frac{\partial f_s^n}{\partial \mathbf{r}_s^i} + \sum_{i=1}^n \sum_{j=0}^n \mathbf{a}_{s,s}^{ij} \cdot \frac{\partial f_s^n}{\partial \mathbf{v}_s^i} + \sum_{i=1}^n \int \mathbf{a}_{s,s}^{i(n+1)} \cdot \frac{\partial f_s^{n+1}}{\partial \mathbf{v}_s^i} dX_s^{n+1} + \sum_{s' \neq s} \sum_{i=1}^n \int \mathbf{a}_{s,s'}^{i0} \cdot \frac{\partial C(f_s^n, f_{s'}^1)}{\partial \mathbf{v}_s^i} = 0. \quad (2.10)$$

The first term of Liouville's equation gives rise to the term $\partial f_s^n / \partial t$, and the next two terms arise from the boundary conditions that $\rho \rightarrow 0$ as $\mathbf{x} \rightarrow \infty$ and as $\mathbf{v} \rightarrow \infty$ respectively. In the second last term the summations from $j = n + 1$ to $j = N$ for $s' = s$ are considered, and as (for a fixed value of i) the symmetry properties of ρ make the integral constant, we can evaluate each of the j terms for $j = n + 1$. There are $N(s) - n - 1$ such terms, so this yields the correct normalisation for f_s^{n+1} . In a similar way for each of the other species each individual particle j gives the same integral for each value of i because of the symmetry of ρ and so can all be evaluated for $j = 1$ leaving the combined distribution function in the integral.

The set of equations (2.10) are known as the BBGKY hierarchy after their development by Bogoliubov, Born, Green, Kirkwood and Yvon. These equations form a set of N coupled integro-differential equations and are therefore just as hard to solve as our original Liouville equation. Their value lies in the fact that we now have a series of equations which, after making a suitable approximation, we can truncate. Hopefully this will leave us with a reduced set of equations - a set which we can solve.

2.3 Truncating The Series - The Vlasov Equation

The simplest way to truncate the BBGKY hierarchy is to consider the particles to be non-interacting. Then all $\mathbf{a}_{s,i}^{ij} = 0$, except for $\mathbf{a}_{s,i}^i$ corresponding to external forces, and the integral terms disappear leaving a solution corresponding to uncorrelated particles, *viz.*

$$f_s^n = \prod_{i=1}^n f_s^1(X_s^i, t) \quad (2.11)$$

$$\rho = \prod_{s=1}^S \prod_{i=1}^{N(s)} f_s^1(X_s^i, t) \quad (2.12)$$

But this approach is clearly inappropriate when considering plasmas – the particles exert electromagnetic forces on each other and, due to the long-range nature of these forces, each particle affects, and is affected by, many others†. However, simple considerations of Debye Length and charge shielding lead to the conclusion the kinetic energy of each plasma particle is much greater than its potential energy‡, and so it may be appropriate to regard the plasma particles as uncorrelated to some extent and introduce a scheme of successive approximation to equations (2.10).

† These long-range forces rule out an alternative approach which was adopted by Boltzmann. He considered a gas of hard spheres and derived the famous Boltzmann Kinetic equation for a neutral gas.

‡ This criteria is true for *ideal plasmas*, i.e. those with a large number of plasma particles in the Debye sphere. There are some plasmas which are *nonideal*, such as inertial confinement plasmas and, surprisingly, the plasma in the centre of the Sun. Strictly speaking the approximations we make do not apply to these plasmas, though in fact many of the final results will be valid.

Let us now consider the electromagnetic forces which the particles in the plasma experience. A plasma particle of species s , having charge q_s and mass m_s , suffers acceleration from external fields \mathbf{E}_0 and \mathbf{B}_0 of

$$\mathbf{a}_{s,}^{i^0} = \frac{q_s}{m_s} [\mathbf{E}_0 + \mathbf{v}_s^i \times \mathbf{B}_0], \quad (2.13)$$

and acceleration due to other plasma particles of

$$\mathbf{a}_{s,}^{i^j} = \frac{q_s}{m_s} [\mathcal{E}_{s,}^{ij} + \mathbf{v}_s^i \times \mathbf{B}_{s,}^{ij}]. \quad (2.14)$$

$\mathcal{E}_{s,}^{ij}$ and $\mathbf{B}_{s,}^{ij}$ are the electric and magnetic fields produced by particle j at the position of particle i , i.e.

$$\mathcal{E}_{s,}^{ij} = \frac{q_{s'}}{4\pi\epsilon_0} \frac{\mathbf{r}_s^i - \mathbf{r}_{s'}^j}{|\mathbf{r}_s^i - \mathbf{r}_{s'}^j|^3}, \quad (2.15)$$

$$\mathbf{B}_{s,}^{ij} = \frac{\mu_0 q_{s'}}{4\pi} \frac{\mathbf{v}_{s'}^j \times (\mathbf{r}_s^i - \mathbf{r}_{s'}^j)}{|\mathbf{r}_s^i - \mathbf{r}_{s'}^j|^3}. \quad (2.16)$$

We are making a hidden assumption in (2.15) and (2.16). To be exact we should account for the finite speed of light, and hence propagation of electromagnetic forces, by considering *retarded potentials* where the field at time t exerted by particles a distance r away is calculated according to the plasma state at a time $t - r/c$. To disregard this effect is to consider a plasma where the timescale of the phenomena examined is much greater than the light travel time across that portion of the plasma which is influencing (and/or being influenced) by that phenomena. In general this means that the Debye Length times the frequency should be less than the speed of light.

We now proceed by pulverising each of the particles in the plasma. That is to say we let $N(s) \rightarrow \infty$ while holding $N(s)q_s$ and $N(s)m_s$ constant. Thus $\frac{q_s}{m_s}$ is constant. This means that $f_s^n = O(N(s)^n)$, $\mathbf{a}_{s,}^{i^0}$ is constant and that $\mathbf{a}_{s,}^{i^j} = O(N(s)^{-1})$. Therefore the third term of (2.10) is one order of magnitude less than the rest of the terms (excepting $j = 0$, the external force term) and can be discarded. Then the truncated set of BBGKY equations is,

$$\frac{\partial f_s^n}{\partial t} + \sum_{i=1}^n \mathbf{v}_s^i \cdot \frac{\partial f_s^n}{\partial \mathbf{r}_s^i} + \sum_{i=1}^n \mathbf{a}_{s,}^{i^0} \cdot \frac{\partial f_s^n}{\partial \mathbf{v}_s^i} + \sum_{i=1}^n \int \mathbf{a}_{s,}^{i^{(n+1)}} \cdot \frac{\partial f_s^{n+1}}{\partial \mathbf{v}_s^i} dX_{n+1} + \sum_{s' \neq s} \sum_{i=1}^n \int \mathbf{a}_{s,}^{i^1} \cdot \frac{\partial C(f_s^n, f_{s'}^1)}{\partial \mathbf{v}_s^i} = 0. \quad (2.17)$$

Seeking a solution which can be expressed in terms of uncorrelated particles, i.e. (2.11) and (2.12) holding, it is easy to see that all the equations will hold if

$$\frac{\partial f_s^1(X_s^1)}{\partial t} + \mathbf{v}_s^1 \cdot \frac{\partial f_s^1(X_s^1)}{\partial \mathbf{r}_s^1} + \left[\mathbf{a}_{s,}^{1^0} + \int \mathbf{a}_{s,}^1 f_s^1(X_2) dX_2 + \sum_{s' \neq s} \int \mathbf{a}_{s,}^{1^1} f_{s'}^1(X_{s'}^1) \right] \cdot \frac{\partial f_s^1}{\partial \mathbf{v}_s^1} = 0. \quad (2.18)$$

i.e.

$$\frac{\partial f^s}{\partial t} + \mathbf{v} \cdot \frac{\partial f^s}{\partial \mathbf{r}} + \mathbf{a}' \cdot \frac{\partial f^s}{\partial \mathbf{v}} = 0, \quad (2.19)$$

where we have now dropped the unnecessary sub and superscripts to arrive at *The Vlasov Equation*. This is one of the most useful equations in plasma physics and describes the evolution of a plasma under external fields and including smoothed self-consistent plasma fields,

$$\mathbf{a}'(\mathbf{r}, \mathbf{v}) = \frac{q_s}{m_s} (\mathbf{E}_0 + \mathbf{v} \times \mathbf{B}_0) + \sum_{s'=1}^S \int \frac{q_{s'}}{m_{s'}} [\mathcal{E}_{s'} + \mathbf{v} \times \mathbf{B}_{s'}] f_{s'}^1(\mathbf{r}_{s'}, \mathbf{v}_{s'}) d\mathbf{r}_{s'} d\mathbf{v}_{s'}. \quad (2.20)$$

($\mathcal{E}_{s'}$ and $\mathbf{B}_{s'}$ are the fields produced by particles of species s' at the (\mathbf{r}, \mathbf{v}) , i.e. (2.15) and (2.16) with $\mathbf{r}_s^i = \mathbf{r}$ and $\mathbf{r}_{s'}^j = \mathbf{r}_{s'}$; $\mathbf{v}_{s'}^j = \mathbf{v}_{s'}$).

2.4 The Fluid Equations

The Vlasov equation ignores the close collisions between particles but other than that it is an excellent description of the plasma. In a sense it is too good, still containing too much information for the tractable analysis of the waves we wish to study. For this reason we continue the process of simplification, this time with the aim of removing much of the information contained in the velocity space portion of the Vlasov equation.

By taking velocity moments of the Vlasov equation we move from six dimensional space plus time, $(\mathbf{r}, \mathbf{v}, t)$, to three dimensional Cartesian space plus time, (\mathbf{r}, t) . Of course, we expect that the set of equations we derive will not be closed, but instead form a chain of linked equations, in much the same way as the BBGKY hierarchy did when it was derived from the full plasma distribution function (although the BBGKY chain did eventually close at Liouville's equation). However, we might hope that a suitable truncation of the set of equations might give a realistic yet tractable theory to work with.

Firstly we shall renormalise the Vlasov equation so that

$$n_s(\mathbf{r}, t) = \int f_s(\mathbf{r}, \mathbf{v}, t) d\mathbf{v} \quad (2.21)$$

is the density of species s in real space. This leads to a sensible redefinition of our ensemble average as

$$\langle Q \rangle(\mathbf{r}, t) = \frac{1}{n_s} \int f_s(\mathbf{r}, \mathbf{v}, t) Q(\mathbf{r}, \mathbf{v}, t) d\mathbf{v}. \quad (2.22)$$

i.e. an average in \mathbf{v} space defined at each point in \mathbf{r} space, so that the plasma fluid velocity, $\langle \mathbf{v} \rangle$, is defined as

$$\mathbf{v}_s = \frac{1}{n_s} \int \mathbf{v} f_s(\mathbf{r}, \mathbf{v}, t) d\mathbf{v}. \quad (2.23)$$

Our zeroth moment in velocity space is simply the integral of (2.19) over $d\mathbf{v}$, i.e.

$$\overbrace{\int \frac{\partial f_s}{\partial t} d\mathbf{v}}^{\circ 1} + \overbrace{\int \mathbf{v} \cdot \frac{\partial f_s}{\partial \mathbf{r}} d\mathbf{v}}^{\circ 2} + \overbrace{\int \mathbf{a}' \cdot \frac{\partial f_s}{\partial \mathbf{v}} d\mathbf{v}}^{\circ 3} = 0. \quad (2.24)$$

This yields

$$\frac{\partial n_s}{\partial t} + \frac{\partial}{\partial \mathbf{r}} (n_s \mathbf{v}_s) = 0, \quad (2.25)$$

The Continuity Equation for species s . The first term arrives from $\circ 1$ by definition, the second by the fact that the spatial derivative in $\circ 2$ is independent of the integral and can be taken outside it. The terms from $\circ 3$ disappear because of boundary conditions that $f_s \rightarrow 0$ as $\mathbf{v} \rightarrow \infty$.

The continuity equation reflects the fact that the number of particles of each species is constant. When we deal with annihilation in e^+e^- plasmas we shall modify this equation accordingly.

Next we multiply by \mathbf{v} and once again integrate the Vlasov equation:

$$\overbrace{\int \mathbf{v} \frac{\partial f_s}{\partial t} d\mathbf{v}}^{\circ 1} + \overbrace{\int \mathbf{v} \mathbf{v} \cdot \frac{\partial f_s}{\partial \mathbf{r}} d\mathbf{v}}^{\circ 2} + \overbrace{\int \mathbf{v} \mathbf{a}' \cdot \frac{\partial f_s}{\partial \mathbf{v}} d\mathbf{v}}^{\circ 3} = 0, \quad (2.26)$$

giving

$$\frac{\partial}{\partial t} (n_s \mathbf{v}_s) + \frac{\partial}{\partial \mathbf{r}} \cdot (n_s \langle \mathbf{v} \mathbf{v} \rangle_s) = \mathbf{a} n_s, \quad (2.27)$$

The Momentum Equation for species s . Here the first term arises from $\circ 1$ by taking the time derivative outside the integral. The second term is similar, this time the spatial derivative being taken out of $\circ 2$ to leave the ensemble average of $\mathbf{v} \mathbf{v}$. In the acceleration term on the RHS of (2.27) we have had to define a new acceleration term \mathbf{a} . This arises from the complex definition of \mathbf{a}' from equation (2.20) which when inserted into term $\circ 3$ of (2.26) gives

$$\int \mathbf{v} \left[\frac{q_s}{m_s} (\mathbf{E}_0 + \mathbf{v} \times \mathbf{B}_0) + \sum_{s'=1}^S \int \frac{q_{s'}}{m_{s'}} [\mathcal{E}_{s'} + \mathbf{v} \times \mathbf{B}_{s'}] f_{s'}^1(\mathbf{r}_{s'}, \mathbf{v}_{s'}) d\mathbf{r}_{s'} d\mathbf{v}_{s'} \right] \cdot \frac{\partial f_s}{\partial \mathbf{v}} d\mathbf{v}. \quad (2.28)$$

Integration by parts of the terms involving electric fields is straightforward but the integration of the terms $\mathbf{v} \times \mathbf{B}$ requires more care. For the external magnetic field integration we have

$$\frac{q_s}{m_s} \int \mathbf{v} (\mathbf{v} \times \mathbf{B}_0) \frac{\partial f_s}{\partial \mathbf{v}} d\mathbf{v}. \quad (2.29)$$

Because of the nature of the $\mathbf{v} \times \mathbf{B}$ term we can include it inside the velocity space integral, i.e.

$$\frac{q_s}{m_s} \int \mathbf{v} \frac{\partial}{\partial \mathbf{v}} [(\mathbf{v} \times \mathbf{B}_0) f_s] d\mathbf{v}. \quad (2.30)$$

Then integrating by parts gives

$$\frac{q_s}{m_s} (\mathbf{v}_s \times \mathbf{B}_0) n_s. \quad (2.31)$$

Similar considerations apply to the acceleration terms integrated over each species in (2.28) and lead to our new acceleration term

$$\mathbf{a} = \frac{q_s}{m_s} [\mathbf{E}_0 + \mathbf{v}_s \times \mathbf{B}_0] + \sum_{s'=1}^S \int \frac{q_s}{m_s} [\mathcal{E}_{s'} + \mathbf{v}_s \times \mathbf{B}_{s'}] f_{s'}^1(\mathbf{r}_{s'}, \mathbf{v}_{s'}) d\mathbf{r}_{s'} d\mathbf{v}_{s'}. \quad (2.32)$$

Of course, it would not be much of a simplification to derive a set of fluid equations for each species but to leave complicated integrations in phase space as the means of deriving the acceleration. We need to simplify this acceleration term further.

This is done by performing the integrals over velocity space in each of the terms $\mathcal{E}_{s'}$ and $\mathbf{B}_{s'}$. This yields a final version of the acceleration term as

$$\mathbf{a} = \frac{q_s}{m_s} [\mathbf{E} + \mathbf{v}_s \times \mathbf{B}], \quad (2.33)$$

where \mathbf{E} and \mathbf{B} have been defined as

$$\mathbf{E} = \mathbf{E}_0 + \sum_{s'=1}^S \int \frac{q_{s'}}{4\pi\epsilon_0} n_{s'} \frac{\mathbf{r} - \mathbf{r}_{s'}}{|\mathbf{r} - \mathbf{r}_{s'}|^3} d\mathbf{r}_{s'} \quad (2.34)$$

$$\mathbf{B} = \mathbf{B}_0 + \sum_{s'=1}^S \int \frac{\mu_0 q_{s'}}{4\pi} n_{s'} \frac{\mathbf{v}_{s'} \times (\mathbf{r} - \mathbf{r}_{s'})}{|\mathbf{r} - \mathbf{r}_{s'}|^3} d\mathbf{r}_{s'} \quad (2.35)$$

For our purposes the first two moments over velocity space are sufficient. As expected, the first equation (governing n_s) involves $n_s \mathbf{v}_s$ and the equation for momentum involves the energy tensor $n_s \langle \mathbf{v} \mathbf{v} \rangle_s$. Were we to continue taking moments, the next equation would govern energy evolution inside the plasma and would involve the rank 3 heat tensor $\langle \mathbf{v} \mathbf{v} \mathbf{v} \rangle_s$. If we are to truncate the series after two equations then it is the term $\langle \mathbf{v} \mathbf{v} \rangle_s$ in the momentum equation which we must find an approximation to.

2.5 The Momentum Equation

The first case that we might consider is where the plasma is *cold*. Then all the plasma particles move at the average species velocity \mathbf{v}_s ,

$$f_s(\mathbf{r}, \mathbf{v}, t) = n_s(\mathbf{r}, t) \delta[\mathbf{v} - \mathbf{v}_s]. \quad (2.36)$$

Then the term $\langle \mathbf{v} \mathbf{v} \rangle_s$ becomes $\mathbf{v}_s \mathbf{v}_s$. Hence

$$\frac{\partial}{\partial t} (n_s \mathbf{v}_s) + \frac{\partial}{\partial \mathbf{r}} (n_s \mathbf{v}_s \mathbf{v}_s) = \mathbf{a} n_s. \quad (2.37)$$

If we multiply the continuity equation, (2.25), by \mathbf{v}_s and expand the derivatives in (2.37) the equation becomes

$$\frac{\partial \mathbf{v}_s}{\partial t} + \left(\mathbf{v}_s \cdot \frac{\partial}{\partial \mathbf{r}} \right) \mathbf{v}_s = \mathbf{a} n_s. \quad (2.38)$$

This is the momentum equation for a cold plasma.

The next case to consider, one more realistic than the last, is a *warm plasma*. Here we do allow the particles to have a thermal spread but we assume that the distribution function is isotropic around \mathbf{v}_s in velocity space. This means that considering

$$\langle \mathbf{v} \mathbf{v} \rangle = \left\langle \begin{pmatrix} v_x v_x & v_x v_y & v_x v_z \\ v_y v_x & v_y v_y & v_y v_z \\ v_z v_x & v_z v_y & v_z v_z \end{pmatrix} \right\rangle \quad (2.39)$$

we can see that all the off diagonal terms must vanish. For the diagonal terms we make a change of variable to $\mathbf{v}' = \mathbf{v} - \mathbf{v}_s$. In this frame each of the terms is equal to the thermal velocity v^T so that

$$\langle \mathbf{v}' \mathbf{v}' \rangle = (v_s^T)^2 \mathbf{I}, \quad (2.40)$$

where \mathbf{I} is the unit tensor. Thus $\langle \mathbf{v} \mathbf{v} \rangle$ becomes

$$\langle \mathbf{v} \mathbf{v} \rangle_s = \langle (\mathbf{v}' + \mathbf{v}_s)(\mathbf{v}' + \mathbf{v}_s) \rangle = \mathbf{v}_s \mathbf{v}_s + \frac{P_s}{n_s m_s} \mathbf{I}, \quad (2.41)$$

where P_s is the isotropic pressure of species s , defined as $P_s = n_s m_s (v_s^T)^2$.

Then the momentum equation for a warm plasma is

$$\frac{\partial}{\partial t} (n_s \mathbf{v}_s) + \frac{\partial}{\partial \mathbf{r}} \cdot (n_s \mathbf{v}_s \mathbf{v}_s) + \frac{1}{m_s} \frac{\partial P_s}{\partial \mathbf{r}} = \mathbf{a} n_s. \quad (2.42)$$

Or using the continuity equation in a way similar to above

$$\frac{\partial \mathbf{v}_s}{\partial t} + \left(\mathbf{v}_s \cdot \frac{\partial}{\partial \mathbf{r}} \right) \mathbf{v}_s = \mathbf{a} - \frac{1}{n_s m_s} \frac{\partial P_s}{\partial \mathbf{r}}. \quad (2.43)$$

2.6 Maxwell's Equations

We have now arrived at the form of the plasma equations needed for the study of plasma waves in the fluid approximation. The equation of continuity (2.25) will be used throughout, together with the appropriate momentum equation: (2.38) for the cold plasma, (2.43) for the warm plasma or (2.27) when we discuss the symmetries of general distributions in chapter three.

However, no study of plasma physics could be undertaken without *Maxwell's Equations*, which give the correct mathematical description of electromagnetic fields.

$$\frac{\partial \mathbf{E}}{\partial \mathbf{r}} = \frac{\rho_t}{\epsilon_0} \quad (2.44)$$

$$\frac{\partial \mathbf{B}}{\partial \mathbf{r}} = 0 \quad (2.45)$$

$$\frac{\partial}{\partial \mathbf{r}} \times \mathbf{E} + \frac{\partial \mathbf{B}}{\partial t} = 0 \quad (2.46)$$

$$\frac{\partial}{\partial \mathbf{r}} \times \mathbf{B} - \epsilon_0 \mu_0 \frac{\partial \mathbf{E}}{\partial t} = \mu_0 \mathbf{j} \quad (2.47)$$

All the symbols have their usual meaning, ρ_t is the charge density and \mathbf{j} is the total current density. When we derived the fluid equations we used \mathbf{E} and \mathbf{B} fields which were derived from Coulomb's law and the Biot-Savart law. These gave difficult integral equations for the electric and magnetic fields in the plasma ((2.34), (2.35)). It is far easier to find the Plasma \mathbf{E} and \mathbf{B} fields from Maxwell's equations. Maxwell's equations (or the *Maxwell, Heaviside, Hertz* equations (Peratt 1992)) give the resulting electric and magnetic fields as the plasma develops different charge and current densities in its structure. It is in this context that we shall employ them, noting that for a multi-species fluid plasma

$$\rho_t = \sum_{s=1}^S q_s n_s, \quad (2.48)$$

$$\mathbf{j} = \sum_{s=1}^S q_s n_s \mathbf{v}_s. \quad (2.49)$$

Chapter 3

Linear Waves In Equal Mass Plasmas

3.1 Introduction

In this chapter the study of the normal wave modes of an infinite homogeneous equal mass plasma is undertaken. The plasma is considered to be in the fluid approximation, so it can be described by a continuity equation and a momentum equation. The mathematical techniques that we will use in this chapter and in chapter four will be those of *Fourier analysis* and *linearisation*. These are both very well known techniques and hardly need any exposition here. Briefly however we note the following.

As the plasma is infinite and homogeneous the problem is simplified. An infinite spatial extent removes the need to tackle boundary conditions and homogeneity means that for linear waves there are no zero order derivatives in the problem.

Fourier analysis (see e.g. Bracewell 1986) involves transforming from (\mathbf{r}, t) space to (\mathbf{k}, ω) space using the transformation

$$\Psi'(\mathbf{k}, \omega) = \iint \Psi(\mathbf{r}, t) \exp(i(\omega t - \mathbf{k} \cdot \mathbf{r})) d\mathbf{r} dt. \quad (3.1)$$

The reverse transformation is

$$\Psi(\mathbf{r}, t) = \left(\frac{1}{2\pi}\right)^4 \iint \Psi'(\mathbf{k}, \omega) \exp(i(\omega t - \mathbf{k} \cdot \mathbf{r})) d\mathbf{k} d\omega. \quad (3.2)$$

The value of the Fourier transformation is that it can change differential equations into algebraic ones. However, these algebraic equations will form an infinite hierarchy unless the equations in (\mathbf{r}, t) space are linear. Consequently the Fourier transform is much more useful if applied to linear equations.

Linearisation is a simple, but powerful, mathematical technique. It has been applied to a wide variety of problems and its use in solving for the normal wave modes in plasmas is well known (Clemmow & Dougherty 1969, Nicholson 1983, Stix 1962). Its essence is that if we have an equilibrium in a complex set of equations, and we disturb this equilibrium by a small (formally infinitesimal) amount, then we can derive a set of equations for the perturbing quantities which are *linear*. This happens because the equilibrium quantities are constant (and are thus just parameters), and the products of perturbing quantities are of second order and can be ignored.

Notation and Figures

In the analysis to follow it will become convenient to label the waves in an equal mass plasma according to the electric field associated with each wave. We shall use the symbol Π to refer to a

wave. Π_x , Π_y or Π_z will refer to a wave with an electric field E_x , E_y or E_z respectively. Π_{xz} will refer to a wave with an associated field in the $x - z$ plane.

In all the figures for chapter three frequency is normalised to ω_p and wave number to k_0 , where $k_0 = c/\omega_p$.

3.2 Dispersion Relation For A Magnetised Plasma

The starting point for the derivation of the dispersion relation are Maxwell's equations for the curl of \mathbf{E} and \mathbf{B} .

$$\frac{\partial}{\partial \mathbf{r}} \times \mathbf{E} + \frac{\partial \mathbf{B}}{\partial t} = \mathbf{0} \quad (2.46)$$

$$\frac{\partial}{\partial \mathbf{r}} \times \mathbf{B} - \epsilon_0 \mu_0 \frac{\partial \mathbf{E}}{\partial t} = \mu_0 \mathbf{j} \quad (2.47)$$

The first step is to perturb these equations from equilibrium, allowing for a zero order homogeneous magnetic field \mathbf{B}_0 but for no zero order electric field or currents. Denoting the perturbed magnetic field as \mathbf{B}_1 these equations then become

$$\frac{\partial}{\partial \mathbf{r}} \times \mathbf{E} + \frac{\partial \mathbf{B}_1}{\partial t} = \mathbf{0}, \quad (3.3)$$

$$\frac{\partial}{\partial \mathbf{r}} \times \mathbf{B}_1 - \epsilon_0 \mu_0 \frac{\partial \mathbf{E}}{\partial t} = \mu_0 \mathbf{j}, \quad (3.4)$$

where \mathbf{E} and \mathbf{j} now represent perturbed quantities.

We now proceed with a Fourier analysis, all perturbed quantities being assumed to vary as $\exp(i(\omega t - \mathbf{k} \cdot \mathbf{r}))$. This gives

$$-\mathbf{k} \times \mathbf{E} + \omega \mathbf{B}_1 = \mathbf{0}, \quad (3.5)$$

$$-\mathbf{k} \times \mathbf{B}_1 - \omega \epsilon_0 \mu_0 \mathbf{E} = \mu_0 \mathbf{j} \quad (3.6)$$

It is convenient to introduce a dimensionless form of the wave vector

$$\mathbf{n} = \frac{\mathbf{k}c}{\omega}, \quad (3.7)$$

and having done this we can use (3.5) to eliminate \mathbf{B}_1 in (3.6) to give

$$\mathbf{n} \times (\mathbf{n} \times \mathbf{E}) = \frac{i\mathbf{j}}{\omega \epsilon_0} - \mathbf{E}. \quad (3.8)$$

It is convenient, though far from essential, to define a coordinate system in which to work. The usual choice is to direct \mathbf{B}_0 along the z axis and to confine \mathbf{k} (the direction of propagation) to the $x - z$ plane, making an angle of θ with the z axis (figure 3.1). Then (3.8) becomes

$$\begin{pmatrix} 1 - n^2 \cos^2 \theta & 0 & n^2 \cos \theta \sin \theta \\ 0 & 1 - n^2 & 0 \\ n^2 \cos \theta \sin \theta & 0 & 1 - n^2 \sin^2 \theta \end{pmatrix} \cdot \mathbf{E} - \frac{i\mathbf{j}}{\omega\epsilon_0} = 0. \quad (3.9)$$

This equation will hold in all cases (we have only used Maxwell's equations to derive it) but we still require to find the response current from our plasma, and so turn to our fluid equations.

3.3 The Cold Plasma

To analyse wave propagation in a cold plasma we start with the cold plasma momentum equation,

$$\frac{\partial \mathbf{v}^s}{\partial t} + \left(\mathbf{v}^s \cdot \frac{\partial}{\partial \mathbf{r}} \right) \mathbf{v}^s = \mathbf{a} n^s. \quad (2.38)$$

Linearising, with no zero order velocity terms, and employing a Fourier analysis as before, yields

$$i\omega \mathbf{v}_s = \frac{q_s}{m_s} (\mathbf{E} + \mathbf{v}_s \times \mathbf{B}_0). \quad (3.10)$$

Adopting the stated coordinate system, this equation can be rearranged to give the velocity components for each species. Then using (2.49) to sum over each species, we obtain the current in the plasma,

$$\begin{aligned} j_x &= \sum_{s=1}^S \frac{q_s^2 n_s}{m_s} \left(\frac{i\omega E_x + \Omega_s E_y}{\Omega_s^2 - \omega^2} \right) \\ j_y &= \sum_{s=1}^S \frac{q_s^2 n_s}{m_s} \left(\frac{i\omega E_y - \Omega_s E_x}{\Omega_s^2 - \omega^2} \right) \\ j_z &= - \sum_{s=1}^S \frac{iq_s^2 n_s E_z}{m_s \omega}, \end{aligned} \quad (3.11)$$

where $\Omega_s = q_s B_0 / m_s$ is the gyro frequency for species s . Note that the usual convention of defining $\Omega > 0$ is not adopted here, instead Ω_s has the same sign as the charge of species s .

Equations (3.11) can be written in terms of a conductivity tensor so that

$$\mathbf{j} = \boldsymbol{\sigma} \cdot \mathbf{E}, \quad (3.12)$$

where

$$\boldsymbol{\sigma} = \sum_{s=1}^S \frac{q_s n_s}{m_s} \begin{pmatrix} \frac{i\omega}{\omega^2 - \Omega_s^2} & \frac{\Omega_s}{\omega^2 - \Omega_s^2} & 0 \\ -\frac{\Omega_s}{\omega^2 - \Omega_s^2} & \frac{i\omega}{\omega^2 - \Omega_s^2} & 0 \\ 0 & 0 & \frac{i}{\omega} \end{pmatrix}. \quad (3.13)$$

Recalling then the dispersion relation, (3.9), we can rewrite the dispersion relation for a cold plasma as

$$\epsilon \cdot \mathbf{E} = 0. \quad (3.14)$$

ϵ is the dielectric tensor,

$$\epsilon = \begin{pmatrix} 1 - \sum_{s=1}^S \frac{\omega_s^2}{\omega^2 - \Omega_s^2} - n^s \cos^2 \theta & \sum_{s=1}^S \frac{i\omega_s^2 \Omega_s}{\omega^2 - \Omega_s^2} & n^2 \cos^2 \theta \sin^2 \theta \\ - \sum_{s=1}^S \frac{i\omega_s^2 \Omega_s}{\omega^2 - \Omega_s^2} & 1 - \sum_{s=1}^S \frac{\omega_s^2}{\omega^2 - \Omega_s^2} - n^s & 0 \\ n^2 \cos^2 \theta \sin^2 \theta & 0 & 1 - \sum_{s=1}^S \frac{\omega_s^2}{\omega^2} - n^s \sin^2 \theta \end{pmatrix}. \quad (3.15)$$

The plasma frequency of species s has been defined as ω_s , where

$$\omega_s^2 = \frac{n_s q_s^2}{m_s \epsilon_0} \quad (3.16).$$

Eigensolutions of (3.14) exist when the determinant of the matrix forming the dielectric tensor is zero.

3.4 The Cold Equal Mass Plasma

The expression for the dielectric tensor, (3.15), is quite general and its solutions, $|\epsilon| = 0$, are well known for electron-ion plasmas (Stix 1962, Clemmow & Dougherty 1969). We now study the form of the solution for an equal mass plasma - two components each of mass m and of charge $\pm q$. Summing over equal mass components σ_{11} , σ_{22} and σ_{33} take on simple forms. However, both σ_{12} and σ_{21} are zero due to the charge/mass symmetry. This is a considerable simplification, yielding the dispersion relation for an equal mass plasma as

$$\begin{vmatrix} 1 - \frac{\omega_p^2}{\omega^2 - \Omega^2} - n^2 \cos^2 \theta & 0 & n^2 \sin \theta \cos \theta \\ 0 & 1 - \frac{\omega_p^2}{\omega^2 - \Omega^2} - n^2 & 0 \\ n^2 \sin \theta \cos \theta & 0 & 1 - \frac{\omega_p^2}{\omega^2} - n^2 \sin^2 \theta \end{vmatrix} = 0. \quad (3.17)$$

The term ω_p is the plasma frequency of the whole equal mass plasma and Ω^2 is the square of gyro frequency of each component, viz.

$$\omega_p^2 = \frac{2nq^2}{m\epsilon_0} \quad (3.18)$$

$$\Omega^2 = \frac{q^2 B_0^2}{m^2} \quad (3.19)$$

Mathematically the extra symmetry of the plasma has removed terms ϵ_{12} and ϵ_{21} . Physically this means that a harmonic electric field in the x direction produces only a current j_x , but $j_y = 0$. Similarly for a field E_y we find that $j_x = 0$. Thus the gyro motion of the plasma does not cause currents to flow.

Taking a specific example to illustrate, consider an oscillating driving field E_x . Then from the equation of motion (3.10) it is seen that

$$v_x = \frac{-iq}{m\omega}(E_x + v_y B_0), \quad (3.20)$$

$$v_y = \frac{iqB_0 v_x}{m\omega}, \quad (3.21)$$

with solutions

$$v_x = \frac{-iqE_x}{m\omega} \left(1 - \frac{q^2 B_0^2}{m^2 \omega^2}\right)^{-1}, \quad (3.22)$$

$$v_y = \frac{q^2 B_0 E_x}{m^2 \omega^2} \left(1 - \frac{q^2 B_0^2}{m^2 \omega^2}\right)^{-1}. \quad (3.23)$$

Recalling that all these solutions are harmonic as $e^{i(\omega t - \mathbf{k} \cdot \mathbf{r})}$ we can see that positively charged particles oscillate, in the x direction, with phase $\pi/2$ behind E_x , whereas the phase of the negative particles is $\pi/2$ ahead. However, the extra factor of q in the solution for v_y means that whatever the charge of the particles they are in phase with the driving field. Hence the current, $\mathbf{j}_s = q_s \mathbf{v}_s$, flows in the opposite direction for each component and no net current flow exists parallel to the harmonic field. This is illustrated schematically in figure 3.2 for both equal mass and electron-proton plasmas. We now look at the special cases of propagation parallel and perpendicular to the magnetic field.

Parallel Solutions

For parallel propagation, $\theta = 0$, hence $|\epsilon| = 0$ becomes

$$\begin{vmatrix} 1 - \frac{\omega_p^2}{\omega^2 - \Omega^2} - n^2 & 0 & 0 \\ 0 & 1 - \frac{\omega_p^2}{\omega^2 - \Omega^2} - n^2 & 0 \\ 0 & 0 & 1 - \frac{\omega_p^2}{\omega^2} \end{vmatrix} = 0. \quad (3.24)$$

The determinant of the diagonal matrix is trivial and yields the solutions

$$n^2 = 1 - \frac{\omega_p^2}{\omega^2 - \Omega^2} \quad (3.25)$$

for waves Π_x and Π_y , and

$$\omega^2 = \omega_p^2 \quad (3.26)$$

for the solution Π_z .

Equation (3.26) is the usual electrostatic plasma oscillation along (and hence unaffected by) the magnetic field.

Equation (3.25) can be rewritten as

$$k^2 = \frac{\omega^2}{c^2} \left(1 - \frac{\omega_p^2}{\omega^2 - \Omega^2} \right). \quad (3.27)$$

The resonance ($k = \infty$) at $\omega = \Omega$ and the cut off ($k = 0$) at $\omega^2 = \omega_p^2 + \Omega^2$ allows us to see the main features of the graph which is plotted in figure 3.3.

At low frequencies the dispersion relation is

$$n^2 \approx 1 + \frac{\omega_p^2}{\Omega^2}, \quad (3.28)$$

so that

$$\omega^2 \approx \frac{v_A^2 k^2}{1 + v_A^2/c^2} \approx v_A^2 k^2, \quad (3.29)$$

where $v_A^2 = B_0^2/\mu_0\rho_m$ is the squared Alfvén speed, ρ_m being the plasma mass density. Thus, the lower portion of the dispersion relation is the transverse Alfvén wave. (So called as the field is compressed perpendicular to the direction of propagation.)

The upper portion of the dispersion relation is easily identified by noting that for high frequencies $\omega \approx kc$, which is just the expected transverse electromagnetic wave.

If $\Omega = 0$, i.e. $B_0 = 0$, we have no Alfvén wave and the TEM cut off is at ω_p , as expected.

Faraday Rotation and Whistler Waves

One of the most instructive ways of examining the special properties of an equal mass plasma is with reference to the more usual electron-ion plasma (Stix 1962, Clemmow & Dougherty 1969, Nicholson 1983). For the case of parallel propagation the solutions to the dispersion relation are given by

$$\begin{vmatrix} \alpha - n^2 & i\beta & 0 \\ -i\beta & \alpha - n^2 & 0 \\ 0 & 0 & \gamma \end{vmatrix} = 0. \quad (3.30)$$

The coefficients of α , β and γ are given by summing over plasma species in (3.15). Using an e^-p^+ plasma to illustrate we have,

$$\alpha = 1 - \frac{\omega_{e-}^2}{\omega^2 - \Omega_{e-}^2} - \frac{\omega_{p+}^2}{\omega^2 - \Omega_{p+}^2}, \quad (3.31)$$

$$\beta = \frac{\omega_{e-}^2 \Omega_{e-}}{\omega^2 - \Omega_{e-}^2} + \frac{\omega_{p+}^2 \Omega_{p+}}{\omega^2 - \Omega_{p+}^2}, \quad (3.32)$$

$$\gamma = 1 - \frac{\omega_{e-}^2}{\omega^2} - \frac{\omega_{p+}^2}{\omega^2}. \quad (3.33)$$

The solution $\gamma = 0$ is just the same electrostatic oscillation of the plasma as was equation (3.26), but the solution of the 2×2 matrix gives two distinct solutions,

$$n^2 = \alpha \pm \beta. \quad (3.34)$$

Obviously these waves consist of oscillations which combine x and y electric field vectors, and substituting the solutions into the dispersion relation reveals that the solution $\alpha + \beta$ is right hand circularly polarised, and the solution $\alpha - \beta$ is left hand circularly polarised. The disappearance of the β term in the equal mass plasma has allowed us to work with modes which are linearly polarised, although circularly polarised modes could equally well be constructed.

A sketch of the solutions of (3.34) is shown in figure 3.4. Two portions of the graph are important. The first, labelled (A) shows the so-called *whistler* wave. It is in this region that both the phase and group velocity of the R.C.P. component increase with frequency. A glance at figure 3.3 reveals that both the phase and group velocity of the equal mass plasma decrease with frequency from $\omega = 0 \rightarrow \Omega$. Thus the whistler wave is absent. Differentiation of (3.25) confirms this.

The second area of interest, labeled (B) in figure 3.4, lies at higher frequencies. Here the split between the circularly polarised modes gives rise to Faraday rotation. This is the rotation, in space, of the plane of polarisation of a linearly polarised wave. An equal mass plasma has no such splittings and consequently Faraday rotation does not occur in these plasmas. This phenomena has already been noted in connection with e^+e^- plasmas (Nordelinger 1978). In §3.7 we shall discuss under what conditions anisotropic distribution functions of an equal mass plasma will maintain this property.

Perpendicular Solutions

For perpendicular propagation ($\theta = \pi/2$) the dispersion relation has solutions given by

$$\begin{vmatrix} 1 - \frac{\omega_p^2}{\omega^2 - \Omega^2} & 0 & 0 \\ 0 & 1 - \frac{\omega_p^2}{\omega^2 - \Omega^2} - n^2 & 0 \\ 0 & 0 & 1 - \frac{\omega_p^2}{\omega^2} - n^2 \end{vmatrix} = 0. \quad (3.35)$$

The determinant is again trivial, yielding solutions

$$\omega^2 = \omega_p^2 + \Omega^2 \quad (3.36)$$

for Π_x ,

$$n^2 = 1 - \frac{\omega_p^2}{\omega^2 - \Omega^2} \quad (3.37)$$

for Π_y (the same solution as in the parallel case) and finally

$$n^2 = 1 - \frac{\omega_p^2}{\omega^2} \quad (3.38)$$

for Π_x .

Equation (3.36) represents a non-propagating oscillation, with the electromagnetic force being enhanced by the gyro motion so that the oscillation is of a higher frequency than the normal plasma frequency oscillation.

The solutions for Π_y have been discussed previously.

Finally, the Π_z result, equation (3.38), is easily recognised as a transverse electromagnetic wave. Since it involves particle motion along the magnetic field, we are then left with the unmagnetised result.

These results are summarised in figure 3.5.

General Propagation

Examining the dispersion relation (3.17) for general angles of propagation it can be seen that the solutions of $|\epsilon| = 0$ can be reduced from a 3×3 determinant to a 1×1 and a 2×2 .

The singular matrix solution, $\epsilon_{22} = 0$, gives rise to a wave Π_y with dispersion relation

$$n^2 = 1 - \frac{\omega_p^2}{\omega^2 - \Omega^2}, \quad (3.39)$$

which has already been discussed. For this wave \mathbf{E} and \mathbf{k} (and hence \mathbf{B}_1) are all perpendicular, which allows us to identify this wave as a transverse electromagnetic wave at high frequencies and a transverse (or fast) Alfvén wave at low frequencies. The other two solutions come from the determinant of the remaining 2×2 matrix :

$$\begin{vmatrix} 1 - \frac{\omega_p^2}{\omega^2 - \Omega^2} - n^2 \cos^2 \theta & n^2 \cos^2 \theta \sin^2 \theta \\ n^2 \cos^2 \theta \sin^2 \theta & 1 - \frac{\omega_p^2}{\omega^2} - n^2 \cos^2 \theta \end{vmatrix} = 0 \quad (3.40)$$

This represents a wave Π_{xz} .

Writing $A = 1 - \omega_p^2/(\omega^2 - \Omega^2)$ and $B = 1 - \omega_p^2/\omega^2$ so as to best illustrate the symmetries of the solution we then have

$$n^2 = \frac{AB}{A \sin^2 \theta + B \cos^2 \theta}. \quad (3.41)$$

Note that this becomes $n^2 = A$ at $\theta = 0$ and $n^2 = B$ at $\theta = \pi/2$.

Examining a plot of the dispersion relation from (3.41) (shown in figure 3.6) it can be seen that the Alfvén wave, which exists at $\theta = 0$, drops off in speed as θ is increased and finally disappears at $\theta = \pi/2$. This wave is of course the shear, or slow, Alfvén wave. Noticing that for low frequencies $B \gg A$, (3.41) becomes (for angles suitably far from $\pi/2$)

$$n^2 \approx \frac{A}{\cos^2 \theta}. \quad (3.42)$$

Using the low frequency approximation for A , (3.29), this becomes

$$\omega \approx v_A k \cos \theta, \quad (3.43)$$

the expected result for the shear Alfvén wave.

The two resonances in the dispersion relation obviously occur when $A \sin^2 \theta + B \cos^2 \theta = 0$. Inserting the expressions for A and B this becomes

$$\omega_{res}^2 = \frac{1}{2} \left(\Omega^2 + \omega_p^2 \pm (\Omega^4 + \omega_p^4 - 2\Omega^2 \omega_p^2 \cos 2\theta)^{1/2} \right), \quad (3.44)$$

which gives the extent of the stop bands for all angles.

If the equilibrium field is weak, such that $\omega_p \gg \Omega$, (3.44) takes on a simpler form through ignoring the term Ω^4 and making a binomial expansion of the square root:

$$\omega_{res}^2 \approx \frac{1}{2} \left(\Omega^2 + \omega_p^2 \pm \omega_p^2 \left(1 - \frac{\Omega^2}{\omega_p^2} \cos 2\theta \right) \right), \quad (3.45)$$

so that the upper and lower resonant frequencies become

$$\omega_{upper\ res}^2 = \omega_p^2 + \Omega^2 \sin^2 \theta, \quad (3.46)$$

$$\omega_{lower\ res}^2 = \Omega^2 \cos^2 \theta. \quad (3.47)$$

As previously noted, the wave combines electric fields in the x and z directions. The dot product of \mathbf{E} and \mathbf{k} is shown in figure 3.7. From this it is obvious that the angle between \mathbf{E} and \mathbf{k} is not a constant, so the high frequency waves arising from this solution can be identified as a form of extraordinary electromagnetic mode, in which the electric field vector is not perpendicular to the direction of propagation. (We have seen though that in the case of propagation parallel and perpendicular to the field equal mass symmetry means that $\mathbf{k} \perp \mathbf{E}$.)

CMA Diagram For Equal Mass Plasmas

The CMA (Clemmow–Mullaly–Allis) diagram is a way of classifying the waves which exist inside a cold plasma. With the two free parameters of the plasma, density and magnetisation, represented on the axes ω_p/ω and Ω/ω respectively, the surface of the diagram represents all the possible states of a uniform cold plasma. All the solutions which we have found so far (e.g. transverse Alfvén waves) exist only for certain frequencies, and on the CMA plot these frequencies are represented as the areas between different bounding surfaces – calculated from the dispersion relation. For the equal mass plasma the two quantities A and B form the bounding surfaces : $A = 0$, $A = \infty$, $B = 0$. Within these regions normalised wave vectors can be plotted. It can be shown (Allis, quoted in Stix 1962) that the wave vector surfaces (essentially surfaces of refractive index) are topologically invariant inside any of the boundary regions, whence the value of the CMA diagram in summarising

the properties of a cold plasma. (It is also possible to plot group velocity surfaces, though more care must be taken (Walker 1977).)

The CMA diagram for the equal mass plasma is shown in figure 3.8. As can be seen there are five distinct regions to the plasma.

- (a) Alfvén Wave Region: here both fast and slow Alfvén waves exist.
- (b) Highly Magnetised Region: here the fast Alfvén wave still exists, but the slow one has become more electromagnetic in character.
- (c) Transition Region: frequencies above ω_p and Ω but below $\sqrt{(\omega_p^2 + \Omega^2)}$. The fast Alfvén wave is cut off, but a semi-transverse EM wave can still be transmitted as long as the particle motion is mainly along \hat{z} , minimising the influence of the magnetic field.
- (d) High Frequency EM Region: ordinary and extraordinary electromagnetic waves propagate in this region.
- (e) Stop Region: below ω_p but above Ω . No waves propagate in this region.

3.5 Warm Equal Mass Plasmas

We now extend our treatment of plasma waves to a warm equal mass plasma. Thus our momentum equation is now

$$\frac{\partial \mathbf{v}}{\partial t} + \left(\mathbf{v} \cdot \frac{\partial}{\partial \mathbf{r}} \right) \mathbf{v} = \mathbf{a} - \frac{1}{nm} \frac{\partial P}{\partial \mathbf{r}}. \quad (2.43)$$

We have temporarily dropped the species subscripts for clarity.

As previously we linearise these equations, additionally letting $P = P_0 + P_1$, where P_0 is an equilibrium pressure and P_1 is a perturbation. This, after Fourier analysing, gives

$$i\omega \mathbf{v} = \frac{q}{m} (\mathbf{E} + \mathbf{v} \times \mathbf{B}_0) + \frac{i}{n_0 m} P_1 \mathbf{k}. \quad (3.48)$$

Now, assuming our plasma to behave as an ideal gas, we can state that for *adiabatic* changes $P_1 = \gamma k_B T n_1$, where γ is the ratio of specific heats, T is the temperature of the species and k_B is Boltzmann's constant. From the continuity equation we easily see that

$$n_1 = \frac{n_0 \mathbf{k} \cdot \mathbf{v}}{\omega}. \quad (3.49)$$

Thus

$$i\omega \mathbf{v} = \frac{q}{m} (\mathbf{E} + \mathbf{v} \times \mathbf{B}_0) + \frac{i\gamma k_B T}{m\omega} \mathbf{k} (\mathbf{k} \cdot \mathbf{v}) \quad (3.50)$$

The resulting equations for the velocity components can be solved in the same way as for the cold plasma, although the expressions are more complex. With the aid of computer algebra (Reduce 3.3) this difficulty is overcome and results in the following

$$\left. \begin{aligned} v_x &= \frac{q(E_x(a^2 k^2 \omega \cos^2 \theta - i\omega^3) + E_y \Omega(a^2 k^2 \cos^2 \theta - \omega^2) + E_z(-ia^2 k^2 \omega \sin \theta \cos \theta))}{m(\omega^2(\omega^2 - \Omega^2) + a^2 k^2(\Omega^2 \cos^2 \theta - \omega^2))}, \\ v_y &= \frac{q(E_x \Omega(-a^2 k^2 \cos^2 \theta + \omega^2) + E_y(ia^2 k^2 \omega - i\omega^3) + E_z \Omega(a^2 k^2 \sin \theta \cos \theta))}{m(\omega^2(\omega^2 - \Omega^2) + a^2 k^2(\Omega^2 \cos^2 \theta - \omega^2))}, \\ v_z &= \frac{q(E_x(-ia^2 k^2 \cos \theta \sin \theta) + E_y \Omega(a^2 k^2 \cos \theta \sin \theta) + E_z(ia^2 k^2 \omega \sin^2 \theta + i\Omega^2 \omega - i\omega^3))}{m(\omega^2(\omega^2 - \Omega^2) + a^2 k^2(\Omega^2 \cos^2 \theta - \omega^2))}, \end{aligned} \right\} \quad (3.51)$$

where the adiabatic sound speed has been introduced:

$$a^2 = \frac{\gamma k_B T}{m} \quad (3.52)$$

We move straight on to the equal mass case, and also note that we consider both species to be at the same temperature. This is not a further restriction over those already inherent in using the warm plasma model. To see why this is the case consider the transfer of momentum in a collision between two particles of masses m_1 and m_2 . The momentum transfer is proportional to m_1/m_2 so that it is much easier to transfer momentum between particles of similar masses than between those of widely different mass. With electron-ion plasmas this means that each species in the plasma can reach self-equilibrium in a far shorter time than it takes for the whole plasma to reach a true equilibrium (Laing 1981), so it is natural at this point to develop a theory with unequal temperatures for the species. Conversely, in an equal mass plasma, the transfer of momentum between species is as easy as the transfer of momentum among an individual species, so that all equilibrium timescales are the same. The equal mass plasma therefore reaches a global equilibrium in the same time as each species could reach a self-equilibrium and so it is natural to make both species temperatures equal.

Looking in detail at equations (3.51) we see that $v_{x,z} = v_{x,z}(E_x, E_y \Omega, E_z)$. Thus the dependence of v_x and v_z upon E_y is factored by Ω which cancels when summed over different equal mass components. Similarly $v_y = v_y(E_x \Omega, E_y, E_z \Omega)$ and the dependence on E_x and E_z cancels in the equal mass sum. The current in a warm equal mass plasma is thus

$$\mathbf{j} = \frac{2inq^2\omega}{m(\omega^2(\omega^2 - \Omega^2) + a^2 k^2(\Omega^2 \cos^2 \theta - \omega^2))} \times \begin{pmatrix} a^2 k^2 \cos^2 \theta - \omega^2 & 0 & -a^2 k^2 \cos \theta \sin \theta \\ 0 & a^2 k^2 - \omega^2 & 0 \\ -a^2 k^2 \cos \theta \sin \theta & 0 & a^2 k^2 \sin^2 \theta + \Omega^2 - \omega^2 \end{pmatrix} \cdot \mathbf{E} \quad (3.53)$$

which has the same symmetries as the cold case.

Turning to the dispersion relation (3.15) and using (3.53) we find

$$\begin{pmatrix} 1 - \Theta(\omega^2 - a^2 k^2 \cos^2 \theta) - n^2 \cos^2 \theta & 0 & \cos \theta \sin \theta (n^2 - \Theta a^2 k^2) \\ 0 & 1 - \Theta(\omega^2 - a^2 k^2) - n^2 & 0 \\ \cos \theta \sin \theta (n^2 - \Theta a^2 k^2) & 0 & 1 - \Theta(\omega^2 - \Omega^2 - a^2 k^2 \sin^2 \theta) - n^2 \sin^2 \theta \end{pmatrix} \cdot \mathbf{E} = 0, \quad (3.54)$$

where

$$\Theta = \frac{\omega_p^2}{\omega^2(\omega^2 - \Omega^2) + a^2 k^2(\Omega^2 \cos^2 \theta - \omega^2)} \quad (3.55)$$

As with the cold equal mass plasma we shall first look at propagation parallel and perpendicular to the field before going on to look at general angles of propagation.

Parallel Solutions

The dispersion relation (3.54) for $\theta = 0$ is

$$\begin{vmatrix} 1 - \Theta_0(\omega^2 - a^2 k^2) - n^2 & 0 & 0 \\ 0 & 1 - \Theta_0(\omega^2 - a^2 k^2) - n^2 & 0 \\ 0 & 0 & 1 - \Theta_0(\omega^2 - \Omega^2) \end{vmatrix} = 0, \quad (3.56)$$

where Θ_0 is given by substitution of $\theta = 0$ into (3.55).

Of course the determinant equation is trivial and yields the following solutions:

$$1 - \frac{\omega_p^2}{(\omega^2 - \Omega^2)} = n^2 \quad (3.55)$$

for waves Π_x and Π_y and

$$1 - \frac{\omega_p^2}{(\omega^2 - a^2 k^2)} = 0 \quad (3.57)$$

for a wave Π_z .

That the solutions of (3.56) for waves Π_x and Π_y are those found for a cold plasma is just what we should expect. This is because for x and y electric fields, the particles move in the $x - y$ plane, thus \mathbf{k} is perpendicular to \mathbf{v} and no pressure force is felt.

The solution (3.57) for Π_z is somewhat altered from the cold plasma case and can be written

$$\omega^2 = \omega_p^2 + a^2 k^2 \quad (3.58)$$

This is of course the electrostatic Langmuir wave (with \mathbf{k} parallel to both \mathbf{E} and \mathbf{B}_0) found in all plasmas. These dispersion curves are shown in figure 3.9.

Perpendicular Solutions

With $\theta = \pi/2$ the dispersion relation becomes

$$\begin{vmatrix} 1 - \Theta_{\pi/2}\omega^2 & 0 & 0 \\ 0 & 1 - \Theta_{\pi/2}(\omega^2 - a^2 k^2) - n^2 & 0 \\ 0 & 0 & 1 - \Theta_{\pi/2}(\omega^2 - \Omega^2 - a^2 k^2) - n^2 \end{vmatrix} = 0, \quad (3.59)$$

with

$$\Theta_{\pi/2} = \frac{\omega_p^2}{\omega^2(\omega^2 - \Omega^2 - a^2 k^2)}. \quad (3.60)$$

Again the symmetry of the plasma reveals itself in three distinct solutions :

$$1 - \frac{\omega_p^2}{\omega^2 - \Omega^2 - a^2 k^2} = 0 \quad (3.61)$$

for waves Π_x ,

$$n^2 = 1 - \frac{\omega_p^2(\omega^2 - a^2 k^2)}{\omega^2(\omega^2 - \Omega^2 - a^2 k^2)} \quad (3.62)$$

for waves Π_y and

$$n^2 = 1 - \frac{\omega_p^2}{\omega^2} \quad (3.63)$$

for waves Π_z .

Taking the Π_z wave first we find the normal transverse electromagnetic wave that existed in the cold plasma. Here of course the particle motion is confined to the z direction and is thus unaffected by the magnetic field, so that $\mathbf{k} \perp \mathbf{v}$ and no density perturbation occurs to produce a pressure force.

Equation (3.62) can be seen to split into two parts, an Alfvén-sound wave (discussed further below) and an electromagnetic wave.

Equation (3.61) can be rewritten as

$$\omega^2 = \omega_p^2 + \Omega^2 + a^2 k^2. \quad (3.63)$$

These waves correspond to upper hybrid waves found in electron-ion plasmas, the upper hybrid frequency just reducing to $\sqrt{(\omega_p^2 + \Omega^2)}$ for an equal mass plasma. These waves can be seen as the magnetised analogue of Langmuir waves and are electrostatic ($\mathbf{k} \parallel \mathbf{E}$).

These results are summarised in figure 3.10.

General Propagation

The symmetries of the equal mass plasma cause the dispersion relation for the warm plasma to have the same form as for the cold case (i.e. $\sigma_{12} = \sigma_{21} = \sigma_{23} = \sigma_{32} = 0$). Thus the solutions to (3.54) reduce once more from a 3×3 determinant to a 1×1 and a 2×2 .

Considering firstly the 1×1 determinant, which gives solutions for Π_y waves, we find

$$n^2 = 1 - \frac{\omega_p^2(\omega^2 - a^2 k^2)}{\omega^4 - \omega^2(\Omega^2 - a^2 k^2) + a^2 k^2 \Omega^2 \cos^2 \theta} \quad (3.64)$$

This is a dispersion relation which is quadratic in k^2 , and solutions for various angles are plotted in figure 3.11, where we see that the electromagnetic wave exists at all angles (as expected) and that the Alfvén and sound waves exhibit various degrees of coupling, from $\theta = 0$, where they are separate, to $\theta = \pi/2$ where they form one single wave. This is a result of the compressional Alfvén wave producing no density perturbation at $\theta = 0$ (because the induced gyro motion along $\hat{\mathbf{x}}$ is still perpendicular to \mathbf{k} – hence the absence of a sound wave), but as θ swings round to $\pi/2$ a density perturbation arises and the Alfvén wave begins to couple to the sound wave via the ∇P force. Notice that we have shown the ‘sound wave’ $\omega^2 = a^2 k^2$ at $\theta = 0$. Although this wave does not exist physically its dispersion relation is an asymptote for the Alfvén-sound wave as $\theta \rightarrow 0$.

Turning to the 2×2 determinant ($\epsilon_{11}\epsilon_{33} - \epsilon_{31}\epsilon_{13} = 0$) this becomes

$$(1 - \Theta(\omega^2 - a^2 k^2 \cos^2 \theta) - n^2 \cos^2 \theta)(1 - \Theta(\omega^2 - \Omega^2 - a^2 k^2 \sin^2 \theta) - n^2 \sin^2 \theta) - \cos^2 \theta \sin^2 \theta (n^2 - \Theta a^2 k^2)^2 = 0 \quad (3.65)$$

Using (3.55) for Θ this becomes a cubic polynomial in k^2 . The dispersion relation is plotted in figure 3.12 for various angles θ .

The figure can be seen at low frequencies to exhibit a similar Alfvén-sound wave behaviour already discussed for the Π_y solution (again we plot the asymptotic solution $\omega^2 = a^2 k^2$ at $\theta = 0$). At higher frequencies we see the extraordinary electromagnetic wave found for cold plasmas and in addition a spectrum of electrostatic waves which can exist at any angle.

3.6 Collisional Effects In A Warm Equal Mass Plasma

The final fluid model that we study for the equal mass plasma is one which incorporates the effect of collisions. This must be done phenomenologically, as the Vlasov equation (2.19), from which we derived the fluid equations, ignores ‘collisions’ (or more correctly ignores close coulomb interactions between two particles in the plasma). Despite this rather *ad hoc* approach the warm plasma model with collisions is very useful. Theoretically we wish to show that the special symmetry found in the equal mass plasma is not destroyed by the inclusion of a collision term.

The phenomenological collision term which we adopt is one which takes the form of momentum dissipation arising from a ‘frictional’ force between two fluid elements. Included in the momentum equation for the warm plasma it gives

$$\frac{\partial \mathbf{v}_s}{\partial t} + \left(\mathbf{v}_s \cdot \frac{\partial}{\partial \mathbf{r}} \right) \mathbf{v}_s = \frac{q_s}{m_s} (\mathbf{E} + \mathbf{v}_s \times \mathbf{B}) - \frac{1}{n_s m_s} \frac{\partial P_s}{\partial \mathbf{r}} - \sum_{s'=1}^S \nu_{s,s'} (\mathbf{v}_s - \mathbf{v}_{s'}). \quad (3.66)$$

$\nu_{s,s'}$ is the ‘collision frequency’ between species s and s' . Various models can be adopted for the form of this term (it can be a function of both \mathbf{v}_s and $\mathbf{v}_{s'}$) but we are not interested in these specifics, rather in how an equation of the form (3.66) behaves for an equal mass plasma.

The analysis of equation (3.66) proceeds exactly as for the warm and cold equal mass plasmas: we first linearise and then take a Fourier transform. However, now the equations of motion are coupled via the collision term:

$$\begin{aligned} i\omega \mathbf{v}_+ &= \frac{q_+}{m}(\mathbf{E} + \mathbf{v}_+ \times \mathbf{B}_0) + \frac{ia^2}{\omega} \mathbf{k}(\mathbf{k} \cdot \mathbf{v}_+) - \nu(\mathbf{v}_+ - \mathbf{v}_-) \\ i\omega \mathbf{v}_- &= \frac{q_-}{m}(\mathbf{E} + \mathbf{v}_- \times \mathbf{B}_0) + \frac{ia^2}{\omega} \mathbf{k}(\mathbf{k} \cdot \mathbf{v}_-) - \nu(\mathbf{v}_- - \mathbf{v}_+) \end{aligned} \quad (3.67)$$

These are the six coupled equations to be solved for the six velocity components of the plasma: \mathbf{v}_+ & \mathbf{v}_- . Physically we have not changed the equations much, but algebraically the additional collision term is far from trivial and the resultant equations are very unwieldy. It is almost essential to use computer algebra to solve these equations – to tackle them by hand is practically impossible. After analysis by Reduce 3.3 the velocity components are obtained. These expressions are long (20 A4 pages) and not particularly useful, so we do not give them, however, we find that the extra symmetry of the problem is not destroyed by the presence of a collision term: the dependences of $v_{x,z}$ on E_y and of v_y on $E_{x,z}$ are still all factored by Ω . So the dispersion relation takes on the same form as before:

$$\begin{pmatrix} \epsilon_{11} & 0 & \epsilon_{13} \\ 0 & \epsilon_{22} & 0 \\ \epsilon_{31} & 0 & \epsilon_{33} \end{pmatrix} \cdot \mathbf{E} = 0 \quad (3.68)$$

But now the non-zero ϵ terms take on an uglier cast:

$$\begin{aligned} \epsilon_{11} = & 1 - \omega_p^2 [a^4 k^4 (2\nu\omega \cos^2 \theta - i\Omega^2 \cos^4 \theta + i\omega^2 \cos^2 \theta) \\ & + a^2 k^2 (4i\nu^2 \omega^2 + 2\nu\Omega^2 \omega \cos^2 \theta - (4 + \cos^2 \theta)\nu\omega^3 \\ & + 2i\Omega^2 \omega^2 \cos^2 \theta - (1 + \cos^2 \theta)i\omega^4) \\ & + (i\omega^6 + 4\nu\omega^5 - i\Omega^2 \omega^4 - 4i\nu^2 \omega^4 - 2\nu\Omega^2 \omega^3)] \div \Xi - n^2 \cos^2 \theta, \end{aligned} \quad (3.69)$$

$$\begin{aligned} \epsilon_{13} = \epsilon_{31} = & \cos \theta \sin \theta (n^2 - a^2 k^2 \omega_p^2 [a^2 k^2 (i\omega^2 + 2\nu\omega - i\Omega^2 \cos^2 \theta) \\ & + \omega^2 (i\omega^2 - 2\nu\omega + i\Omega^2)] \div \Xi), \end{aligned} \quad (3.70)$$

$$\begin{aligned} \epsilon_{22} = & 1 - \omega_p^2 [a^4 k^4 (i\omega^2 + 2\nu\omega - i\Omega^2 \cos^2 \theta) \\ & + a^2 k^2 (-2i\omega^4 - 6\nu\omega^3 + i\omega^2 \nu^2 + i\omega^2 \Omega^2 (1 + \cos^2 \theta) + 2\nu\omega \Omega^2) \\ & + (i\omega^6 + 4\omega^5 \nu - i\omega^4 \Omega^2 - 4i\omega^4 \nu^2 - 2\nu\Omega^2 \omega^3)] \div \Xi - n^2 \end{aligned} \quad (3.71)$$

$$\begin{aligned} \epsilon_{33} = & 1 - \omega_p^2 [a^4 k^4 \cos^2 \theta \sin^2 \theta (i\omega^2 + 2\nu\omega - i\Omega^2) \\ & + a^2 k^2 (4i\nu^2 + (2 + 2\cos^2 \theta)\Omega^2 \omega - (4 + 2\sin^2 \theta)\nu\omega^3 \\ & - i\Omega^4 \cos^2 \theta + 2i\Omega^2 \omega^2 - i(1 + \sin^2 \theta)\omega^4) \\ & + (i\omega^6 + 4\nu\omega^5 - 2i\Omega^2 \omega^4 - 4i\nu^2 \omega^4 - 4\nu\Omega^2 \omega^3 + i\Omega^4 \omega^2)] \div \Xi - n^2 \sin^2 \theta, \end{aligned} \quad (3.72)$$

where the factor Ξ is equal to

$$\begin{aligned}
& a^4 k^4 (i\omega^4 + 4\nu\omega^3 - 2i\Omega^2\omega^2 \cos^2 \theta - 4\nu\Omega^2\omega \cos^2 \theta + i\Omega^4 \cos^4 \theta) \\
& + a^2 k^2 \omega (-i\omega^5 - 5\nu\omega^4 + 8i\nu^2\omega^3 + i\Omega^2\omega^3 \cos^2 \theta + 4\nu^3\omega^2 + 3(1 + \cos^2 \theta)\nu\Omega^2\omega^2 \\
& - 2i(1 + \cos^2 \theta)\Omega\nu^2\omega^2 - i\Omega^4\omega \cos^2 \theta - \nu\Omega^4 \cos^2 \theta) \\
& + \omega^3 (i\omega^5 + 6\nu\omega^4 - 12i\nu^2\omega^3 - 2i\Omega^2\omega^3 - 8\nu^3\omega^2 - 8\nu\Omega^2\omega^2 + 8i\nu^2\Omega^2\omega + i\Omega^4\omega + 2\nu\Omega^4).
\end{aligned} \tag{3.73}$$

Solutions For Waves Π_y

This class of solutions is obtained by setting $\epsilon_{22} = 0$. It yields a third order polynomial in k^2 . The extra solution turns out to be a repeated root of the sound wave solution and the full solution is broadly the same as for a warm plasma. The solution is shown in figure 3.13. As all the waves are damped there is no ambiguity between $\Re(k)$, which is always positive, and $\Im(k)$, which is always negative (lying to the left of the ω axis). To plot these solutions we have used a simple Coulomb collision term (Nicholson 1983) of the form

$$\nu = \frac{8\pi n q^4 \ln \Lambda}{m^2 v_T^3}, \tag{3.74}$$

where Λ is the Coulomb logarithm and v_T is the thermal speed.

As the damping is proportional to v_T^{-3} , in figure 3.13 the temperature is lower than for the dispersion relations shown in the warm plasma section. The characteristic damping behaviour is more evident as the collision frequency is the same order as the gyro and plasma frequencies. Broadly, the solutions are the same as found in the warm plasma model. The second sound wave solution is seen to be more heavily damped than the first, thus it might be less important for wave propagation, but more so for heating.

Solutions For Waves Π_{xz}

The second class of solutions is derived from the dispersion relation by setting $\epsilon_{11}\epsilon_{33} - \epsilon_{13}\epsilon_{31} = 0$. A fifth order polynomial in k^2 results. On plotting the solutions the two new roots are found, as before, to be repeated sound wave solutions. As before, it is more instructive to look at damping when the collision frequency is high and this is shown in figure 3.14. The features of the warm plasma are carried over with the inclusion of damping. The plot shows that of the two additional sound wave solutions, one is almost an exact double root of the original sound wave and the other is a more heavily damped wave.

3.7 Equal Mass Symmetry in General Distributions

The three fluid models studied so far all show an extra symmetry inherent in an equal mass plasma. Mathematically this takes the form of the disappearance of terms ϵ_{12} , ϵ_{21} , ϵ_{32} and ϵ_{23}

in the dielectric tensor. This has enabled us to characterise waves into two general classes, those with an associated y electric field, Π_y and those with an associated electric field in the xz plane, Π_{xz} . It has also removed the important phenomena of Faraday rotation from the plasma. However, real plasmas are not fluids and are more accurately modelled by considering kinetic theory. Can we expect our equal mass symmetries to carry over to kinetic description? In fact, we can make progress simply by studying the open form of the plasma momentum equation (2.27).

$$\frac{\partial}{\partial t}(n_s \mathbf{v}_s) + \frac{\partial}{\partial \mathbf{r}} \cdot (n_s \langle \mathbf{v} \mathbf{v} \rangle_s) = \mathbf{a} n_s, \quad (2.27)$$

As noted before, this equation is open. The term $\langle \mathbf{v} \mathbf{v} \rangle$ relates it to the energy equation and thence to the rest of the infinite hierarchy of fluid equations. As our symmetry involves the dielectric tensor, derived from the momentum equation, it is sufficient to work with this term only – *but to make no assumptions regarding the term involving $\langle \mathbf{v} \mathbf{v} \rangle$* . This ensures that the additional information concerning the plasma distribution function can come into play.

To restate the problem, the open momentum equations for an equal mass plasma are

$$\frac{\partial}{\partial t}(n_{\pm} \mathbf{v}_{\pm}) + \frac{\partial}{\partial \mathbf{r}} \cdot (n_{\pm} \langle \mathbf{v} \mathbf{v} \rangle_{\pm}) = \mathbf{a} n_{\pm}. \quad (3.75)$$

If the dispersion relation derived from these equations – making no assumptions regarding $\langle \mathbf{v} \mathbf{v} \rangle$ – has $\epsilon_{12} = \epsilon_{21} = \epsilon_{32} = \epsilon_{23} = 0$, then equal mass symmetry will persist.

Derivation of Symmetry Conditions

Fourier analysing and then linearising equations (3.75) we derive

$$i\omega \mathbf{v}_{\pm} - i\alpha^{\pm} n_{1\pm} = \frac{q_{\pm}}{m} n_0 (\mathbf{E} + \mathbf{v}_{\pm} \times \mathbf{B}_0), \quad (3.76)$$

where we have written $\mathbf{k} \cdot \langle \mathbf{v} \mathbf{v} \rangle_{\pm} = \alpha^{\pm}$. We now calculate $\mathbf{j} = n_0(q_+ \mathbf{v}_+ + q_- \mathbf{v}_-)$ and examine the appropriate terms in σ . The set of linear equations for \mathbf{v}_{\pm} were solved with the aid of computer algebra (Reduce 3.3) and the results for the relevant components for σ are shown below.

$$\sigma_{12} \propto B_0 k_z \kappa (\alpha_y^- \alpha_z^+ + \alpha_y^+ \alpha_z^-) + B_0 \kappa (\alpha_y^- + \alpha_y^+) + k_z (\alpha_z^- \alpha_x^+ - \alpha_x^- \alpha_z^+) + (\alpha_x^+ - \alpha_x^-) \quad (3.77)$$

$$\begin{aligned} \sigma_{21} \propto & B_0 k_z \kappa (\alpha_x^- \alpha_z^+ - \alpha_x^+ \alpha_z^-) + B_0 \kappa (\alpha_x^- - \alpha_x^+) \\ & + k_x (\alpha_x^- \alpha_y^+ + \alpha_y^- \alpha_x^+) + k_z (\alpha_y^- \alpha_z^+ + \alpha_z^- \alpha_y^+) + (\alpha_y^- + \alpha_y^+) \end{aligned} \quad (3.78)$$

$$\begin{aligned} \sigma_{23} \propto & B_0^3 k_z \kappa^3 (\alpha_x^- \alpha_z^+ - \alpha_x^+ \alpha_z^-) + B_0^3 \kappa^3 (\alpha_x^- - \alpha_x^+) + B_0^2 k_x \kappa^2 (\alpha_x^- \alpha_y^+ + \alpha_y^- \alpha_x^+) \\ & + B_0^2 k_z \kappa^2 (\alpha_y^- \alpha_z^+ + \alpha_z^- \alpha_y^-) + B_0^2 \kappa^2 (\alpha_y^- + \alpha_y^+) + B_0 k_z \kappa (\alpha_x^- \alpha_z^+ - \alpha_x^+ \alpha_z^-) \\ & + B_0 \kappa (\alpha_x^- - \alpha_x^+) + k_x (\alpha_x^- \alpha_y^+ + \alpha_y^- \alpha_x^+) + k_z (\alpha_y^- \alpha_z^+ + \alpha_z^- \alpha_y^-) + (\alpha_y^+ + \alpha_y^-) \end{aligned} \quad (3.79)$$

$$\sigma_{32} \propto B_0^2 \kappa^2 (\alpha_z^- - \alpha_z^+) + B_0 k_x \kappa (\alpha_y^- \alpha_z^+ + \alpha_z^- \alpha_y^+) + k_x (\alpha_z^- \alpha_x^+ - \alpha_x^- \alpha_z^+) + (\alpha_z^- - \alpha_z^+) \quad (3.80)$$

We have written $\kappa = |q|/im\omega$. To interpret equations (3.77)-(3.80) we shall look for solutions which do not involve special cases of B_0 or \mathbf{k} , but instead rely on cancellation between the α terms. Examining each of the equations in turn we see that they are all equal to zero on the same criterion :

$$\alpha_x^+ = \alpha_x^- \quad \alpha_y^+ = -\alpha_y^- \quad \alpha_z^+ = \alpha_z^- \quad (3.81)$$

Recalling that $\alpha = \mathbf{k} \cdot \langle \mathbf{v} \mathbf{v} \rangle$ and requiring that our criterion should not involve \mathbf{k} , this translates into conditions on the values of the components of $\langle \mathbf{v} \mathbf{v} \rangle$:

$$\langle v_x v_y \rangle_+ = - \langle v_x v_y \rangle_-, \quad (3.82)$$

$$\langle v_z v_y \rangle_+ = - \langle v_z v_y \rangle_-, \quad (3.83)$$

$$\langle v_x v_x \rangle_+ = \langle v_x v_x \rangle_-, \quad (3.84)$$

$$\langle v_x v_z \rangle_+ = \langle v_x v_z \rangle_-, \quad (3.85)$$

$$\langle v_z v_z \rangle_+ = \langle v_z v_z \rangle_-, \quad (3.86)$$

with no restriction on the values of $\langle v_y v_y \rangle_{\pm}$.

Now we must also bear in mind that our plasma was initially in equilibrium. This means two things for us. Firstly that we have no zero order velocity components: $\langle \mathbf{v} \rangle_{\pm} = 0$; and secondly that the distribution function must be symmetric about the magnetic field: $f_{\pm} = f_{\pm}(v_{\perp}, v_{\parallel})$. The second of these conditions has a profound impact on the moment criteria above. It means that $\langle v_x v_y \rangle$, $\langle v_z v_y \rangle$ and $\langle v_x v_z \rangle$ must all be identically equal to zero. Thus the 'equal mass' criteria is automatically satisfied for (3.82), (3.83) and (3.85) and we need only concern ourselves with (3.84) and (3.86).

Interpretation of Criteria

To interpret the requirements of our symmetry criteria we must first understand the nature of the term that they refer to in the momentum equation, $\frac{\partial}{\partial \mathbf{r}} n_{\pm} \langle \mathbf{v} \mathbf{v} \rangle_{\pm}$. On multiplying by m we see that the term in question is actually

$$\frac{\partial}{\partial \mathbf{r}} n_{\pm} \mathbf{P}_{\pm}, \quad (3.87)$$

where \mathbf{P} is the pressure tensor. Linearising and Fourier analysing this becomes

$$n_1 \mathbf{k} \cdot \mathbf{P} \quad (3.88)$$

This term contributes forces that arise from pressure inside the plasma, and in examining the mathematical constraints on this term we look physically at the form that the pressure force must take for our equal mass symmetry to be preserved.

Our requirement can easily be related to our previous discussion concerning the disappearance of currents induced by gyro motion. Recall that the gyro motion produced currents which cancelled when summed over equal mass components, so that no current flowed along \hat{y} when an E_x field was applied and *vice versa*. Now, when the plasma is perturbed, pressure forces come into play, and if the symmetry of the plasma is to be preserved these too must ensure that no current flows along \hat{y} when an E_x field was applied (and *vice versa*).

Allowed Distributions

The requirements of (3.84) and (3.86) are, as we stated above, related to the pressure forces inside the plasma. We require for the two components of the plasma to have the same pressure force along \hat{x} and \hat{z} . This means that the plasma components must have the same temperature along the magnetic field and across it, but that these temperatures may be different. In addition our symmetry conditions stated that the plasma must have no zero order velocity and be symmetric around the magnetic field. In figure 3.15 we show an example of a distribution which will satisfy these criteria.

It is the case however, that even if some of these conditions are not met, and that waves may start to couple if the equal mass symmetry is broken, Faraday rotation will not reappear. This is a specific effect related to the behaviour of the circularly polarized modes of a normal plasma arising from the charge/mass asymmetry of electron-ion plasmas – our plasma will always retain its charge/mass symmetry even if it loses the wave decoupling effect and so it will never exhibit Faraday rotation.

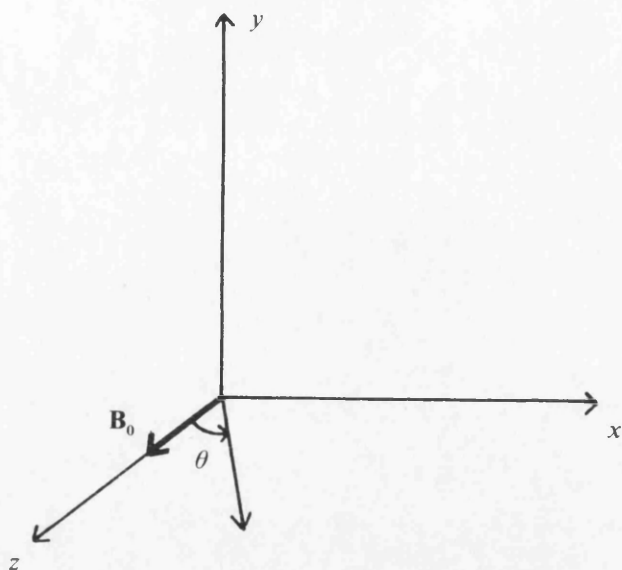


Figure 3.1. Coordinate system.

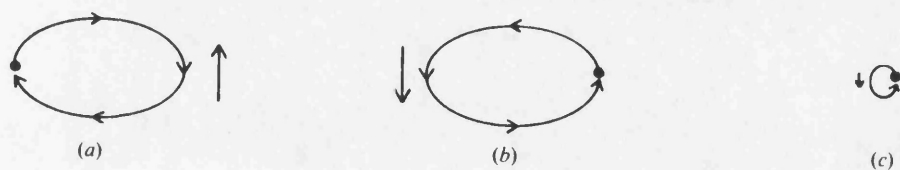


Figure 3.2. Orbits of particles in a harmonic electric field E_x : (a) negative equal mass particles; (b) positive equal mass particles; (c) positive heavy ions. The arrow indicates the current j_y produced at phase π in the orbit. Note the cancellation of currents in the equal mass case.

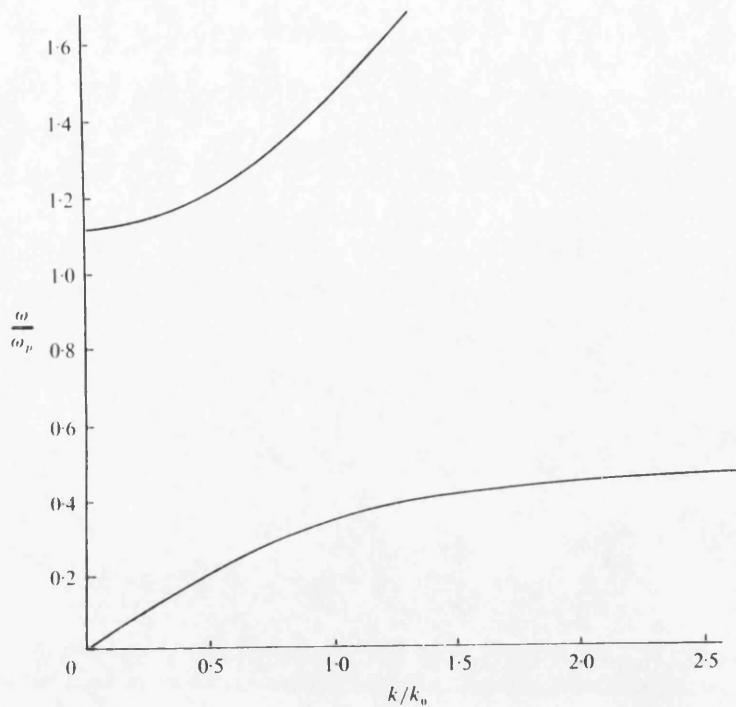


Figure 3.3. Dispersion relation for a cold equal mass plasma with waves propagating along the magnetic field.

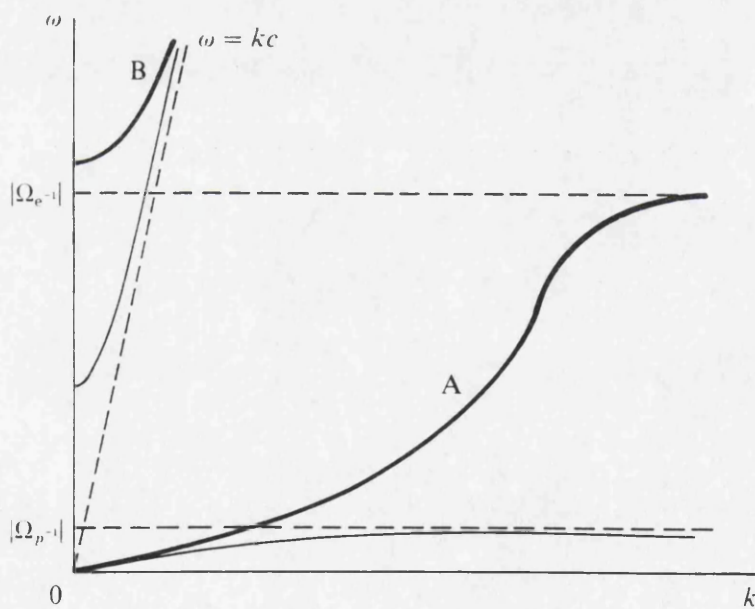


Figure 3.4. Schematic drawing of the dispersion relation for an electron/ion plasma:——, RCP waves; ———, LCP waves.

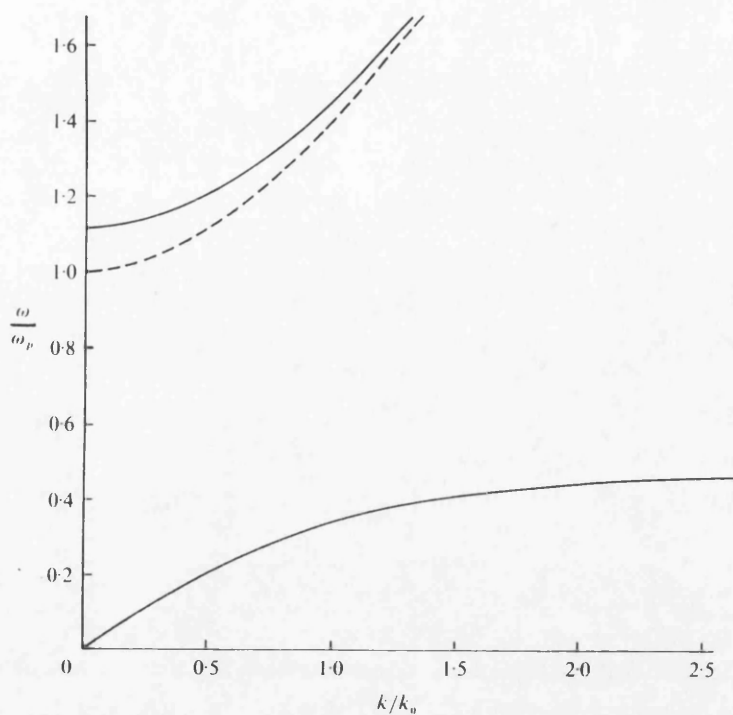


Figure 3.5. Dispersion relation for a cold equal mass plasma with waves propagating perpendicular to the magnetic field: —, Π_y ; ---, Π_z .

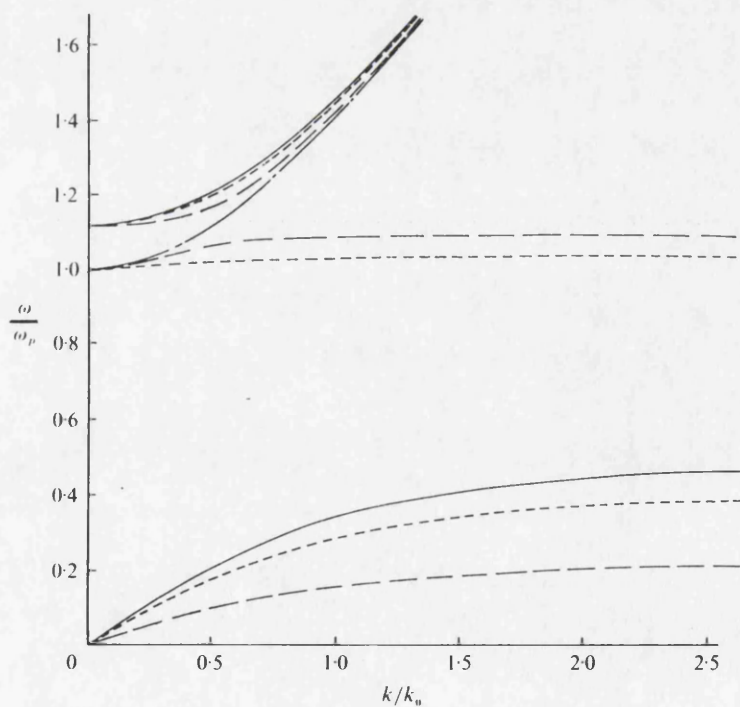


Figure 3.6. Dispersion relation for waves Π_{xz} in a cold equal mass plasma: —, $\theta = 0$; ----, $\pi/6$; — —, $\pi/3$; — — —, $\pi/2$.

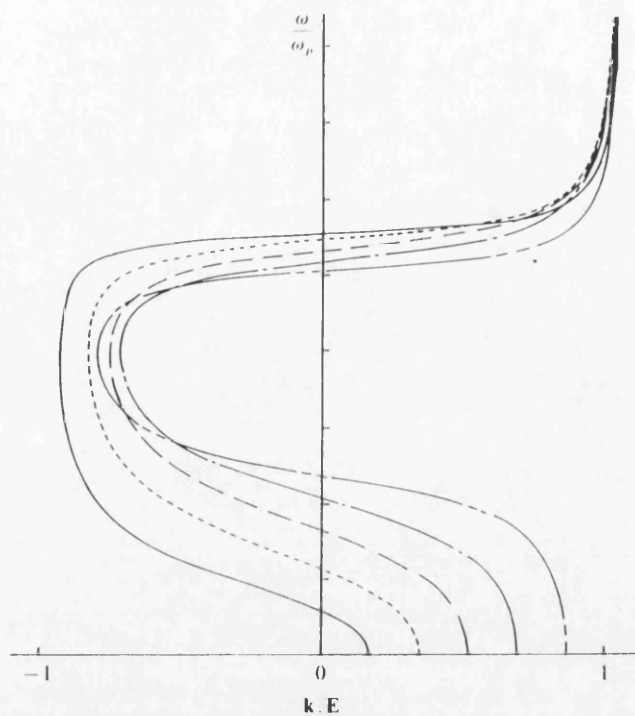


Figure 3.7. Angle between direction of propagation and electric field vector for Π_{xz} waves at various angles to the magnetic field: —, $\pi/12$; - - - - , $\pi/6$; — — —, $\pi/4$; - · - · -, $\pi/3$; — · — · —, $5\pi/6$.

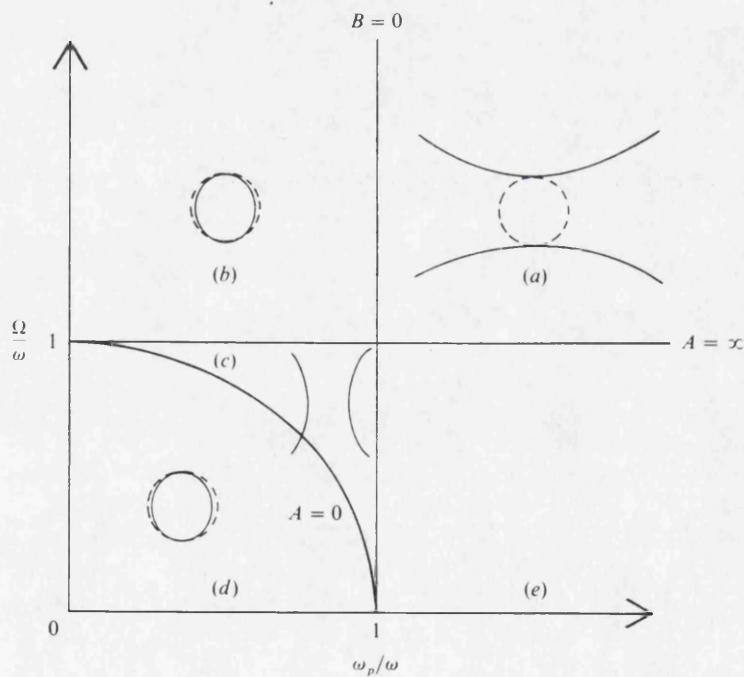


Figure 3.8. CMA diagram for equal mass plasmas: —, Π_{xz} ; - - - - , Π_y .

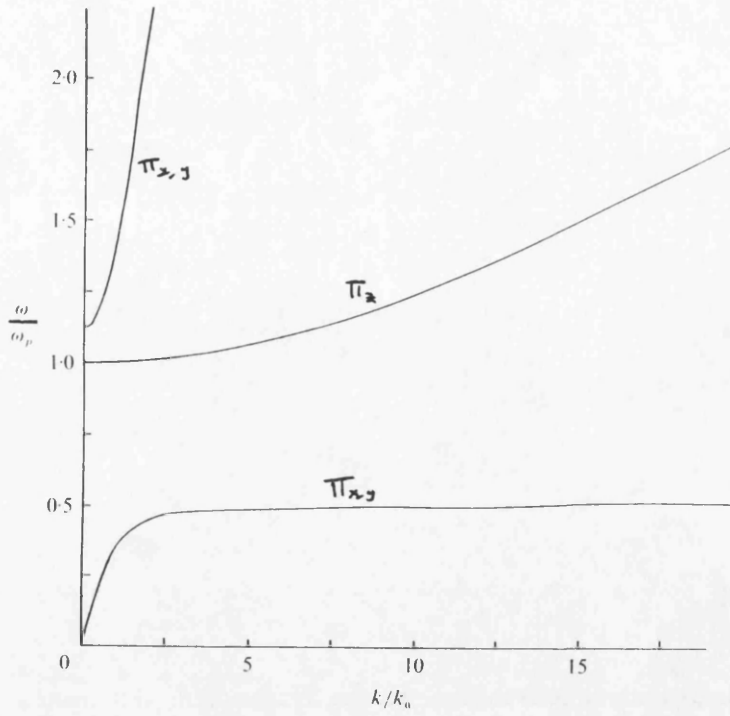


Figure 3.9. Dispersion relation for wave propagation parallel to the field in a warm equal mass plasma. The sound speed is $0.07c$.

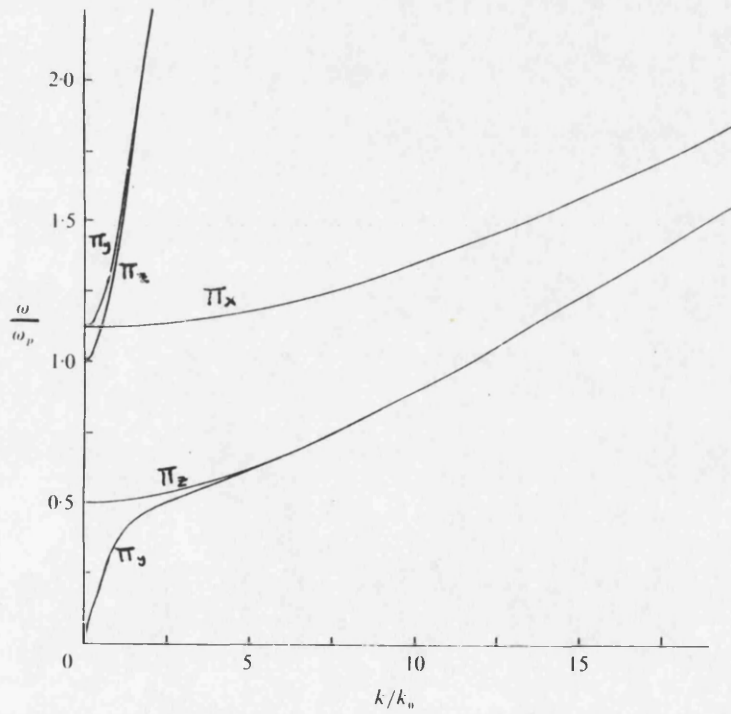


Figure 3.10. Dispersion relation for wave propagation perpendicular to the field in a warm equal mass plasma. The sound speed is $0.07c$.

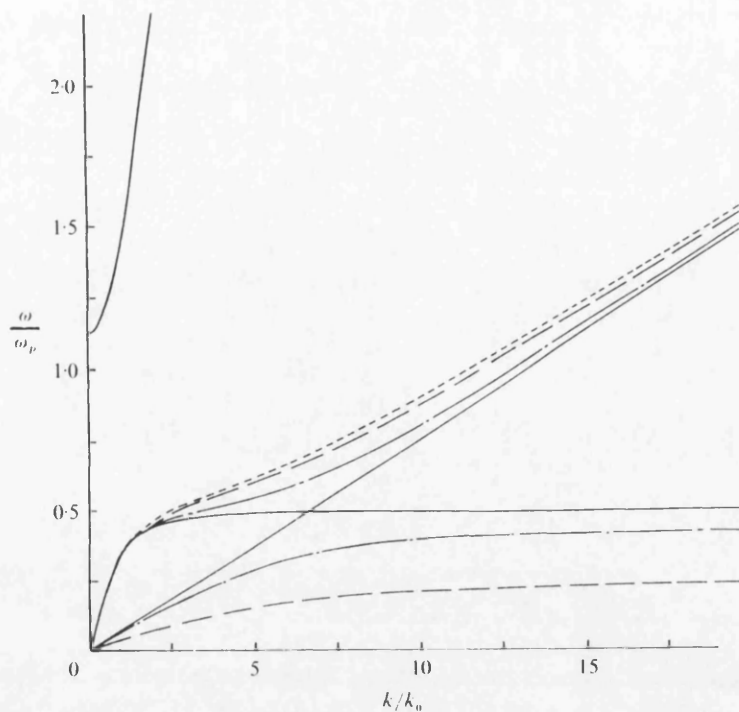


Figure 3.11. Dispersion relation for Π_y waves propagating at various angles to the magnetic field. The sound speed is $0.07c$: —, $\theta = 0$; ---, $\pi/6$; - - -, $\pi/3$; - · - ·, $\pi/2$.

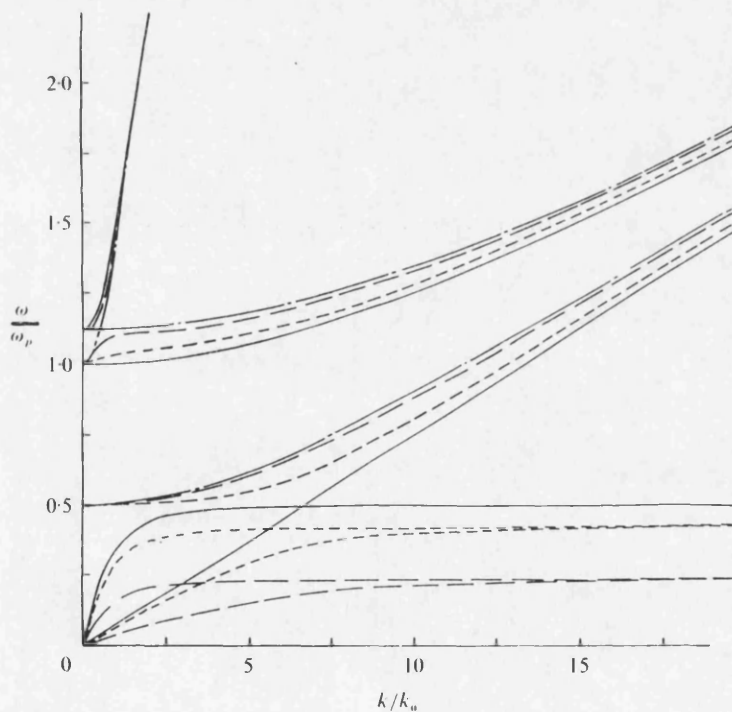


Figure 3.12. Dispersion relation for Π_{xz} waves propagating at various angles to the magnetic field. The sound speed is $0.07c$: —, $\theta = 0$; ---, $\pi/6$; - - -, $\pi/3$; - · - ·, $\pi/2$.

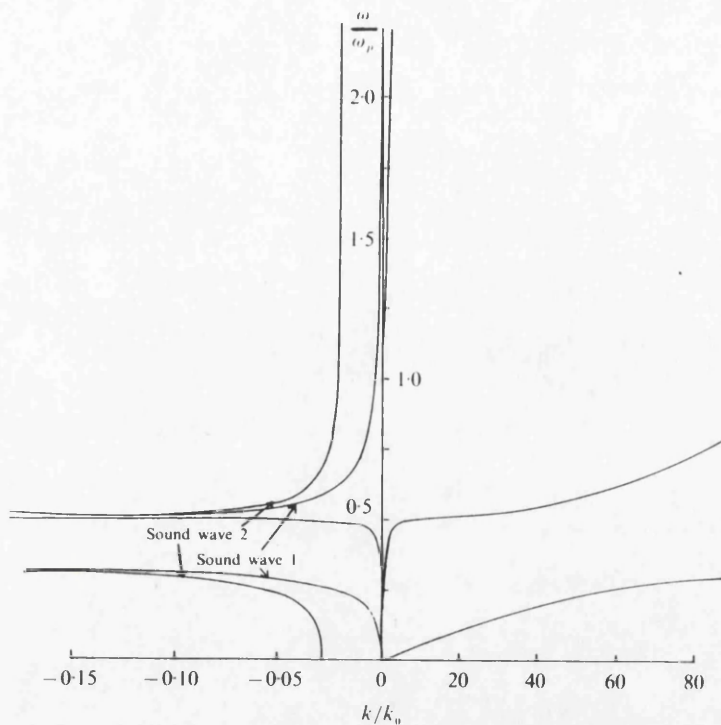


Figure 3.13. Dispersion relation for Π_y waves propagating at 45° to the magnetic field, incorporating the effects of collisions. The sound speed is $0.007c$:

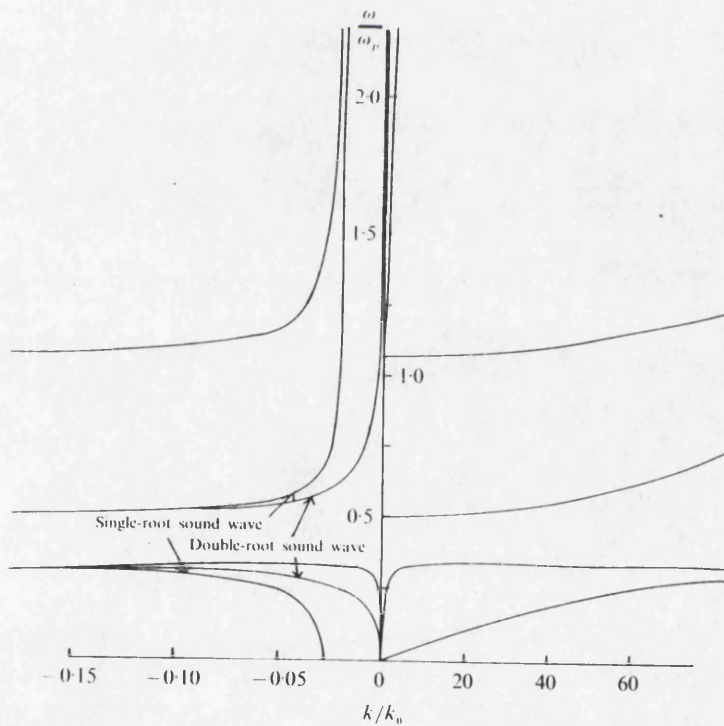


Figure 3.14. Dispersion relation for Π_{xz} waves propagating at 45° to the magnetic field, incorporating the effects of collisions. The sound speed is $0.007c$:

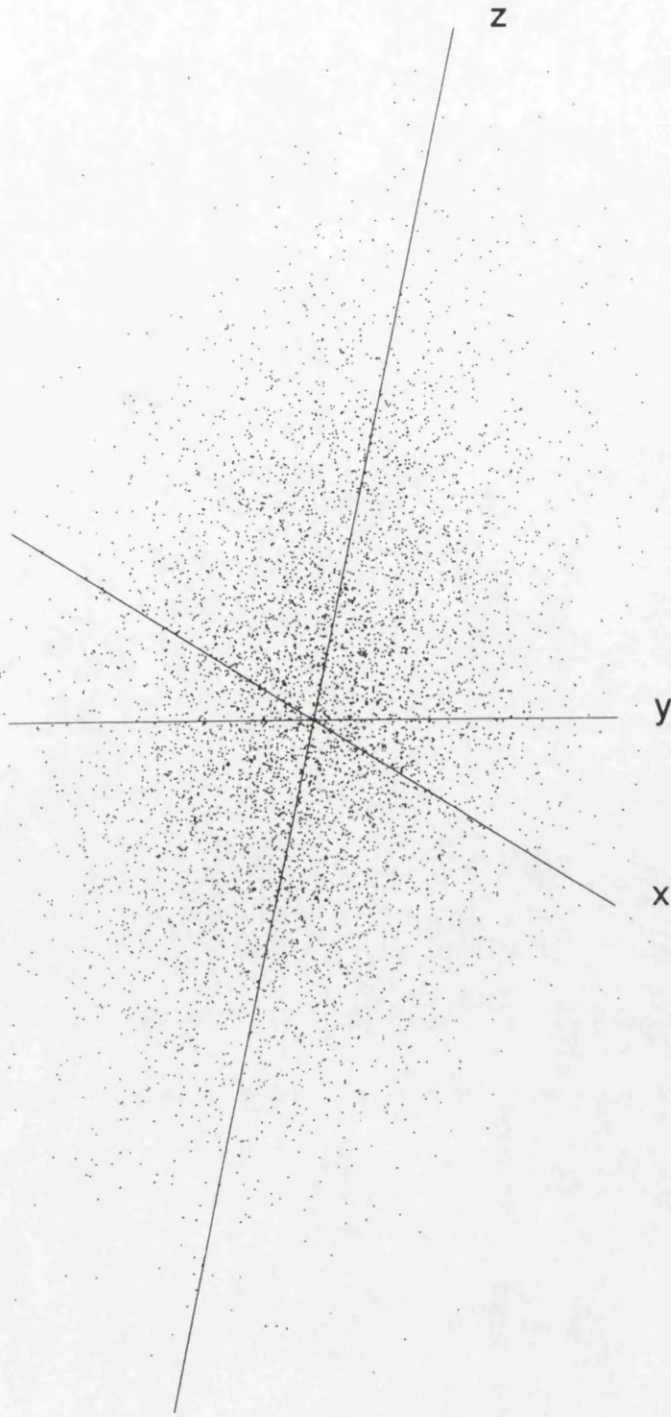


Figure 3.15. A 3-D view of a distribution function satisfying the conditions for equal mass symmetry. Both species have the same distribution - a Maxwellian modified to have different temperatures along the field and across it.

Chapter 4

Linear Waves In Electron-Positron Plasmas

4.1 Introduction

In chapter one it was seen that plasmas of electrons and positrons are of particular interest to the astrophysical community. It is obvious that these will be equal mass plasmas and that consequently some of the results of chapter three will be embodied within these plasmas. However, other physics must be included as well - most obviously we would expect annihilation and creation processes to be going on within the plasma and, if the plasma is to be in equilibrium, that the plasma temperatures will most likely be relativistic.

The extra physics that we shall include will obviously complicate our results. In this respect the results of chapter three will be useful - although they themselves will not be directly applicable to e^+e^- plasmas they will be an important stepping stone in understanding the results we obtain. This is particularly true of the results including annihilation and creation effects, where the algebraic complexity of the equations is considerable. In particular, we might expect that the important result of the disappearance of Faraday rotation and whistler waves will be preserved. Recall from our short review of electron-ion plasmas that this arose from the appearance of nonzero terms in the dielectric tensor (ϵ_{12} & ϵ_{21}) and that the absence of these terms led to an absence of the effect in equal mass plasmas. If these terms are also absent from the e^+e^- plasma dispersion relation then Faraday rotation and whistler waves will not occur. In addition, should the plasma exhibit the symmetry demonstrated throughout chapter three, i.e. a dielectric tensor of the form

$$\begin{pmatrix} \epsilon_{11} & 0 & \epsilon_{13} \\ 0 & \epsilon_{22} & 0 \\ \epsilon_{31} & 0 & \epsilon_{33} \end{pmatrix}, \quad (4.1)$$

then the splitting of waves into two classes, Π_y and Π_{xz} , will still occur (with the attendant simplifications of the solutions - both in algebra and ease of interpretation).

If the plasma temperature is high and the density is diffuse, then annihilation timescales will be far longer than the plasma period and the gyro period - the relevant periods for wave propagation; and this means that from the point of view of wave propagation we can ignore annihilation and creation (this will simplify the equations enormously).

Lightman (1983) gives the annihilation time for electron-positron pair annihilation as

$$t_{ann} \approx \frac{\Gamma^2}{2c\sigma_T n_0 \ln \Gamma}. \quad (4.2)$$

Where Γ is the thermal Lorentz γ factor† (which we will write as Γ to avoid confusion with the ratio of specific heats of an ideal gas) and σ_T is the Thompson cross section. This equation is valid when $\Gamma \gg 1$.

This means that the ratio of the plasma frequency to the annihilation frequency is

$$\frac{\omega_p}{\omega_{ann}} = \sqrt{\frac{2n_0 q^2}{\Gamma m \epsilon_0}} / \frac{c \sigma_T n_0 \ln \Gamma}{\pi \Gamma^2}, \quad (4.3)$$

or

$$\frac{\omega_p}{\omega_{ann}} \approx \frac{10^{22} \Gamma^{3/2}}{\sqrt{n_0} \ln \Gamma}. \quad (4.4)$$

Thus we must satisfy the approximate criterion $n_0 \ll 10^{44}$ to be able to ignore annihilation.

How does this compare to the densities of electrons and positrons in thermal equilibrium? It is quite straightforward to use statistical mechanics to evaluate the equilibrium densities and Chapman (1936) derives the result that the pair density in thermal equilibrium is

$$\begin{aligned} n &= \frac{32\pi c^3 m_e^3}{h^3} T_*^3 \exp(-T_*^{-1}), \\ &= 7 \times 10^{36} T_*^3 \exp(-T_*^{-1}) \end{aligned} \quad (4.5)$$

Where $T_* = kT/m_e c^2$. This means that at $T_* = 1$ the pair density is 8 orders of magnitude smaller than the maximum density allowable for ignoring annihilation. Thus we are well justified in treating wave propagation without considering annihilation. (Note though that strictly speaking equation (4.2) is only correct if $\Gamma \gg 1$, which is clearly not the case when $T_* = 1$. However, it will not be too far from the correct value and given that we have 8 orders of magnitude to spare in density we can still be confident in our result.)

Equation (4.5) assumed a plasma in thermal equilibrium with its radiation field. Such a plasma would emit like a blackbody and, as Lightman (1982) points out, “There exist no objects of astronomical size that have relativistic temperatures and emit like blackbodies — the energy requirements would be prodigious.” Lightman goes on to consider a different class of equilibria, that of ‘effectively thin’ plasmas (which we discussed in chapter one). This finite plasma is optically thin to radiation of pair producing energies – it is not a true thermal equilibrium, the plasma loses energy from escaping radiation, but it is a more realistic model of the electron-positron plasmas

† Defined as the ensemble average of Γ , i.e.

$$\int \frac{f(\mathbf{r}, \mathbf{v}, t)}{\sqrt{1 - \mathbf{v}^2/c^2}} d\mathbf{v}$$

found in nature. These equilibria are controlled (in part) by a seed number of electron-proton pairs, but it is found that it is possible to have equilibria which are mass dominated by electron-positron pairs – thus justifying ignoring the protons in the plasma. And, if the seed density is low enough, then we should be able to satisfy the criterion of equation (4.4).

Even if the models we study prove not to be physically reasonable then when we have more advanced models, containing all the physics required, our understanding of the results will be greatly helped by models which are simpler and easier to interpret. To this end we shall first study waves in an infinite homogeneous electron-positron plasma including relativistic effects but ignoring annihilation. Later we shall consider annihilation and creation, but we will retain our simplistic infinite homogeneous plasma.

Figures

In all the figures for chapter four frequency is normalised to ω_p and wave number to k_0 , where $k_0 = c/\omega_p$.

4.2 Relativistic Electron-Positron Plasmas

To deal fully with relativistic effects, special relativity must be employed. However, to do plasma physics in a 4-vector form is very complicated (a glance at the energy-momentum tensor reveals just how difficult fluids are to deal with, never mind plasma fluids). The main task of relativity is however, to explain the invariance of physics in different reference frames. At the present time we are not interested in doing this; to be able to explain the waves propagating in the plasma frame would be sufficient for our purposes. Therefore, we can stay with a Cartesian frame in 3-dimensions and simply use a modified momentum equation to describe the plasma. This is the momentum equation used by Tajima & Taniuti (1990) and it accounts for relativistic effects by including a Γ factor in the first term of the momentum equation. †

$$\frac{d(\Gamma n_s m_0 \mathbf{v}_s)}{dt} = q n_s [\mathbf{E} + \mathbf{v}_s \times \mathbf{B}] - \frac{\partial P_s}{\partial \mathbf{r}}. \quad (4.6)$$

Dispersion Relation

We now proceed to subject equation (4.6) to the analysis developed in chapter three, i.e. linearisation and Fourier analysis. In linearising the equation we can neglect changes in Γ because the fluid velocity has no zero order component. This gives,

† To see why this is, imagine a box full of gas at a relativistic temperature, and of rest mass M . While the box is stationary the fluid velocity is zero. If we try to move the box with a force F we must impart momentum to relativistic particles, so the effective mass of the box is $M\Gamma$ and the acceleration will be $F/M\Gamma$.

$$i\omega n_0 m_0 \Gamma \mathbf{v}_\pm - i\mathbf{k} P_{1\pm} = n_\pm q_\pm [\mathbf{E} + \mathbf{v}_\pm \times \mathbf{B}_0]. \quad (4.7)$$

Now, as the equation of state of the plasma is the same as in the nonrelativistic warm plasma we can carry the result from the continuity equation across, i.e.

$$n_1 = \frac{n_0 \mathbf{k} \cdot \mathbf{v}}{\omega}. \quad (3.49)$$

Now, again assuming adiabatic changes, $P_1 = \gamma k_B T n_1$ we can write the momentum equation as

$$i\omega \mathbf{v}_\pm = \frac{ia^2}{\omega} \mathbf{k}(\mathbf{k} \cdot \mathbf{v}_\pm) + \frac{q_\pm}{\Gamma m_0} \mathbf{E} + \mathbf{v}_\pm \times \Omega_\pm, \quad (4.8)$$

where we have chosen to define a relativistic sound speed and a synchrotron frequency:

$$a^2 = \frac{\gamma k_B T}{\Gamma m_0} \quad \Omega_\pm = \frac{q_\pm \mathbf{B}_0}{\Gamma m_0}. \quad (4.9)$$

The procedure for solving these sets of linear equations is exactly the same as that employed in chapter three. Again we use Reduce 3.3 to find the solutions, which are of the form,

$$\mathbf{v}_\pm = \frac{q}{\Delta} \begin{pmatrix} v_{11} & \Omega_\pm v_{12} & v_{13} \\ \Omega_\pm v_{21} & v_{22} & \Omega_\pm v_{23} \\ v_{31} & \Omega_\pm v_{32} & v_{33} \end{pmatrix} \cdot \mathbf{E}, \quad (4.10)$$

where

$$\left. \begin{aligned} v_{11} &= ia^2 k^2 \omega \cos^2 \theta - i\omega^3 & v_{12} &= a^2 k^2 \cos^2 \theta - \omega^2 & v_{13} &= -ia^2 k^2 \omega \cos \theta \sin \theta \\ v_{21} &= -a^2 k^2 \cos^2 \theta + \omega^2 & v_{22} &= ia^2 k^2 \omega - i\omega^3 & v_{23} &= a^2 k^2 \cos \theta \sin \theta \\ v_{31} &= -ia^2 k^2 \omega \cos \theta \sin \theta & v_{32} &= -a^2 k^2 \cos \theta \sin \theta & v_{33} &= ia^2 k^2 \omega \sin^2 \theta + i\omega \Omega^2 - \omega^3 \end{aligned} \right\} \quad (4.11)$$

$$\Delta = \Gamma m_0 (\omega^2 (\omega^2 - \Omega^2) + a^2 k^2 (\Omega^2 \cos^2 \theta - \omega^2)). \quad (4.12)$$

Of course we notice immediately the factoring of the four terms in equation (4.10) by Ω_\pm , which means that when we sum over our two species to obtain the current in the plasma we have,

$$\mathbf{j} = n_0 q (\mathbf{v}_+ - \mathbf{v}_-) =$$

$$\frac{i\epsilon_0 \omega}{\Delta'} \begin{pmatrix} a^2 k^2 \cos^2 \theta - \omega^2 & 0 & -a^2 k^2 \cos \theta \sin \theta \\ 0 & a^2 k^2 - \omega^2 & 0 \\ -a^2 k^2 \cos \theta \sin \theta & 0 & a^2 k^2 \sin^2 \theta + \Omega^2 - \omega^2 \end{pmatrix} \cdot \mathbf{E}, \quad (4.13)$$

where

$$\Delta' = \frac{\Delta}{\Gamma \omega^2 m_0}, \quad (4.14)$$

and the plasma frequency of our relativistic plasma has been defined as

$$\omega_p^2 = \frac{2n_0 q^2}{\Gamma m_0 \epsilon_0}. \quad (4.15)$$

Obviously Maxwell's equations are the same for our relativistic plasma, so that the current need only be combined with equation (3.9) to yield the dispersion relation as,

$$\begin{pmatrix} 1 - (\omega^2 - a^2 k^2 \cos^2 \theta) / \Delta' - n^2 \cos^2 \theta & 0 & \cos \theta \sin \theta (n^2 + a^2 k^2 / \Delta') \\ 0 & 1 - (\omega^2 - a^2 k^2) / \Delta' - n^2 & 0 \\ \cos \theta \sin \theta (n^2 - a^2 k^2 / \Delta') & 0 & 1 - (\omega^2 - \Omega^2 a^2 k^2 \sin^2 \theta) / \Delta' - n^2 \sin^2 \theta \end{pmatrix} \cdot \mathbf{E} = 0 \quad (4.16)$$

Most importantly we see the symmetry associated with equal mass plasmas ($\epsilon_{12} = \epsilon_{21} = \epsilon_{23} = \epsilon_{32} = 0$) is maintained – this means the disappearance of Faraday rotation and whistler waves and the splitting of waves into two classes associated with fields E_y and $E_x + E_z$. This result is in accordance with the observations of very low Faraday rotation in extragalactic sources (Jones & O'Dell 1977) where it is believed that electron-positron plasmas might exist (see chapter one).

Dispersion Relation For Waves Π_y

The solutions for waves with an electric field E_y are found by setting $\epsilon_{22} = 0$ in equation (4.16). The dispersion relation for these waves is thus,

$$\frac{k^4 a^2 c^2 (\omega^2 - \Omega^2 \cos^2 \theta) + k^2 \omega^2 (a^2 \Omega^2 \cos^2 \theta - a^2 \omega^2 + a^2 \omega_p^2 + c^2 \Omega^2 - c^2 \omega^2) + \omega^4 (\omega^2 - \Omega^2 - \omega_p^2)}{\omega^2 (k^2 a^2 (\Omega^2 \cos^2 \theta - \omega^2) + \omega^2 (\omega^2 - \Omega^2))} = 0. \quad (4.17)$$

This is not the most transparent of equations, but it is possible to take high and low frequency limits to see what its solutions might be.

At high frequencies we have an approximate dispersion relation,

$$\frac{k^4 a^2 c^2 - k^2 \omega^2 (c^2 + a^2) + \omega^4}{\omega^4 - k^2 a^2 \omega^2} = 0. \quad (4.18)$$

The numerator is a quadratic equation in ω^2 with solutions

$$\omega^2 = k^2 c^2, \quad \omega^2 = k^2 a^2, \quad (4.19)$$

i.e. an electromagnetic wave and a sound wave.

When θ is far from $\pi/2$ the dispersion relation takes the following form at low frequencies,

$$\frac{\omega^4 (\Omega^2 + \omega_p^2) - k^2 \omega^2 (a^2 \Omega^2 \cos^2 \theta + a^2 \omega_p^2 + c^2 \Omega^2) + k^4 a^2 c^2 \Omega^2 \cos^2 \theta}{\omega^2 (k^2 a^2 \Omega^2 \cos^2 \theta - \omega^2 \Omega^2)} = 0. \quad (4.20)$$

Again there is a quadratic numerator in ω^2 so that the solutions are,

$$\omega^2 = \frac{k^2(a^2\Omega^2 \cos^2 \theta + a^2\omega_p^2 + c^2\Omega^2) \pm \sqrt{k^4(a^2\Omega^2 \cos^2 \theta + a^2\omega_p^2 + c^2\Omega^2)^2 - 4k^4a^2c^2\Omega^2(\Omega^2 + \omega_p^2)}}{2(\omega_p^2 + \Omega^2)}. \quad (4.21)$$

Unfortunately the discriminant of this equation does not factor to give a perfect square, *unless* $\cos \theta = 1$. So let us set $\theta = 0$ and continue. In this case the two solutions become,

$$\omega^2 = k^2a^2, \quad \omega^2 = \frac{k^2c^2\Omega^2}{\Omega^2 + \omega_p^2}. \quad (4.22)$$

Of course, the first of these two solutions is a sound wave and is spurious. At $\theta = 0$ $\mathbf{k} \perp \mathbf{v}$ so that no pressure force is produced. The solution appears in this analysis as we neglected the denominator, which would have cancelled out the sound wave solution.

The second solution corresponds to Alfvén waves in a relativistic plasma. To see this, notice that it has the same properties as the nonrelativistic Alfvén wave in a cold plasma (equation (3.29)) in that if the plasma is of low density or high field (such that $\Omega \gg \omega_p$) the dispersion relation is,

$$\omega^2 \approx k^2c^2. \quad (4.23)$$

And if the plasma is of high density or low field (such that $\Omega \ll \omega_p$) we have,

$$\omega^2 \approx \frac{k^2c^2\Omega^2}{\omega_p^2} = \frac{k^2c^2B_0^2\epsilon_0}{2\Gamma m_0 n_0} = v_A^2 k^2, \quad (4.24)$$

where, as before, $v_A^2 = B_0^2/\mu_0\rho_m$ is the squared Alfvén speed, ρ_m being the plasma mass density (now including a relativistic Γ).

If $\theta = \pi/2$ another low frequency analysis can be done. In this case the dispersion relation is,

$$\frac{k^4a^2c^2 + k^2(a^2\omega_p^2 + c^2\Omega^2) - \omega^2(\Omega^2 + \omega_p^2)}{-k^2a^2\omega^2 - \omega^2\Omega^2} = 0, \quad (4.25)$$

so that,

$$\omega^2(\Omega^2 + \omega_p^2) = k^4a^2c^2 + k^2(a^2\omega_p^2 + c^2\Omega^2). \quad (4.26)$$

If we apply a high density/low magnetisation criterion then

$$\omega^2 \approx k^2a^2, \quad (4.27)$$

i.e. a sound wave. Conversely if the high magnetisation/low density condition is applicable then

$$\omega^2 \approx k^2c^2, \quad (4.28)$$

so that an electromagnetic wave exists. Notice that in both cases there is no Alfvén wave.

In figure 4.1 a plot of equation (4.17) is shown for various angles. In this case $\omega_p = 2\Omega$ and $a > v_A$. At high frequencies the electromagnetic wave and the sound wave exist – in accordance with our high frequency analysis. At low frequencies the sound wave also exists in addition to an Alfvén wave, which drops in speed as θ swings round from 0 and disappears at $\pi/2$ (as expected from the low frequency $\pi/2$ analysis).

In figure 4.2 equation (4.17) is plotted, this time for $\Omega = 5\omega_p$. Again, at high frequencies the expected electromagnetic and sound waves exist. At low frequencies the Alfvén wave exhibits the same behaviour as before, (notice at $\theta = 0$ it is practically $\omega^2 = k^2 c^2$ as predicted) dropping to zero at $\theta = \pi/2$. The ‘sound wave’ at low frequencies is seen to have a dispersion relation $\omega^2 \approx k^2 c^2$, again in accordance with our low frequency $\theta = \pi/2$ predictions, but at other angles this relationship also seems to hold. The fact that the sound wave has this curious low frequency dispersion relation reveals the true nature of this low frequency wave to be magnetosonic. Thus, when $a > v_A$ its low frequency dispersion is $\omega^2 \approx k^2 a^2$, however in figure 4.2, where $a < v_A$ its dispersion relation is $\omega^2 \approx k^2 c^2$ – but when $\omega_p \ll \Omega$ then $v_A \approx c$, so that the dispersion relation is really just $\omega^2 \approx k^2 v_A^2$.

Dispersion Relation For Waves Π_{xz}

To find the dispersion relations for waves with fields $E_x + E_z$ we must return to equation (4.16) and set $\epsilon_{11}\epsilon_{33} - \epsilon_{13}\epsilon_{31} = 0$. This gives the unpleasant equation for Π_{xz} waves as

$$\begin{aligned}
& \left[k^6 a^4 c^2 (\omega^4 - 2\Omega^2 \omega^2 \cos^2 \theta + \Omega^4 + \cos^4 \theta) \right. \\
& + k^4 a^2 \left(\omega^6 (-2c^2 - a^2) \right. \\
& + \omega^4 (c^2 \omega_p^2 + 2c^2 \Omega^2 + a^2 \omega_p^2 + 2c^2 \Omega^2 \cos^2 \theta + 2a^2 \Omega^2 \cos^2 \theta) \\
& + \omega^2 (-a^2 \Omega^4 \cos^4 \theta - a^2 \Omega^2 \omega_p^2 \cos^2 \theta - 2c^2 \Omega^4 \cos^2 \theta - 2c^2 \Omega^2 \omega_p^2 \cos^2 \theta) \\
& + 2c^2 \Omega^4 \omega_p^2 \cos^4 \theta) \\
& + k^2 \omega^2 \left(\omega^6 (c^2 + 2a^2) \right. \\
& + \omega^4 (-2a^2 \Omega^2 \cos^2 \theta - 2a^2 \Omega^2 - 3a^2 \omega_p^2 - 2c^2 \Omega^2 - c^2 \omega_p^2) \\
& + \omega^2 (2a^2 \Omega^4 \cos^2 \theta + 2a^2 \Omega^2 \omega_p^2 \cos^2 \theta \\
& + c^2 \Omega^2 \omega_p^2 \cos^2 \theta + 2a^2 \Omega^2 \omega_p^2 + a^2 \omega_p^4 + c^2 \Omega^4 + c^2 \Omega^2 \omega_p^2) \\
& - (a^2 \Omega^4 \omega_p^2 \cos^2 \theta + a^2 \Omega^2 \omega_p^4 \cos^2 \theta + c^2 \Omega^4 \omega_p^2 \cos^2 \theta) \Big) \\
& + \omega^4 \left(-\omega^6 + \omega^4 (2\Omega^2 + 2\omega_p^2) - \omega^2 (\Omega^4 + 3\Omega^2 \omega_p^2 + \omega_p^4) + \Omega^4 \omega_p^2 + \Omega^2 \omega_p^4 \right) \Big] \\
& \div \left(k^4 a^4 \omega^2 (-\omega^4 + 2\Omega^2 \omega^2 \cos^2 \theta - \Omega^4 \cos^4 \theta) \right. \\
& \left. + 2k^2 a^2 \omega^4 (\omega^4 - \Omega^2 \omega^2 (1 + \cos^2 \theta) + \Omega^4 \cos^2 \theta) + \omega^6 (-\omega^4 + 2\Omega^2 \omega^2 - \Omega^4) \right) = 0
\end{aligned} \tag{4.29}$$

It is obvious from (4.29) that even a limiting frequency analysis would not make the solutions of this equation more transparent. However, looking at the dielectric tensor (equation (4.16)), when the wave vector is parallel or perpendicular to the magnetic field ($\theta = 0, \pi/2$) the 2×2 determinant solutions factor into two 1×1 determinants†, i.e. the waves have decoupled into one wave with a field E_x and one with a field E_z rather than two waves both with a combined field. The solutions to the dispersion relation are now just $\epsilon_{11} = 0$ and $\epsilon_{33} = 0$, and it is possible to make a frequency limit analysis of these equations.

Taking propagation parallel to the field first, the equation $\epsilon_{11} = 0$ for waves Π_x is,

$$\frac{k^4 a^2 c^2 (\omega^2 - \Omega^2) + k^2 \omega^2 (a^2 \Omega^2 - a^2 \omega^2 + a^2 \omega_p^2 + c^2 \Omega^2 - c^2 \omega^2) + \omega^4 (\omega^2 - \Omega^2 - \omega_p^2)}{\omega^2 (k^2 a^2 (\Omega^2 - \omega^2) + \omega^2 (\omega^2 - \Omega^2))} = 0. \tag{4.30}$$

This is the same equation as for waves Π_y , (4.17), with θ set to 0. So the results of analysing this equation at high frequencies will be the same, viz. a sound wave and an electromagnetic wave (equation (4.19)), although the sound wave is not a real solution ($\mathbf{k} \perp \mathbf{v}$, again it appears as we ignored the numerator).

At low frequencies we will get the same results as the low frequency analysis at $\theta = 0$ for Π_y waves, equations (4.22), an Alfvén wave and a spurious sound wave.

† This happens because ϵ_{13} and ϵ_{31} are both factored by $\cos \theta \sin \theta$.

Turning to the solutions to $\epsilon_{33} = 0$, at $\theta = 0$ these are very simple,

$$\frac{k^2 a^2 - \omega^2 + \omega_p^2}{k^2 a^2 - \omega^2} = 0, \quad (4.31)$$

with the solution,

$$\omega^2 = \omega_p^2 + k^2 a^2, \quad (4.32)$$

a relativistic Langmuir wave. There are no solutions for $\omega < \omega_p$.

For wave propagation perpendicular to the magnetic field the Π_x dispersion relation is simple,

$$\frac{k^2 a^2 + \Omega^2 - \omega^2 + \omega_p^2}{k^2 a^2 + \Omega^2 - \omega^2} = 0, \quad (4.33)$$

with a solution corresponding to an upper hybrid wave,

$$\omega^2 = k^2 a^2 + \Omega^2 + \omega_p^2. \quad (4.34)$$

The solution for Π_z waves at $\theta = \pi/2$ is,

$$\frac{\omega^4 - \omega^2(\omega_p^2 + \Omega^2 + k^2 a^2 + k^2 c^2) + \Omega^2 \omega_p^2 + k^2(a^2 \omega_p^2 + c^2 \Omega^2) + k^4 a^2 c^2}{\omega^2(\omega^2 - \Omega^2 - k^2 a^2)} = 0. \quad (4.35)$$

At high frequencies a quadratic in ω^2 results,

$$\omega^4 - \omega^2(k^2 a^2 + k^2 c^2) + k^2(a^2 \omega_p^2 + c^2 \Omega^2 + k^2 a^2 c^2) = 0, \quad (4.36)$$

with solutions,

$$\omega^2 = \frac{k^2 c^2 + k^2 a^2 \pm \sqrt{k^4 a^4 + k^4 c^4 - 2k^4 a^2 c^2 - 4k^2 a^2 \omega_p^2 - 4k^2 c^2 \Omega^2}}{2}. \quad (4.37)$$

The discriminant will be a perfect square if we assume (not unreasonably) that at high frequencies the wavelengths of the waves will be very short. This will mean that $k^2 a^2, k^2 c^2 \gg \omega_p^2, \Omega^2$ and then the solutions are just

$$\omega^2 = k^2 c^2, \quad \omega^2 = k^2 a^2, \quad (4.19)$$

an electromagnetic wave and a sound wave (just what we would expect).

At low frequencies the dispersion relation is linear in ω^2 :

$$\omega^2 = \frac{k^2(a^2 \omega_p^2 + c^2 \Omega^2) + \Omega^2 \omega_p^2}{\omega_p^2 + \Omega^2}. \quad (4.38)$$

To proceed further we might wish to assume that the plasma has $\omega_p \gg \Omega$. In this case the dispersion relation is

$$\omega^2 = k^2 a^2 + \Omega^2. \quad (4.39)$$

But this predicts $\omega > \Omega$, in contradiction to our low frequency assumption. Similarly, if we were to assume that $\Omega \gg \omega$ then we have a dispersion relation

$$\omega^2 = k^2 a^2 + \omega_p^2, \quad (4.40)$$

where obviously $\omega > \omega_p$, again in contradiction to the low frequency assumption. However, we might tentatively conclude that the failure of our analysis predicts that there will be no low frequency waves for Π_z at $\theta = \pi/2$. But we will have to return to the full dispersion relation to confirm this.

Figure 4.3 shows the dispersion relation (4.29) plotted when $\omega_p = 2\Omega$ at $\theta = 0$. All the predicted waves are seen to exist: Alfvén, Langmuir, electromagnetic. In figure 4.4 (4.29) is plotted for $\Omega = 5\omega_p$, and again all the expected waves exist.

Figure 4.5 shows (4.29) plotted when $\omega_p = 2\Omega$ at $\theta = \pi/2$. The predicted electromagnetic and sound waves exist at high frequencies, along with the electrostatic upper hybrid wave. However, below Ω no wave exists, as we expected from our low frequency analysis. In figure 4.6 (4.29) is plotted when $\Omega = 5\omega_p$ at $\theta = \pi/2$. The electromagnetic wave exists above ω_p (this is a Π_z wave, plasma motion along the field and so unaffected by it in both cases). The upper hybrid wave is also present, as is the sound wave. Again there are no low frequency waves.

Figure 4.7 shows the dispersion relation for various angles when $\omega_p = 2\Omega$. At high frequencies there is a sound wave, an electromagnetic wave and an electrostatic wave (very similar in form to the warm equal mass plasma of chapter three). At low frequencies there is an Alfvén wave which dies as $\theta \rightarrow \pi/2$ and coupling produces a magnetosonic wave at low frequencies which resonates at the same frequency as the Alfvén wave. In 4.8 the plot is for $\Omega = 5\omega_p$. Essentially the same behaviour is observed as in the previous graph, but notice that between ω_p and Ω the mid angle magnetosonic waves lie close to $\omega = kc$, confirming their nature. (This is similar to the behaviour of the Π_y waves.)

4.3 Annihilation And Creation In Electron-Positron Plasmas

We noted at the start of the chapter that there were situations where it might be possible to ignore annihilation and creation inside the plasma. However, a mixed plasma of particle-anti-particle pairs cannot avoid annihilation for ever, and so it would seem relevant to extend our analysis to include some measure of annihilation and creation effects. Such processes are complex and highly nonlinear, with many reactions needing to be considered. However, for the purposes of wave propagation we should bear a few facts in mind which will enable us to make a simplified analysis. Principally waves will propagate on a fast timescale and as such the long term evolution and equilibrium of

the plasma (see chapter one) need not concern us. Also, as the waves we have been considering are of infinitesimal amplitude, we can linearise all the relevant equations.

Annihilation and creation are expressed mathematically in the continuity equation, so that we might write,

$$\frac{\partial n_{\pm}}{\partial t} + \frac{\partial n_{\pm} \mathbf{v}_{\pm}}{\partial \mathbf{r}} = \nu_C(n_+, n_-) - \nu_A(n_+, n_-), \quad (4.41)$$

where ν_C represents the creation of pairs and ν_A the annihilation. Note that we have allowed for $\nu_{C,A}$ to be functions of the local densities of electrons and positrons. In practice they will also be functions of the local spectrum of photons, but we shall assume that the perturbations in the plasma will be so small that the effect on the local photon spectrum can be ignored. There is no contradiction in assuming the perturbation to affect the electron and positron densities but to be too small to effect the photons if we also assume that the plasma is optically thin to high energy photons. If there is then any disturbance in the photon spectrum, it will be communicated at the speed of light across the whole wave and the perturbation in the spectrum will be at least of second order – and hence ignorable. As we noted at the beginning of this chapter (and in chapter one) electron-positron plasmas might well be expected to be thin to such radiation, so this assumption would be justified.

What exact form should we take for $\nu_{C,A}$? To the lowest order in the fine structure constant, the following processes exist which create pairs,

$$\gamma + \gamma \rightarrow e^+ + e^-, \quad (4.42)$$

$$\gamma + e^{\pm} \rightarrow e^{\pm} + e^+ + e^-, \quad (4.43)$$

$$e^{\pm} + e^{\pm} \rightarrow e^{\pm} + e^{\pm} + e^+ + e^-, \quad (4.44)$$

i.e. pair creation by photon collisions with other photons, photon collisions with electrons or positrons, or electron and positron collisions with electrons or positrons.

Again to the lowest order in the fine structure constant, there is only one annihilation process which is relevant,

$$e^+ + e^- \rightarrow \gamma + \gamma, \quad (4.45)$$

i.e. two body pair annihilation.

What form do these reactions take when linearised? The creation rate ν_C is

$$\nu_C = \nu_{C\gamma\gamma} + \nu_{C\gamma e}(n_+ + n_-) + \nu_{Cee}(n_+ + n_-)(n_+ + n_-). \quad (4.46)$$

$\nu_{C\gamma\gamma}$ is the rate of reaction (4.42) and $\nu_{C\gamma e}$ is the rate of (4.43) (notice it is proportional to the densities) and ν_{Cee} is the rate of (4.44) (proportional to densities squared). When linearised this becomes

$$\begin{aligned}\nu_C = & \nu_{C\gamma\gamma} + \nu_{C\gamma e}(n_{0+} + n_{0-} + n_{1+} + n_{1-}) + \nu_{Cee}(n_{0+}n_{0+} + 2n_{0+}n_{0-} \\ & + n_{0-}n_{0-} + 2(n_{0+}n_{1-} + n_{0+}n_{1+} + n_{0-}n_{1-} + n_{0-}n_{1+})).\end{aligned}\quad (4.47)$$

For the processes of annihilation we write

$$\nu_A = \nu_{A2}n_+n_-, \quad (4.48)$$

where ν_{A2} is the rate of two body annihilation, and then linearise,

$$\nu_A = \nu_{A2}(n_{0+}n_{0-} + n_{0+}n_{1-} + n_{0-}n_{1+}). \quad (4.49)$$

Now we assume that the rates of zero order creation and annihilation balance, so that the net rate of particle creation is

$$\begin{aligned}\nu_{C\gamma e}(n_{1+} + n_{1-}) + 2\nu_{Cee}(n_{0+}n_{1-} + n_{0+}n_{1+} + n_{0-}n_{1-} + n_{0-}n_{1+}) \\ - \nu_{A2}(n_{0+}n_{1-} + n_{0-}n_{1+}).\end{aligned}\quad (4.50)$$

But all the terms we have are linear in $n_{1+} + n_{1-}$, so we can define ν such that

$$\nu_C - \nu_A = -\nu(n_{1+} + n_{1-}). \quad (4.51)$$

In fact it is obvious that no matter which annihilation and creation reactions are considered, once they are linearised they will be factored by $n_{1+} + n_{1-}$ and can be included in the above definition of ν . Thus we can consider a generic continuity equation (albiet with a complex parameter ν) of the form

$$i\omega n_{1\pm} - in_{0\pm}\mathbf{k} \cdot \mathbf{v}_{\pm} = -\nu(n_{1+} + n_{1-}). \quad (4.52)$$

Dispersion Relation

Solving the linearised continuity equation (4.52) gives,

$$n_{1\pm} = \frac{in_{0\pm}\omega\mathbf{k} \cdot \mathbf{v}_{\pm} \pm \nu(n_{0+}\mathbf{k} \cdot \mathbf{v}_+ - n_{0-}\mathbf{k} \cdot \mathbf{v}_-)}{\omega(2\nu + i\omega)}. \quad (4.53)$$

As we wish our results to be applicable to astrophysical situations then it is appropriate to adopt the relativistic model of the plasma momentum equation discussed in §4.2.

$$\frac{d(\Gamma n_s m_0 \mathbf{v}_s)}{dt} = q n_s [\mathbf{E} + \mathbf{v}_s \times \mathbf{B}] - \frac{\partial P_s}{\partial \mathbf{r}}. \quad (4.6)$$

Linearised in the same way as the previous section, this gives

$$i\omega n_0 m_0 \Gamma \mathbf{v}_\pm - i\mathbf{k} P_{1\pm} = n_\pm q_\pm [\mathbf{E} + \mathbf{v}_\pm \times \mathbf{B}_0]. \quad (4.7)$$

We now have to substitute the more complex solution for $n_{1\pm}$ into this equation. Of course, the real problem is the same as occurred in chapter three when we considered a collisional model (§3.6). Instead of two sets of three equations for the plasma species velocities we now have one set of six equations as the solution of the continuity equation involves both \mathbf{v}_+ and \mathbf{v}_- . However, the mathematical techniques have not changed and the extra algebraic difficulties can be overcome again through the use of computer algebra (Reduce 3.3).

The solutions to the velocity equations are long and complex (~30 A4 pages). They do not reveal much information so they are omitted. It is the case however, that the dependence of $v_{x\pm}$ on E_y is factored by Ω , and similarly the dependence of $v_{z\pm}$ on E_y , $v_{y\pm}$ on E_x and $v_{y\pm}$ on E_z are also factored by Ω . This means that both the conductivity tensor and the dielectric tensor have the same form as was found throughout chapter three, and that Faraday rotation disappears and the waves will split into two classes of solution. The dielectric tensor is

$$\epsilon = \begin{pmatrix} \epsilon_{11} & 0 & \epsilon_{13} \\ 0 & \epsilon_{22} & 0 \\ \epsilon_{31} & 0 & \epsilon_{33} \end{pmatrix} \cdot \mathbf{E}, \quad (4.54)$$

where the nonzero components are,

$$\begin{aligned} \epsilon_{11} = & 1 - [k^4 a^4 \omega_p^2 \cos^2 \theta (\omega^5 - 6i\nu\omega^4 - \omega^3(12\nu^2 + \Omega^2 \cos^2 \theta) \\ & + i\nu\omega^2(8\nu^2 + 6\Omega^2 \cos^2 \theta) + 12\nu^2\Omega^2\omega \cos^2 \theta - 8i\nu^3\Omega^2 \cos^2 \theta) \\ & + k^2 a^2 \omega_p^2 \omega (-\omega^6(1 + \cos^2 \theta) + i\nu\omega^5(6 + 8\cos^2 \theta) + \omega^4(12\nu^2 + 2\Omega^2 \cos^2 \theta) \\ & + 24\nu^2 \cos^2 \theta) - i\nu\omega^3 \cos^2 \theta(14\Omega^2 + 32\nu^2) - \nu^2\omega^2 \cos^2 \theta(36\Omega^2 + 16\nu^2) \\ & + 40i\nu^3\Omega^2\omega \cos^2 \theta + 16\nu^2\Omega^2 \cos^2 \theta) \\ & + \omega_p^2 \omega^3 (\omega^6 - 8i\nu\omega^5 - \omega^4(\Omega^2 + 24\nu^2) + i\nu\omega^3(8\Omega^2 + 32\nu^3) + \nu^2\omega^2(24\Omega^2 + 16\nu^2) \\ & - 32i\nu^3\Omega^4\omega - 16\nu^4\Omega^2)] \div \Xi - n^2 \cos^2 \theta \end{aligned} \quad (4.55)$$

$$\begin{aligned}
\epsilon_{22} = & 1 - [k^4 a^4 \omega_p^2 (\omega^5 - 6i\nu\omega^4 - \omega^3(\Omega^2 \cos^2 \theta + 12\nu^2) \\
& + i\nu\omega^2(6\Omega^2 \cos^2 \theta + 8\nu^2) + 12\nu^2\Omega^2\omega \cos^2 \theta - 8i\nu^3\Omega^2 \cos^2 \theta) \\
& + k^2 a^2 \omega_p^2 \omega (-2\omega^6 + 14i\nu\omega^5 + \omega^4(\Omega^2 + \Omega^2 \cos^2 \theta + 36\nu^2) - i\nu\omega^3(6\Omega^2 + 8\Omega^2 \cos^2 \theta + 40\nu^2) \\
& - \nu^2\omega^2(12\Omega^2 + 24\Omega^2 \cos^2 \theta + 16\nu^2) + i\nu^3\omega(8\Omega^2 + 32\Omega^2 \cos^2 \theta) + 16\nu^4\Omega^2 \cos^2 \theta) + \\
& \omega_p^2 \omega^3 (\omega^6 - 8i\nu\omega^5 - \omega^4(\Omega^2 + 24\nu^2) + i\nu\omega^3(8\Omega^2 + 32\nu^2) + \nu^2\omega^2(24\Omega^2 + 16\nu^2) \\
& - 32i\nu^3\Omega^2\omega - 16\nu^4\Omega^2)] \div \Xi - n^2
\end{aligned} \tag{4.56}$$

$$\begin{aligned}
\epsilon_{33} = & 1 - [k^4 a^4 \omega_p^2 (\omega^5 \sin^2 \theta - 6i\nu\omega^4 \sin^2 \theta + \omega^3(\Omega^2 \cos^2 \theta + \Omega^2 \cos^4 \theta - 12\nu^2 \sin^2 \theta) \\
& + i\nu\omega^2(8\nu^2 \sin^2 \theta + 6\Omega^2 \cos^2 \theta + 6\Omega^2 \cos^4 \theta) + 12\nu^2\Omega^2\omega \cos^2 \theta \sin^2 \theta - 8i\nu^3\Omega^2 \cos^2 \theta \sin^2 \theta \\
& + k^2 a^2 \omega_p^2 (\omega^7 (\cos^2 \theta - 2) + i\nu\omega^6 (14 - 8 \cos^2 \theta) + \omega^5 (2\Omega^2 + 36\nu^2 - 24\nu^2 \cos^2 \theta) \\
& + i\nu\omega^4 (2\Omega^2 \cos^2 \theta - 14\Omega^2 + 32\nu^2 \cos^2 \theta + \omega^3 (12\nu^2\Omega^2 \cos^2 \theta - 36\nu^2\Omega^2 \\
& - \Omega^4 \cos^2 \theta - 16\nu^4 \sin^2 \theta) + i\nu\omega^2 (40\nu^2\Omega^2 + 6\Omega^4 \cos^2 \theta - 24\nu^2\Omega^2 \cos^2 \theta) \\
& + \nu^2\Omega^2\omega (16\nu^2 \sin^2 \theta + 12\Omega^2 \cos^2 \theta) - 8i\nu^3\Omega^4 \cos^2 \theta)] \div \Xi - n^2 \sin^2 \theta
\end{aligned} \tag{4.57}$$

$$\begin{aligned}
\epsilon_{13} = \epsilon_{31} = & \cos \theta \sin \theta ([k^4 a^4 \omega_p^2 (-\omega^5 + 6i\nu\omega^4 \\
& + \omega^3(12\nu^2 + \Omega^2 \cos^2 \theta) - i\nu\omega^2(8\nu^2 + 6\Omega^2 \cos^2 \theta) - 12\nu^2\Omega^2\omega \cos^2 \theta \\
& + 8i\nu^3\Omega^2 \cos^2 \theta) + k^2 a^2 \omega_p^2 (\omega^6 - 8i\nu\omega^5 - \omega^4(\Omega^2 + 24\nu^2) + i\nu\omega^3(8\Omega^2 + 32\nu^2) \\
& + \nu^2\omega^2(24\Omega^2 + 16\nu^2) - 32i\nu^3\Omega^2\omega - 16\nu^4\Omega^2)] \div \Xi + n^2)
\end{aligned} \tag{4.58}$$

Where the factor Ξ is equal to

$$\begin{aligned}
\Xi = & k^4 a^4 [\omega^7 - 6i\nu\omega^6 - \omega^5(12\nu^2 + 2\Omega^2 \cos^2 \theta) + i\nu\omega^4(12\Omega^2 \cos^2 \theta + 8\nu^2) \\
& + \omega^2 \cos^2 \theta(24\nu^2\Omega^2 + \Omega^2 \cos^2 \theta) - i\nu\Omega^2\omega^2 \cos^2 \theta(16\nu^2 + 6\Omega^2 \cos^2 \theta) \\
& - 12\nu^2\Omega^4\omega \cos^4 \theta + 8i\nu^3\Omega^4 \cos^4 \theta] + 2k^2 a^2 \omega [-\omega^8 + 7i\nu\omega^7 + \omega^6(\Omega^2 + \Omega^2 \cos^2 \theta + 18\nu^2) \\
& - i\nu\omega^5(7\Omega^2 + 7\Omega^2 \cos^2 \theta + 20\nu^2) - \omega^4(\Omega^4 \cos^2 \theta + 18\nu^2\Omega^2 + 18\nu^2\Omega^2 \cos^2 \theta + 8\nu^4) \\
& + i\nu\omega^3(7\Omega^4 \cos^2 \theta + 20\nu^2\Omega^2 + 20\nu^2\Omega^2 \cos^2 \theta) + \nu^2\Omega^2\omega^2(18\Omega^2 \cos^2 \theta + 8\nu^2 \cos^2 \theta + 8\nu^2) \\
& + \omega^3[\omega^8 - 8i\nu\omega^7 - \omega^6(2\Omega^2 + 24\nu^2) + i\nu\omega^5(16\Omega^2 + 32\nu^2) + \omega^4(\Omega^4 + 48\nu^2\Omega^2 + 16\nu^4) \\
& - i\nu\Omega^2\omega^3(8\Omega^2 + 64\nu^2) - \nu^2\Omega^2\omega^2(24\Omega^2 + 32\nu^2) + 32i\nu^3\Omega^4\omega + 16\nu^4\Omega^4]
\end{aligned} \tag{4.59}$$

This dispersion relation is the most complex studied so far; clearly it is impossible to attempt to gain algebraic insight into the behaviour of the equations as they stand. Even a limiting frequency analysis is not a great deal of use – either all the information about damping is lost and we are left with results similar to those in §6.2 or a slightly simplified, but still intractable equation, is derived and still no algebraic insight is possible. Clearly we should now proceed graphically and

attempt to interpret the plots of the dispersion relations.

Solutions For Waves Π_y

In figure 4.9 the dispersion relation is plotted corresponding to the solution $\epsilon_{22} = 0$. In this case $\omega_p = 2\Omega = 2\nu$ and $\theta = \pi/4$ †. $\Re(k)$ is plotted on the left of the y -axis, $\Im(k)$ to the right. The real part of the solutions accord with the waves which we found when we studied relativistic effects without annihilation: the electromagnetic wave, sound wave, magnetosonic wave and Alfvén wave are all present. However, there is one additional solution – at low frequencies there is a wave which has a dispersion curve close to the sound wave and resonates at the same frequency as the Alfvén wave. Above the synchrotron frequency the new solution appears again, becoming rather like the sound wave in character at high frequencies. An important point to make is that this wave is (in both cases) *essentially undamped*. The Alfvén wave and sound wave are heavily damped. This is because they involve the density perturbations which cause annihilation and creation – and this absorbs energy from the wave. The new solutions cannot involve significant density perturbations as their damping is of the order of 10^{-17} (i.e. $\Im(k)/\Re(k) = O(10^{-17})$). This is to be compared with the Alfvén wave or the sound wave: $\Im(k)/\Re(k) = O(10^{-1})$ and with the electromagnetic wave: $\Im(k)/\Re(k) = O(10^{-3})$. This wave would appear to be something of a problem to understand. It would seem at first that it must involve no density perturbations – otherwise it would be damped. But the fact that at high frequencies it has a sound wave dispersion seems to indicate that it must have density perturbations associated with its propagation. However, it is possible to have a density perturbation without damping if we look at the form of the continuity equation (4.52). It is linear in $n_+ + n_-$, so that if the perturbations in n_+ and n_- are *out of phase* then no annihilation will occur – hence the wave will remain undamped. One thing which remains to be investigated is whether this wave is physical or not.

The damping is shown on a larger scale in figure 4.10, the damping of each wave being identified. In figure 4.11 the dispersion relation for Π_y waves is plotted for $\omega_p = \nu = \Omega/4$, again at $\theta = \pi/4$. All of the waves found in §6.2 exist again, and have the same behaviour in $\Re(k)$. The new solution is also present, with the same cut off, resonance and high frequency behaviour as before, and the damping is still negligible.

Solutions For Waves Π_{xz}

The solutions for the second class of waves, corresponding to fields $E_x + E_z$ and found from $\epsilon_{11}\epsilon_{33} - \epsilon_{13}\epsilon_{31} = 0$, is shown in figure 4.12. Here $\omega_p = 2\Omega = 2\nu$ and $\theta = \pi/4$. Once again the

† This is almost certainly an unrealistically high damping rate. It is chosen, not for realism, but to give a general understanding of the behaviour of the equations under study. It is much easier to interpret the graphs if the damping is high.

solutions found when damping was not considered correspond to the $\Re(k)$ dispersion relations for the sound wave, the magnetosonic wave, the Alfvén wave, the electromagnetic wave and the electrostatic wave. However, the dispersion relation is 5th order in k^2 and two new solutions arise. At low frequencies one of the new solutions is a second root to the sound wave. The other has a dispersion curve above that of both the sound wave and the Alfvén wave. This wave is almost undamped ($\Im(k)/\Re(k) = O(10^{-15})$) as is the Alfvén wave ($\Im(k)/\Re(k) = O(10^{-14})$). The sound wave is strongly damped ($\Im(k)/\Re(k) = O(1)$), revealing that it is associated with a strong *in phase* density perturbation. At high frequencies the new solutions reveal themselves as a continued double root to the sound wave and another solution which closely follows the sound wave dispersion curve. The electromagnetic and electrostatic waves are lightly damped as is the new solution close to the sound wave (all have $\Im(k)/\Re(k) = O(10^{-14})$). The sound wave is heavily damped ($\Im(k)/\Re(k) = O(10^{-1})$).

In figure 4.13 the dispersion relation is plotted for $\omega_p = \nu = \Omega/4$, $\theta = \pi/4$. Again similar waves exist to those found in the previous figure. The double root magnetosonic wave still exists at low frequencies, and is heavily damped throughout ($\Im(k)/\Re(k) = O(1)$). The Alfvén wave and the other new solution also exist here and they are very lightly damped ($\Im(k)/\Re(k) = O(10^{-14})$). At high frequencies the electromagnetic wave is lightly damped ($\Im(k)/\Re(k) = O(10^{-14})$), as is the electrostatic wave ($\Im(k)/\Re(k) = O(10^{-11})$). Also lightly damped is the new partner wave to the sound wave ($\Im(k)/\Re(k) = O(10^{-11})$), but the double root sound wave itself is heavily damped ($\Im(k)/\Re(k) = O(10^{-1})$).

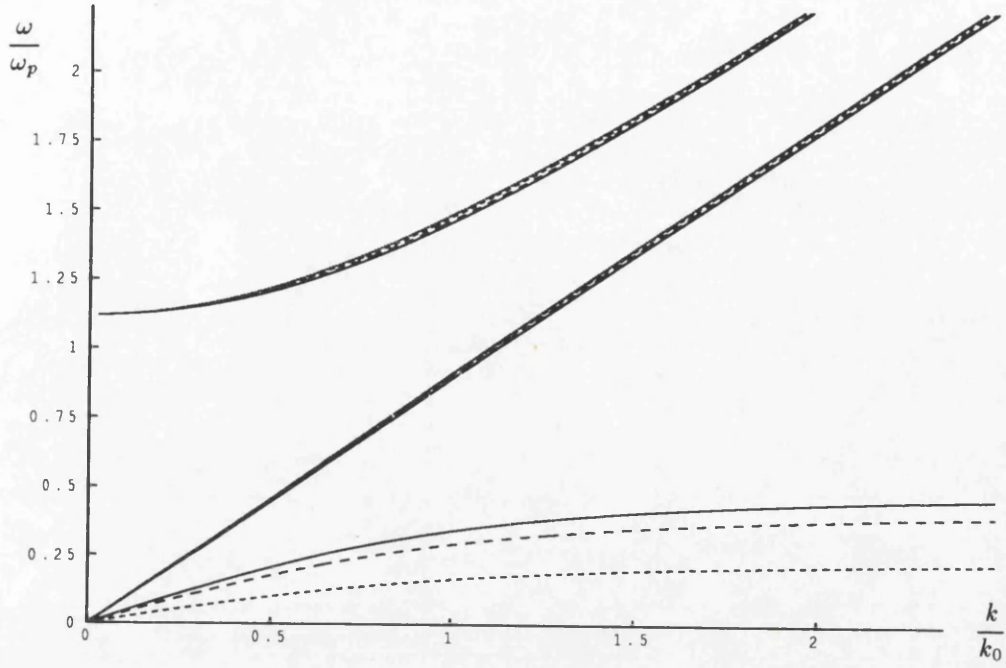


Figure 4.1. Dispersion relation of Π_y waves in an e^+e^- plasma, $\Gamma = 10$ and $\omega_p = 2\Omega$:
 —, $\theta = 0$; ---, $\pi/6$; ·····, $\pi/3$; — · — ·, $\pi/2$.

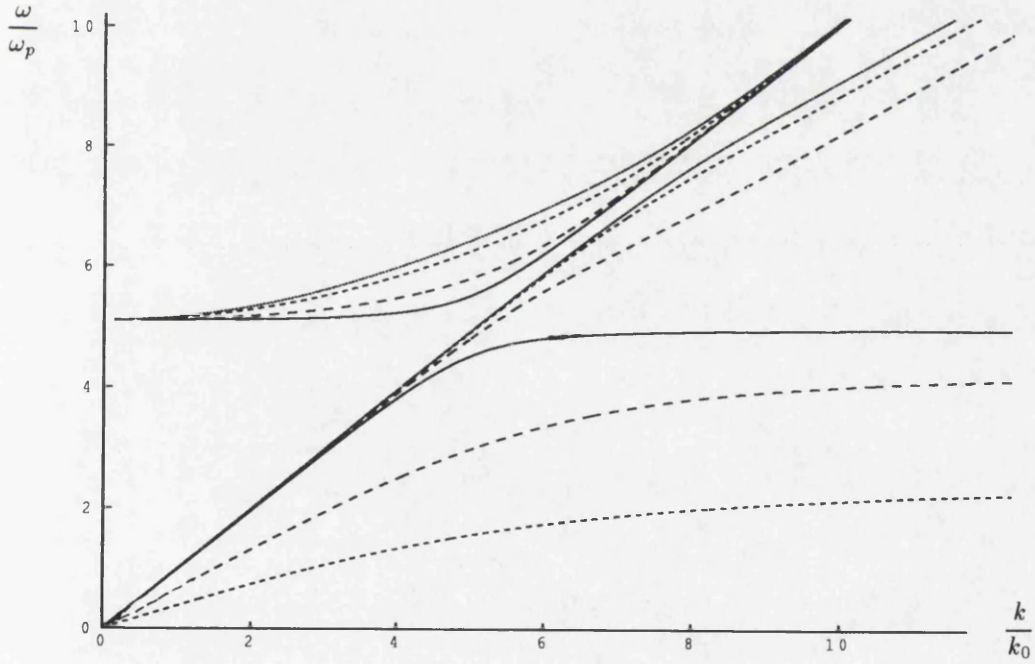


Figure 4.2. Dispersion relation of Π_y waves in an e^+e^- plasma, $\Gamma = 3$ and $5\omega_p = \Omega$:
 —, $\theta = 0$; ---, $\pi/6$; ·····, $\pi/3$; — · — ·, $\pi/2$.

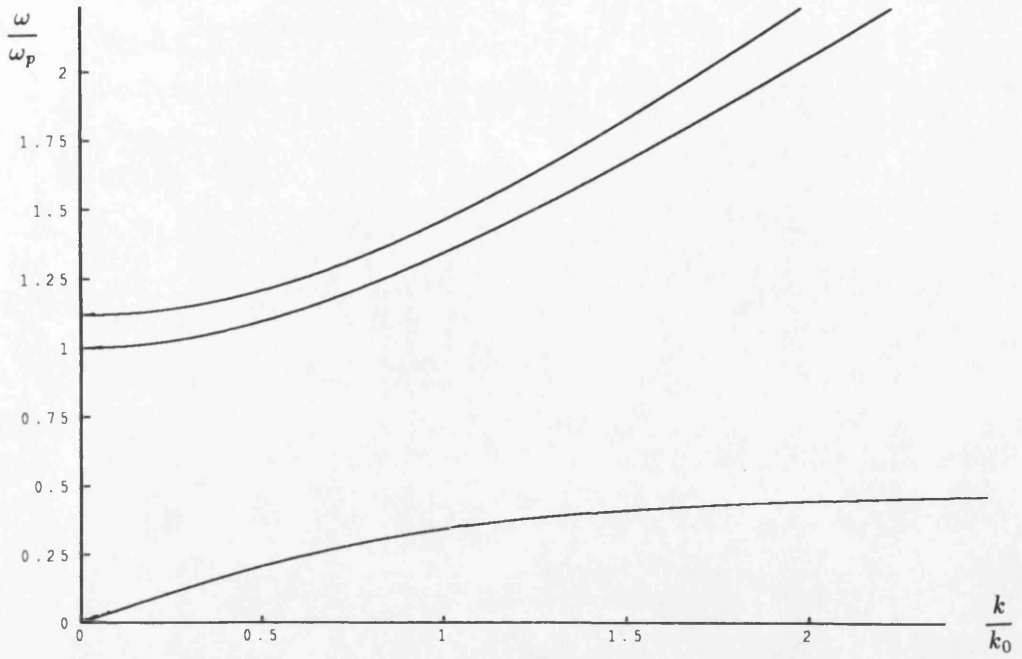


Figure 4.3. Dispersion relation of Π_{xz} waves parallel to the magnetic field in an e^+e^- plasma, $\Gamma = 10$ and $\omega_p = 2\Omega$.

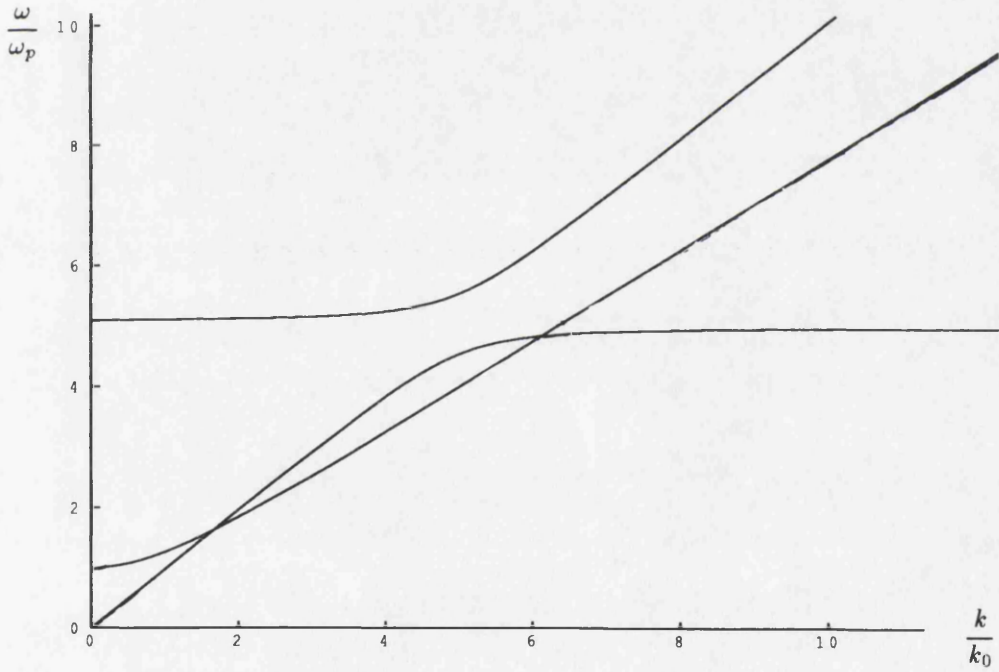


Figure 4.4. Dispersion relation of Π_{xz} waves parallel to the magnetic field in an e^+e^- plasma, $\Gamma = 3$ and $5\omega_p = \Omega$.

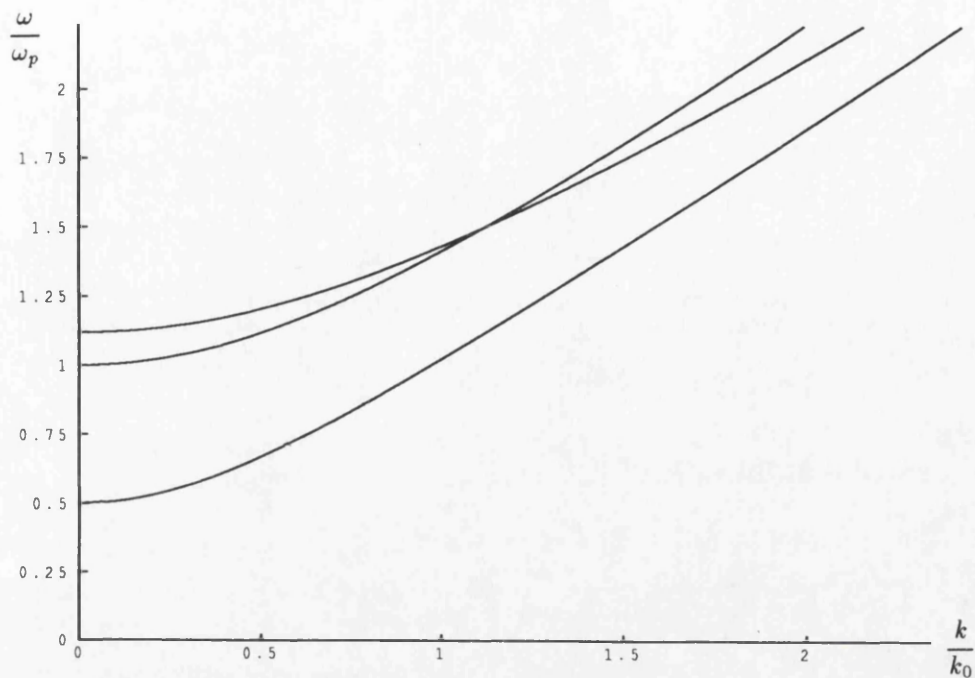


Figure 4.5. Dispersion relation of Π_{xz} waves perpendicular to the magnetic field in an e^+e^- plasma, $\Gamma = 10$ and $\omega_p = 2\Omega$.

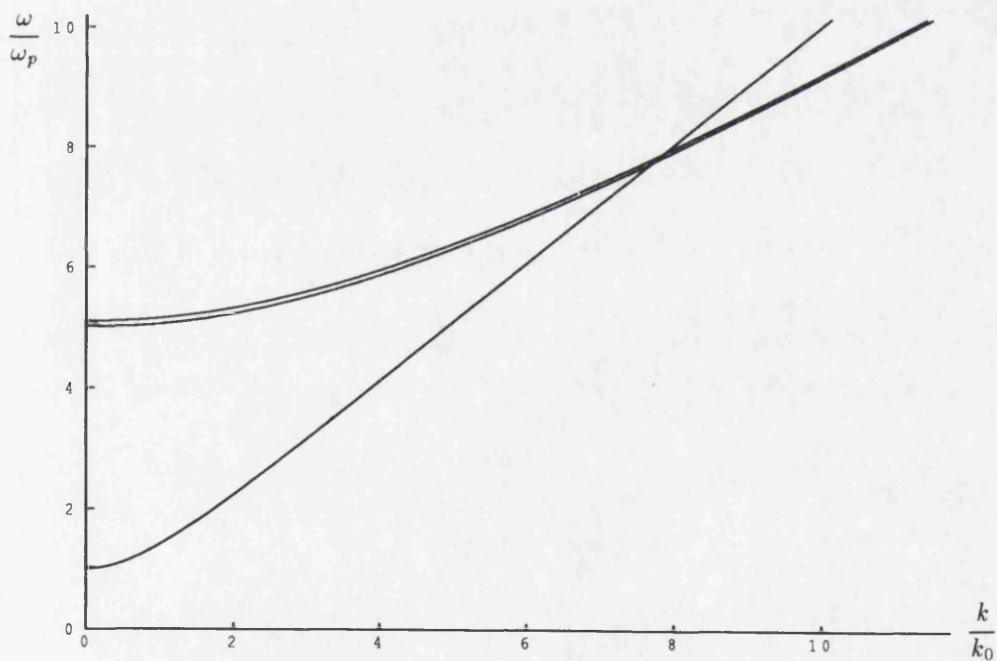


Figure 4.6. Dispersion relation of Π_{xz} waves perpendicular to the magnetic field in an e^+e^- plasma, $\Gamma = 3$ and $5\omega_p = \Omega$.

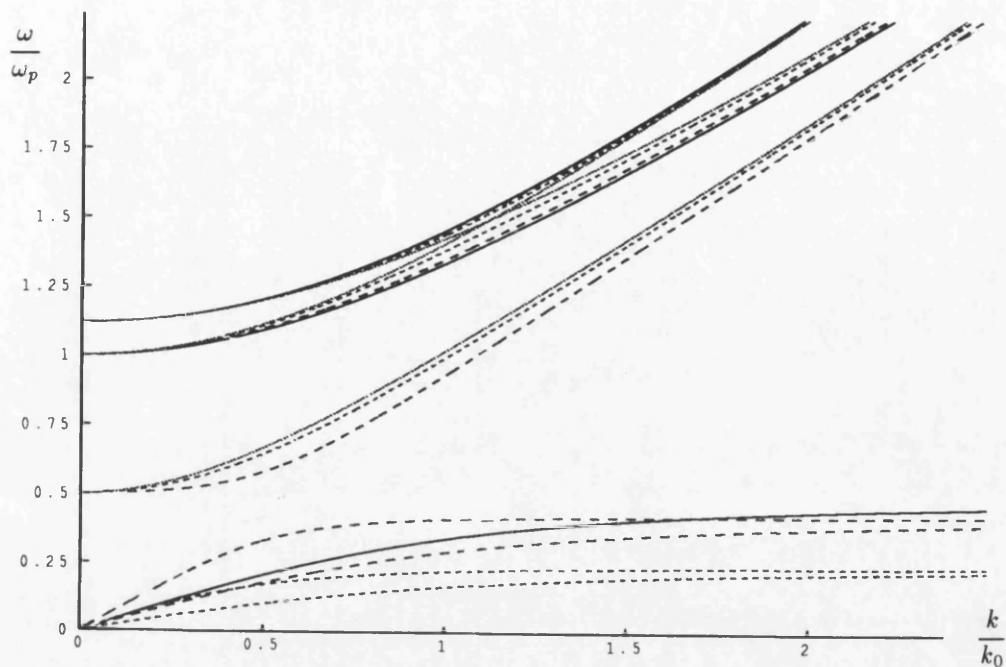


Figure 4.7. Dispersion relation of Π_{xz} waves at various angles in an e^+e^- plasma, $\beta = 10$ and $\omega_p = 2\Omega$: —, $\theta = 0$; ---, $\pi/6$; - · - · -, $\pi/3$; · · · · ·, $\pi/2$.

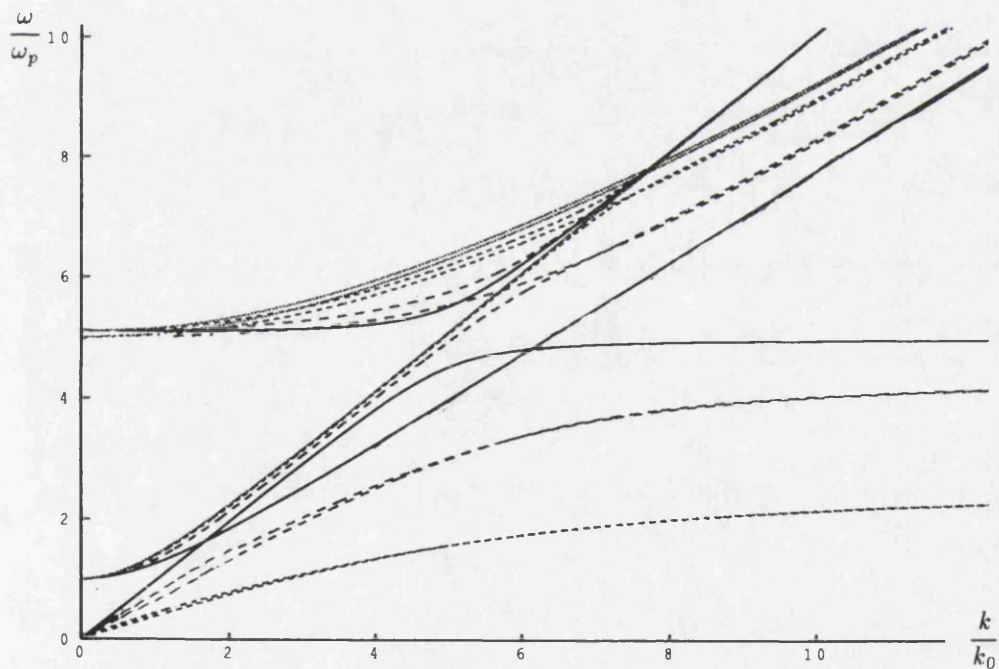


Figure 4.8. Dispersion relation of Π_{xz} waves at various angles in an e^+e^- plasma, $\beta = 3$ and $5\omega_p = \Omega$: —, $\theta = 0$; ---, $\pi/6$; - · - · -, $\pi/3$; · · · · ·, $\pi/2$.

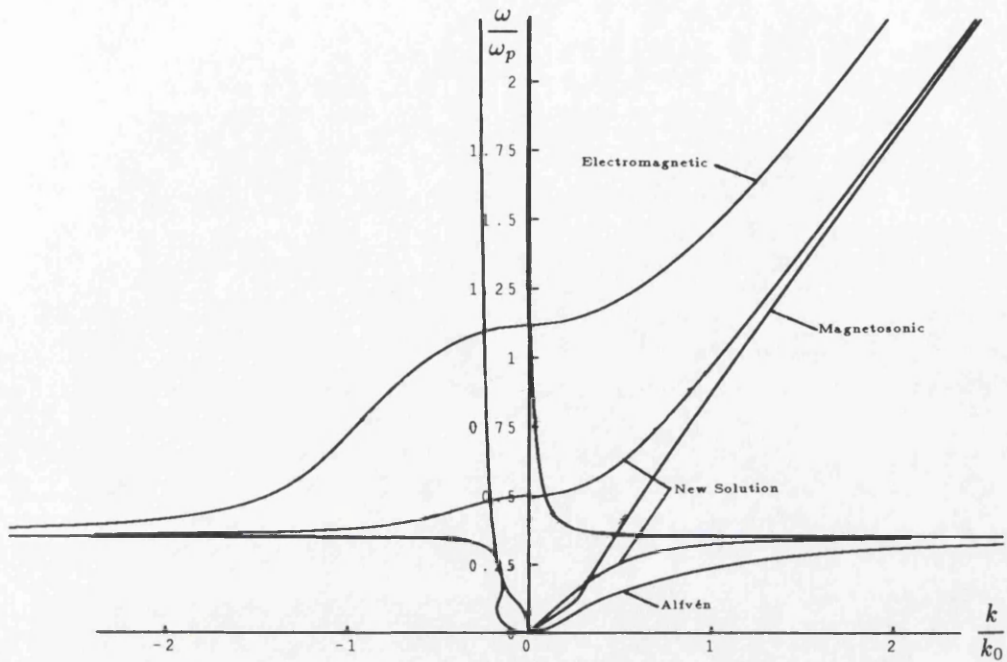


Figure 4.9. Dispersion relation of Π_y waves at $\theta = 45^\circ$ to the field in an e^+e^- plasma with annihilation, $\Gamma = 10$ and $\omega_p = 2\nu = 2\Omega$.

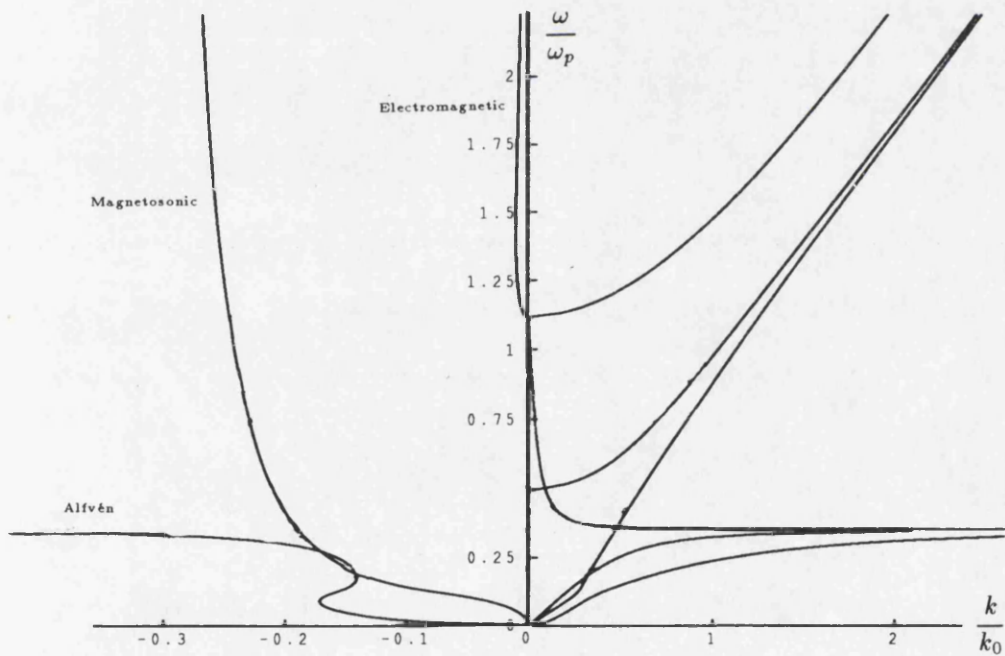


Figure 4.10. Dispersion relation of Π_y waves at $\theta = 45^\circ$ to the field in an e^+e^- plasma with annihilation, $\Gamma = 10$ and $\omega_p = 2\nu = 2\Omega$. The scale on the left of the k axis has been expanded.

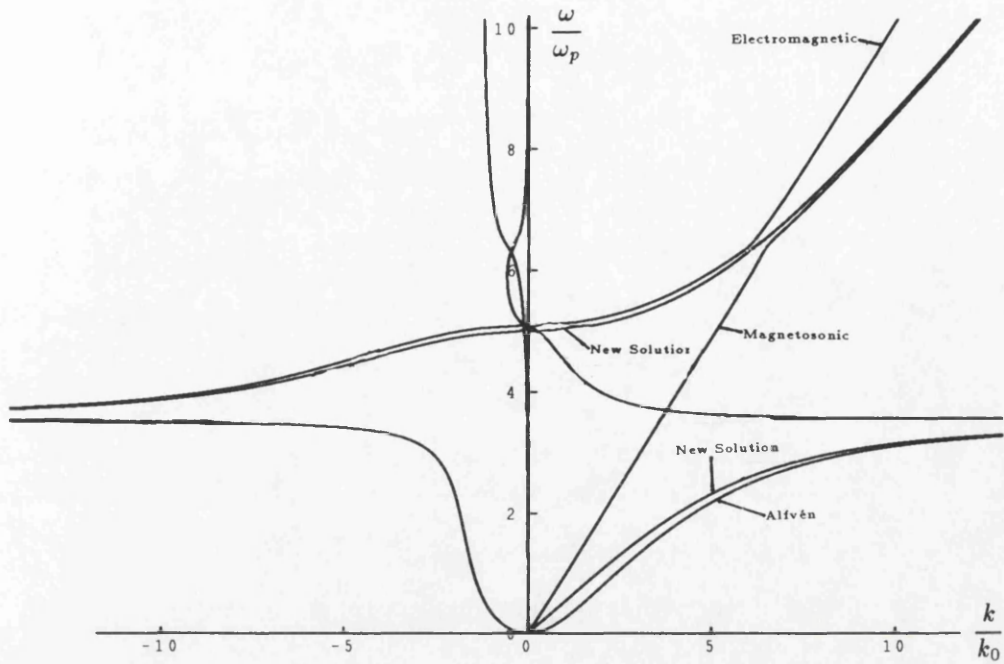


Figure 4.11. Dispersion relation of Π_y waves at $\theta = 45^\circ$ to the field in an e^+e^- plasma with annihilation, $\Gamma = 3$ and $5\omega_p = 5\nu = \Omega$.

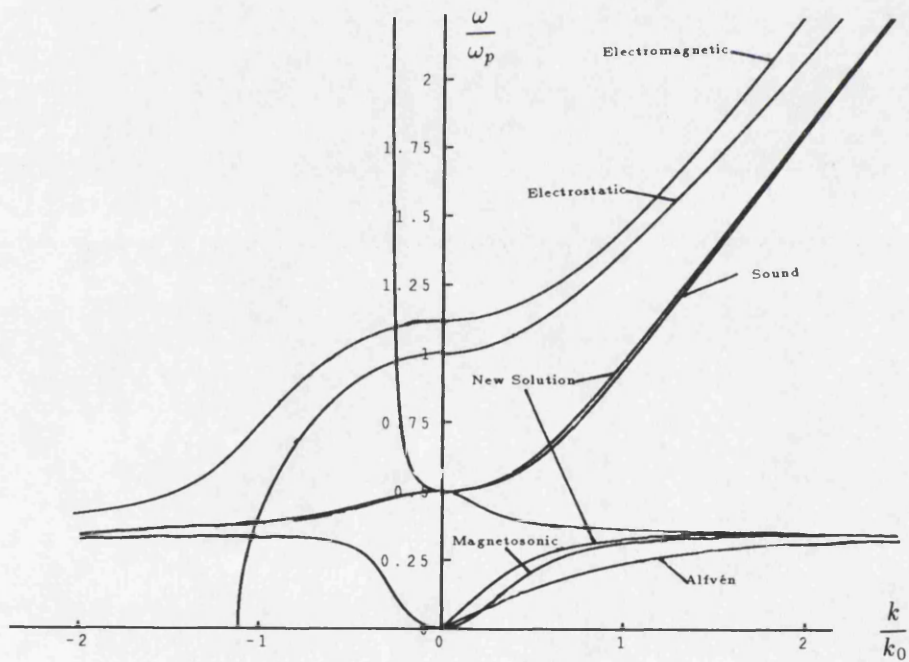


Figure 4.12. Dispersion relation of Π_{xz} waves at $\theta = 45^\circ$ to the field in an e^+e^- plasma with annihilation, $\Gamma = 10$ and $\omega_p = 2\nu = 2\Omega$.

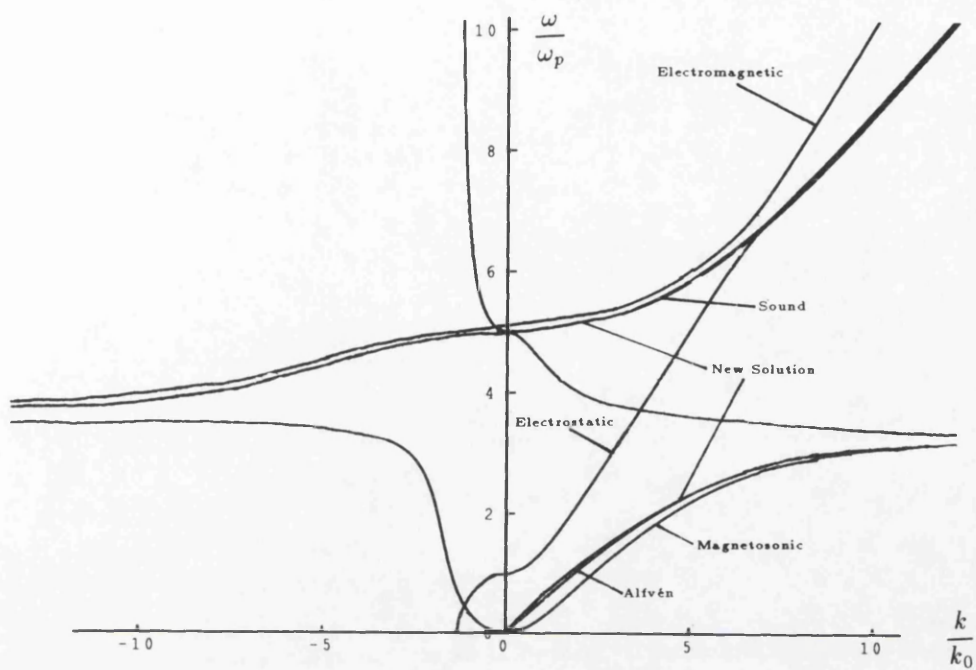


Figure 4.13. Dispersion relation of Π_{xz} waves at $\theta = 45^\circ$ to the field in an e^+e^- plasma with annihilation, $\Gamma = 3$ and $2\omega_p = 2\nu = \Omega$.

While natural science up to the end of the last century was predominantly *collecting* science, a science of finished things, in our century it is essentially a *classifying* science, a science of processes, of the origin and development of these things and of the interconnection which binds all these processes into one great whole.

Fredrich Engels, *Thesis on Feuerbach*

Chapter 5

Nonlinear Waves In Equal Mass Plasmas

5.1 Nonlinear Physics

Over the past 15 years there has been a paradigm change in our understanding of the natural world. In all scientific disciplines – chemistry, biology, mathematics and physics – new ideas about nonlinear systems have come to the fore and are playing a key role in understanding nature. These ideas (loosely grouped under the flag of ‘chaos’, but more accurately termed nonlinear dynamics) are concerned with understanding the behaviour of nonlinear systems – the type of systems of which the real world is primarily composed.

The simplest of nonlinear systems are now known to exhibit fantastically complex behaviour and, most importantly, given the initial conditions of the system, we will not be able to predict its motion for all time, so sensitive is it to these conditions. However, the fact that simple systems with low degrees of freedom (e.g. the ‘standard map’, $x_{n+1} = 4\lambda x_n(1 - x_n)$; (Feignbaum 1980, May 1976) or the Hénon Attractor; (Hénon 1976)) exhibit complex behaviours means that perhaps systems with complex observed behaviours are actually controlled by essentially simple systems of equations (or at least their qualitative behaviour can be modeled by a much simplified system, e.g. Lorenz’s (Lorenz 1963) famous ‘butterfly’ attractor which reproduces the complex behaviour of weather systems after a seemingly absurd truncation of the Navier-Stokes equations).

In plasma physics one of the most important lessons we should learn is that often the linear and nonlinear behaviours of a system are very different. The forced simple pendulum is a case in point (Baker & Gollub 1990). As we are almost invariably dealing with equations which are highly nonlinear, we should expect nonlinear effects to be of great importance, and indeed, they have had a substantial impact upon the field (Infeld & Rowlands 1990, Sagdeev et al 1988). In view of this we shall now go on to start the study of nonlinear effects in equal mass plasmas, and we shall start with the most basic plasma phenomena – electrostatic oscillations.

5.2 Electrostatic Plasma Waves in Electron-Ion Plasmas

One of the simplest cases of nonlinear plasma theory is that of the problem of one dimensional electrostatic waves inside an electron-ion plasma. For such waves inside a plasma with infinitely massive ions, the electron motion is described by the following equations,

$$\frac{\partial n_e}{\partial t} + \frac{\partial(n_e v_e)}{\partial x} = 0, \quad (5.1)$$

$$\frac{\partial v_e}{\partial t} + v_e \frac{\partial v_e}{\partial x} = \frac{-e}{m_e} E, \quad (5.2)$$

$$\frac{\partial E}{\partial x} = \frac{e}{\epsilon_0} (n_0 - n_e). \quad (5.3)$$

The linear solution to these equations is trivial and was first found by Langmuir & Tonks (1929) who derived the result that

$$\omega_0 = \sqrt{\frac{e^2 n_0}{m_e \epsilon_0}}, \quad (5.4)$$

i.e. The plasma frequency oscillation — the most fundamental and important parameter in plasma physics.

As plasma frequency oscillations are so important it was not surprising that they were one of the first plasma wave problems to be tackled nonlinearly. The first approach, by Sturrock (1957), was to expand the equations in terms of a small parameter ϵ . Adopting the linear solution as his zero order solution he analysed the transfer of energy between different modes of the oscillations. In particular he found that in the 1-D case, when averaged over time, no dispersion occurred.

The exact solution to the 1-D electron plasma problem followed not far behind Sturrock's approximate solution. Konyukov (1960) was able to solve equations (5.1)-(5.3) by transforming to Lagrangian coordinates, and a similar analysis was performed by Davidson & Schram (1968) in the following way.†

Firstly we supplement equations (5.1)-(5.3) with the x component of the $\nabla \times \mathbf{B}$ Maxwell equation,

$$\frac{\partial E}{\partial x} = -\frac{1}{\epsilon_0} j. \quad (5.5)$$

Although this equation is not necessary — equations (5.1)-(5.3) describe the plasma completely — it is a useful addition when we apply the following change of variables:

$$\tau = t, \quad (5.6)$$

† The equations for nonlinear electron plasma oscillations can also be solved by using stream functions (Kalman 1960).

$$\chi = x - \int_0^\tau v_e(\chi, \tau') d\tau'. \quad (5.7)$$

From these relations it is easy to see that the space and time derivatives transform in the following way:

$$\frac{\partial}{\partial x} = \left[1 + \int_0^\tau \frac{\partial}{\partial \chi} v_e(\chi, \tau') d\tau' \right]^{-1} \frac{\partial}{\partial \chi}, \quad (5.8)$$

$$\frac{\partial}{\partial t} = \frac{\partial}{\partial \tau} - v_e(\chi, \tau) \left[1 + \int_0^\tau \frac{\partial}{\partial \chi} v_e(\chi, \tau') d\tau' \right]^{-1} \frac{\partial}{\partial \chi}. \quad (5.9)$$

Now, the great advantage of Lagrangian variables is that they follow each individual fluid element. This means that the convective derivative is simply

$$\frac{\partial}{\partial t} + v_e \frac{\partial}{\partial x} = \frac{\partial}{\partial \tau}. \quad (5.10)$$

Thus, in terms of the new variables the momentum equation just becomes

$$\frac{\partial v_e(\chi, \tau)}{\partial \tau} = -\frac{e}{m_e} E(\chi, \tau), \quad (5.11)$$

with the continuity equation transforming to

$$\frac{\partial}{\partial \tau} \left\{ n_e(\chi, \tau) \left[1 + \int_0^\tau \frac{\partial}{\partial \chi} v_e(\chi, \tau') d\tau' \right] \right\} = 0. \quad (5.12)$$

The value of introducing the $\nabla \times \mathbf{B}$ equation is now seen as we can write

$$\left[\frac{\partial}{\partial t} + v_e \frac{\partial}{\partial x} \right] E = \frac{en_0 v_e}{\epsilon_0}, \quad (5.13)$$

i.e.

$$\frac{\partial E}{\partial \tau} = \frac{en_0 v_e(\chi, \tau)}{\epsilon_0}. \quad (5.14)$$

From equations (5.11) and (5.14) it is evident that the equation for v_e has the form of a simple harmonic oscillator,

$$\frac{\partial^2 v_e(\chi, \tau)}{\partial \tau^2} + \omega_e^2 v_e(\chi, \tau) = 0. \quad (5.15)$$

Now χ has appeared as a parameter in a linear equation for $v_e(\chi, \tau)$. This means that the general solution to equations (5.11) to (5.14) are

$$v_e(\chi, \tau) = V(\chi) \cos \omega_e \tau + \omega_e X(\chi) \sin \omega_e \tau, \quad (5.16)$$

$$E(\chi, \tau) = \frac{m_e}{e} (\omega_e V(\chi) \sin \omega_e \tau - \omega_e^2 X(\chi) \cos \omega_e \tau), \quad (5.17)$$

and

$$n_e(\chi, \tau) = \frac{n_e(\chi, 0)}{\left[1 + \frac{1}{\omega_e} \frac{\partial V(\chi)}{\partial \chi} \sin \omega_e \tau + \frac{\partial X(\chi)}{\partial \chi} (1 - \cos \omega_e \tau)\right]}. \quad (5.18)$$

$V(\chi)$ and $X(\chi)$ can be found from the initial velocity and electric field profiles:

$$V(\chi) = v_e(\chi, 0), \quad X(\chi) = \frac{-e}{m_e \omega_e^2} E(\chi, 0). \quad (5.19)$$

Also $X(\chi)$ is related to the initial density ($n_e(\chi, 0)$) through Poisson's equation at $\tau = 0$:

$$\frac{\partial X(\chi)}{\partial \chi} = \frac{n_e(\chi, 0)}{n_0} - 1. \quad (5.20)$$

The transformation equations can be expressed in terms of V and X ,

$$\tau = t, \quad x = \chi + \frac{V(\chi)}{\omega_e} \sin \omega_e \tau + X(\chi)(1 - \cos \omega_e \tau). \quad (5.21)$$

However, to make the transformation from Lagrangian back to Eulerian via. equation (5.21) requires the specification of the initial conditions $V(\chi)$ and $X(\chi)$. This usually means having to solve a transcendental equation, however, it is obvious from the Lagrangian solutions to the problem that coherent oscillations at frequency ω_e are maintained over the region of the initial perturbation. Davidson (1972) gives an example of the inversion to Eulerian variables, but we shall not do so.

5.3 Electrostatic Plasma Waves in Equal Mass Plasmas : Numerical Simulation

As plasma frequency oscillations are of such a fundamental nature it is of interest to see what the behaviour of these waves is inside an equal mass plasma. Having established that the equations can be solved exactly for an electron plasma the first thing to do is to see if the same methods can be applied to an equal mass plasma.

The equations for equal mass plasma oscillations are almost exactly the same as for the electron plasma, but include the dynamics of both plasma components:

$$\frac{\partial n_{\pm}}{\partial t} + \frac{\partial(n_{\pm} v_{\pm})}{\partial x} = 0, \quad (5.22)$$

$$\frac{\partial v_{\pm}}{\partial t} + v_{\pm} \frac{\partial v_{\pm}}{\partial x} = \frac{q_{\pm}}{m} E, \quad (5.23)$$

$$\frac{\partial E}{\partial x} = \frac{e}{\epsilon_0} (n_+ - n_-). \quad (5.24)$$

It is the inclusion of the dynamics of the second plasma component that invalidates the approach adopted for the electron plasma. A Lagrangian transformation can be made, but as we have two fluid components we need two changes of variable and hence separate variables describe the evolution of the positive and negative species. However, when we calculate the field we need to know the

densities of both species at one point in space. Hence we must relate both of our sets of Lagrangian variables to each other. This can only be done by transforming back to Eulerian coordinates and thus the benefits accrued from transformation are lost.

If we try to adopt the alternative approach of Kalman (using stream functions) a similar problem arises. Two stream functions are needed and a reverse transformation needs to be done to calculate the electric field.

Having failed to get an exact solution we must try another approach. The most obvious method is to numerically integrate equations (5.22)-(5.24).

Numerical Integration

The numerical integration of the 1-D electrostatic equal mass equations is straight forward enough. For simple first order Euler integration our equations would become,

$$E(x+1, t) = E(x, t) + \frac{(n_+(x, t) - n_-(x, t)) + (n_+(x+1, t) - n_-(x+1, t))}{2} \Delta x, \quad (5.25)$$

$$v_{\pm}(x, t+1) = v_{\pm}(x, t) + \left[\pm E(x, t) - v_{\pm}(x, t) \frac{v_{\pm}(x+1, t) - v_{\pm}(x-1, t)}{2\Delta x} \right] \Delta t, \quad (5.26)$$

$$n_{\pm}(x, t+1) = n_{\pm}(x, t) - \left[n(x, t) \frac{v_{\pm}(x+1, t) - v_{\pm}(x-1, t)}{2\Delta x} + v(x, t) \frac{n_{\pm}(x+1, t) - n_{\pm}(x-1, t)}{2\Delta x} \right] \Delta t, \quad (5.27)$$

where $(x+1, t)$ refers to the variable evaluated at position $x + \Delta x$ etc. and we have set all constants (q, m, ϵ_0) equal to 1.

Writing the equations in this order makes the most sense in terms of numerical integration and physical intuition. Differences in density cause an electric field. This field causes forces to act which change the velocity of the plasma fluids. The velocity of the plasma causes the density to change. The numerical integration consists of two distinct steps; firstly the spatial integration of n_{\pm} to determine the field, then the temporal integration of n and v .

Although a first order Euler integration method is very simple it can be unstable (Tajima 1971) so we would like to improve on this technique. It would seem at first glance that these equations would be suitably integrated by the *leap frog* method – evaluating E and n at time t , then finding v at $t + 1/2$, then E and n at time $t + 1$ etc. However, the evolution of v involves not only n (through E) but also v itself. The equation for n is similarly a function of n . This means that we are better using the *predictor-corrector* method.

The principal problem of the Euler method is that while we wish to integrate our equation by stepping from t to $t + 1$, it only evaluates the variables on the RHS of the finite differenced equations at time t . Figure 5.1 illustrates the problem. The predictor-corrector method overcomes

this difficulty by using the first order Euler scheme to make a prediction of $n(x, t+1)$ and $v(x, t+1)$ (called $n_{pred}(x, t+1)$ and $v_{pred}(x, t+1)$). Then we evaluate the time centred values of the variables by averaging, i.e. $n(x, t+1/2) = (n(x, t) + n_{pred}(x, t+1))/2$. Finally we use these time centred variables to evaluate the final corrected values of $n(x, t+1)$ and $v(x, t+1)$, i.e.

$$n_{\pm}(x, t+1) = n_{\pm}(x, t) - \left[n(x, t+1/2) \frac{v_{\pm}(x+1, t+1/2) - v_{\pm}(x-1, t+1/2)}{2\Delta x} + v(x, t+1/2) \frac{n_{\pm}(x+1, t+1/2) - n_{\pm}(x-1, t+1/2)}{2\Delta x} \right] \Delta t, \quad (5.28)$$

and similarly for v_{\pm} . This makes this method of integration more accurate and stable than the first order Euler.

Because our equations are spatial in extent, it is difficult to calculate the amplification matrix (with five variables across a spatial mesh of size \mathcal{M} the amplification matrix would be $5\mathcal{M} \times 5\mathcal{M}$). However, there is one simple check which can be used to see if our numerical integration is stable. The equations we are using do not conserve energy explicitly – only implicitly. If we calculate the energy of the plasma during the numerical simulations it should be constant, and if it is we can have confidence in our results. There is another check that we can employ. Analytic results are available for the electron-ion plasma oscillation. Our numerical experiment must be able to duplicate these analytic results.

Numerical Integration of Electron-Ion Plasma

Equations (5.1)-(5.3) were integrated using the predictor-corrector method described above with periodic boundary conditions. In figure 5.2 the results of the simulation are shown. As can be seen, the initial sinusoidal wave form is highly distorted when it evolves towards $t = 1/2 T_p$, with electrostatic forces bunching the electrons and forming a peak density of 5.5. The exact solution (given by Davidson 1972) also predicts a peak density of 5.5. In addition it can be seen that the wave is harmonic with a period $\omega_e = 1$ so that the results of the exact solution have been duplicated by our numerical simulation.

Finally in figure 5.3 we plot the total plasma energy as a function of time though the simulation run. As can be seen it is very steady, fluctuating only by 0.0125%. In figure 5.4 we plot the energy as found from a simulation which uses the first order Euler method to integrate the equations. The improvement in energy conservation is impressive – the Euler integration leads to a secular increase of 1.8% in the plasma energy, clearly an undesirable feature.

Numerical Integration of Equal Mass Plasma

Utilising the predictor corrector method again, figure 5.5 shows the evolution of the negative density component of an electrostatic wave in an equal mass plasma when a perturbation 0.1 is applied. It is seen immediately that the character of the evolution is qualitatively different from the evolution

of the electron plasma. Instead of steady oscillations, the plasma oscillates to higher and higher peaks – and eventually these peaks become so high that they are finer than the mesh spacing of the program and the simulation breaks down. If we look at the evolution of the positive density component of our plasma (figure 5.6) then what is happening becomes clear.

When the electrons in the electron-ion plasma are bunched together by electrostatic forces there exists a heavy neutralising background which pulls down the electron fluid and restores the original sinusoidal shape. In the equal mass plasma a similar sort of evolution exists – each component suffers electrostatic bunching and forms a density peak (as the perturbation of the plasma is small, the peak is much smaller than that of the electrons in figure 5.2, where the perturbation was 0.45. If this large a perturbation is applied to the equal mass plasma it goes unstable in under half a plasma period.) However, in this case there is no heavy background. Instead, the other species is also light, so that although the ‘spiking’ species is pulled down by electrostatic attraction, the ‘neutralising’ species is pulled up. And the simulation shows that it is pulled up into an even higher spike, because the electric field, being an integral over density, is concentrated in the centre of the density perturbation. This higher spike is now ‘neutralised’ by the original spiking component and in doing so is pulled up, in the same way as before, into an even higher spike. This process continues *ad infinitum* until the mesh limit of the simulation is reached. A graph of the electric field evolution is shown in figure 5.7. This clearly shows the evolution of the field from a smooth sinusoid to a sharp – almost step – function in the density peaks.

These results are so different from the electron plasma that some concern must be held regarding them; however, if we graph the energy of the plasma (figure 5.8) it is clear that the simulation is stable – the energy rises slightly towards the end of the simulation when the density spikes are very high, but even then the energy growth is only 0.002%. Although the plasma is being forced into higher and higher spikes, the density differences (which lead to electric fields) stay roughly constant, and so there is no increase in energy. This fact – together with the excellent duplication of the electron-ion plasma results – must lead us to have confidence in the simulation results.

It is obvious from figures 5.5 and 5.6 that the density distribution of the positive and negative plasma components are symmetrical. This can be proved from the evolution equations (5.22) to (5.24). In the simulations x varied over the range $[0, 2\pi)$ so consider the following two coordinate changes:

$$X = x - \pi, \quad X' = \pi - x. \quad (5.29)$$

Thus $X = -X'$. Now consider a solution of the type

$$\rho_+(X) = \rho_-(X'), \quad v_+(X) = -v_-(X'), \quad (5.30)$$

i.e. a symmetry solution with positive and negative densities being reflections in $x = \pi$.

The density equation then becomes

$$\begin{aligned}
& \frac{\partial \rho_+(X)}{\partial t} + \frac{\partial(n_+(X)v_+(X))}{\partial X} = 0, \\
\Rightarrow & \frac{\partial \rho_-(X')}{\partial t} - \frac{\partial(n_-(X')v_-(X'))}{\partial X} = 0, \\
\Rightarrow & \frac{\partial \rho_-(X')}{\partial t} + \frac{\partial(n_-(X')v_-(X'))}{\partial X'} = 0.
\end{aligned} \tag{5.31}$$

And the momentum equation becomes

$$\begin{aligned}
& \frac{\partial v_+(X)}{\partial t} + v_+(X) \frac{\partial v_+(X)}{\partial X} = E(X), \\
\Rightarrow & -\frac{\partial v_-(X')}{\partial t} + v_-(X') \frac{\partial v_-(X')}{\partial X} = E(X), \\
\Rightarrow & -\frac{\partial v_-(X')}{\partial t} - v_-(X') \frac{\partial v_-(X')}{\partial X'} = -E(X'), \\
\Rightarrow & \frac{\partial v_-(X')}{\partial t} + v_-(X') \frac{\partial v_-(X')}{\partial X'} = E(X').
\end{aligned} \tag{5.32}$$

These transforms show that if the solution (5.30) holds at one point in time then it will hold for all time. Thus, if our initial conditions satisfy (5.30) then we only need examine one component of the plasma to find the evolution of the whole plasma. Simply reflecting the density in $x = \pi$ will give the density distribution of the other plasma component.

Although a density perturbation of 10% is much smaller than the 45% applied to the electron plasma, it is very much in the nonlinear regime. We wish to know whether enhancement of the density spikes occurs when the plasma perturbation is very much smaller. To this end figure 5.9 shows the evolution of electron density when the initial perturbation is 1%.

As can be seen the same process is occurring. The initial perturbation of 1% has grown to 5.4% after 6 plasma periods. The energy of the simulated plasma is again almost constant (figure 5.10 shows it constant to 0.0002

Fourier Analysis

The nonlinear evolution of the equal mass plasma can be seen in terms of the plasma acquiring finer and finer spatial detail. If we were to Fourier analyse the plasma density in space, then as we start with a sinusoidal perturbation at $t = 0$, only one Fourier component would be non-zero. However, as the plasma evolves, higher and higher Fourier modes are being excited.

The Fourier analysis can be done on the original equations (5.22)-(5.24). Before we do this it is convenient to introduce a perturbation density ρ_{\pm} , i.e.

$$\rho_{\pm} = n_{\pm} - n_0. \tag{5.33}$$

(In the numerical simulations $n_0 = 1$.)

We now take a Fourier analysis *in space only*. As all the quantities we are dealing with are real, then for any quantity Ψ the Fourier terms will be Hermitian (i.e. $\Psi^k = c.c.\Psi^{-k}$, Bracewell 1986). Our equations now become

$$\frac{d\rho_{\pm}^k}{dt} + ikv_{\pm}^k = -ik[\rho_{\pm}^k, v_{\pm}^k], \quad (5.34)$$

$$\frac{dv_{\pm}^k}{dt} \mp E^k = -ik[v_{\pm}^k, v_{\pm}^k], \quad (5.35)$$

$$ikE^k = \rho_+^k - \rho_-^k. \quad (5.36)$$

We have introduced the notation $[\Phi^k, \Psi^k]$ to stand for the following convolution

$$[\Phi^k, \Psi^k] = \sum_{k1} \Psi^{k1} \Phi^{k-k1}. \quad (5.37)$$

In this form the troublesome nonlinear terms are now the convolution terms. Without them the problem is (obviously) linear, with a general solution

$$E_0 = Ae^{i\omega_p t} + A^\dagger e^{-i\omega_p t}, \quad (5.38)$$

$$\rho_{0\pm} = \pm \frac{ik}{2} \left(Ae^{i\omega_p t} + A^\dagger e^{-i\omega_p t} \right) + C, \quad (5.39)$$

$$v_{0\pm} = \pm \frac{i\omega_p}{2} \left(-Ae^{i\omega_p t} - A^\dagger e^{-i\omega_p t} \right), \quad (5.40)$$

where the k superscript has been dropped for ease of notation, but it should be remembered in the following that we are talking of Fourier amplitudes, not of physical quantities.

It is easy to numerically integrate equations (5.34)-(5.36) directly, again using a predictor-corrector technique. When this is done for an initial perturbation of 0.1 then the results (figure 5.11) are seen to be the same as those derived from Eulerian variables (figure 5.5), further increasing our confidence in the results of the simulations. If we now plot the amplitude of the first few Fourier components (figure 5.12) then the excitation of higher and higher Fourier modes is clear.

5.4 Electrostatic Plasma Waves in Equal Mass Plasmas : Quasilinear Analysis

We have seen that it is not possible to solve the equations for electrostatic waves exactly. However, having Fourier analysed the equations it is possible to make a quasilinear analysis of the plasma evolution.

The basis of this analysis will be to assume that the amplitude of the plasma oscillation is small (or at least is small when we apply this analysis). Looking then at our Fourier equations (5.34)-(5.36) we see that all terms are of first order in amplitude except for the convolution terms – these are second order. If we can assume that the amplitudes are small, then to first order, we can ignore the

convolution terms. This leads to the linear solution (5.38)-(5.40). Then to second order we have the following equations:

$$\frac{d\rho_{1\pm}}{dt} + ikv_{1\pm} = -ik[\rho_{0\pm}, v_{0\pm}], \quad (5.41)$$

$$\frac{dv_{1\pm}}{dt} \mp E_1 = -i[kv_{0\pm}, v_{0\pm}], \quad (5.42)$$

$$ikE_1 = \rho_{1+} - \rho_{1-}. \quad (5.43)$$

We are aiming to derive the next order of solutions ($\rho_{1\pm}$ etc.) by considering only the convolutions of linear solutions. As we know these solutions, we are able to evaluate the convolution terms explicitly to give

$$\frac{d\rho_{1\pm}}{dt} + ikv_{1\pm} = \frac{i\omega_p k}{4} \left(-[kA, A]e^{2i\omega_p t} - [kA^\dagger, A] + [kA, A^\dagger] + [kA^\dagger, A^\dagger]e^{-2i\omega_p t} \right), \quad (5.44)$$

$$\frac{dv_{1\pm}}{dt} \mp E_1 = \frac{i\omega_p^2}{4} \left([kA, A]e^{2i\omega_p t} - [kA^\dagger, A] - [kA, A^\dagger] + [kA^\dagger, A^\dagger]e^{-2i\omega_p t} \right), \quad (5.45)$$

$$ikE_1 = \rho_{1+} - \rho_{1-}. \quad (5.46)$$

Notice that the terms inside the linear convolution have split into two types: those which are harmonic in time and those which are constant. Let us treat the harmonic and secular terms separately ($\rho_{1+} = \rho_{h+} + \rho_{s+}$).

$$\frac{d\rho_{h\pm}}{dt} + ikv_{h\pm} = \frac{ik\omega_p}{4} \left(-[kA, A]e^{2i\omega_p t} + [kA^\dagger, A^\dagger]e^{-2i\omega_p t} \right), \quad (5.47)$$

$$\frac{dv_{h\pm}}{dt} \mp E_h = \frac{i\omega_p^2}{4} \left([kA, A]e^{2i\omega_p t} + [kA^\dagger, A^\dagger]e^{-2i\omega_p t} \right), \quad (5.48)$$

$$ikE_h = \rho_{h+} - \rho_{h-}. \quad (5.49)$$

Differentiate (5.46) w.r.t t and then substitute for $dv_{h\pm}/dt$ from (5.47),

$$\frac{d^2\rho_{h\pm}}{dt^2} \pm ikE_h = \frac{3k\omega_p^2}{4} \left([kA, A]e^{2i\omega_p t} + [kA^\dagger, A^\dagger]e^{-2i\omega_p t} \right). \quad (5.50)$$

Now substitute for E_h from (5.48) to get equations for $\rho_{h\pm}$:

$$\frac{d^2\rho_{h+}}{dt^2} + (\rho_{h+} - \rho_{h-}) = \frac{3k\omega_p^2}{4} \left([kA, A]e^{2i\omega_p t} + [kA^\dagger, A^\dagger]e^{-2i\omega_p t} \right), \quad (5.51)$$

$$\frac{d^2\rho_{h-}}{dt^2} - (\rho_{h+} - \rho_{h-}) = \frac{3k\omega_p^2}{4} \left([kA, A]e^{2i\omega_p t} + [kA^\dagger, A^\dagger]e^{-2i\omega_p t} \right). \quad (5.52)$$

We now introduce new variables ψ_h and ϕ_h , where

$$\psi_h = \rho_{h+} + \rho_{h-}, \quad \phi_h = \rho_{h+} - \rho_{h-}. \quad (5.53)$$

From (5.50) and (5.51) we find equations governing ψ_h and ϕ_h :

$$\frac{d^2\psi_h}{dt^2} = \frac{2k\omega_p^2}{3} \left([kA, A]e^{2i\omega_p t} + [kA^\dagger, A^\dagger]e^{-2i\omega_p t} \right), \quad (5.53)$$

$$\frac{d^2\phi_h}{dt^2} = -2\phi_h. \quad (5.54)$$

The equation for ϕ_h is just a harmonic oscillator and recalling that here $\omega_p = \sqrt{2}$ we see that the solution is just

$$\phi_h = B_h e^{i\omega_p t} + B_h^\dagger e^{-i\omega_p t}. \quad (5.55)$$

The equation for ψ_h also has a straightforward solution,

$$\psi_h = -\frac{k}{6} \left([kA, A]e^{2i\omega_p t} + [kA^\dagger, A^\dagger]e^{-2i\omega_p t} \right) + C_h t + D_h. \quad (5.56)$$

B_h , C_h and D_h are all arbitrary constants. We can see that ψ_h and ϕ_h both contain harmonic components. In addition, there is the possibility of secular growth in ψ_h through the term $C_h t$. However, as this involves an arbitrary constant controlling the growth rate it cannot be a satisfactory explanation for the behaviour of the equal mass plasma.

These solutions can be substituted back into (5.48) to find E_h and then (5.47) for $v_{h\pm}$ (ρ_{h+} and ρ_{h-} are trivially found from (5.52)):

$$E_h = -\frac{i}{k} \left(B_h e^{i\omega_p t} + B_h^\dagger e^{-i\omega_p t} \right), \quad (5.57)$$

$$v_{h\pm} = \frac{\omega_p}{8} \left([kA, A]e^{2i\omega_p t} + [kA^\dagger, A^\dagger]e^{-2i\omega_p t} \right) \mp \frac{\omega_p}{k} \left(B_h e^{i\omega_p t} - B_h^\dagger e^{-i\omega_p t} \right) + D'_h. \quad (5.58)$$

Notice that E_h is purely harmonic and, as we have no flow velocities in the plasma, D'_h must also be zero so that $v_{h\pm}$ is also purely harmonic.

Now we return to (5.46)-(5.48), but this time we consider the secular terms:

$$\frac{d\rho_{s\pm}}{dt} + ikv_{s\pm} = \frac{i\omega_p k}{4} \left([kA, A^\dagger] - [kA^\dagger, A] \right), \quad (5.59)$$

$$\frac{dv_{s\pm}}{dt} \mp E_s = -\frac{i\omega_p^2}{4} \left([kA, A^\dagger] + [kA^\dagger, A] \right), \quad (5.60)$$

$$ikE_s = \rho_{s+} - \rho_{s-}. \quad (5.61)$$

Now we differentiate (5.59) and substitute in (5.60):

$$\frac{d^2\rho_{s\pm}}{dt^2} \pm ikE_s = \frac{k\omega_p^2}{4} \left([kA, A^\dagger] + [kA^\dagger, A] \right). \quad (5.62)$$

Now substitute for E_s to give

$$\frac{d^2 \rho_{s+}}{dt^2} + (\rho_{s+} - \rho_{s-}) = \frac{k\omega_p^2}{4} \left([kA, A^\dagger] + [kA^\dagger, A] \right), \quad (5.63)$$

$$\frac{d^2 \rho_{s-}}{dt^2} - (\rho_{s+} - \rho_{s-}) = \frac{k\omega_p^2}{4} \left([kA, A^\dagger] + [kA^\dagger, A] \right). \quad (5.64)$$

Again it is useful to change variables, this time to ψ_s and ϕ_s defined in the same way as before:

$$\psi_s = \rho_{s+} + \rho_{s-} \quad \phi_s = \rho_{s+} - \rho_{s-}. \quad (5.65)$$

This gives the following equation for ϕ_s

$$\frac{d^2 \phi_s}{dt^2} = -2\phi_s, \quad (5.66)$$

with solution

$$\phi_s = B_s e^{i\omega_p t} + B_s^\dagger e^{-i\omega_p t}. \quad (5.67)$$

The equation for ψ_s is

$$\frac{d^2 \psi_s}{dt^2} = \frac{k\omega_p^2}{2} \left([kA, A^\dagger] + [kA^\dagger, A] \right), \quad (5.68)$$

and as the RHS of this equation is constant, the solutions are

$$\psi_s = \frac{k\omega_p^2}{4} \left([kA, A^\dagger] + [kA^\dagger, A] \right) t^2 + C_s t + D_s. \quad (5.69)$$

The equation for ϕ_s is once again purely harmonic and means that the solutions for E_s and $v_{s\pm}$ are

$$E_s = -\frac{i}{k} \left(B_s e^{i\omega_p t} - B_s^\dagger e^{-i\omega_p t} \right), \quad (5.70)$$

$$v_{s\pm} = \mp \frac{\omega_p}{k} \left(B_s e^{i\omega_p t} - B_s^\dagger e^{-i\omega_p t} \right) - \frac{i\omega_p^2}{4} \left([kA, A^\dagger] + [kA^\dagger, A] \right) t + D'_s. \quad (5.71)$$

Now a key difference between these solutions and the ones found for the harmonic quasilinear terms is that this time we have predicted a secular growth in the second order variables. ψ_s has a term in t^2 and $v_{s\pm}$ has a term in t (E_s is still purely harmonic). The fact that E_s remains harmonic accords with an intuitive view of the numerical results – E sharpens around the density peaks but does not itself grow in amplitude.

Combining the harmonic and secular parts of the solution gives us the final values of the second order quantities. These are

$$\psi = \psi_h + \psi_s = \frac{k\omega_p^2}{4} ([kA, A^\dagger] + [kA^\dagger, A]) t^2 - \frac{k}{6} ([kA, A]e^{2i\omega_p t} + [kA^\dagger, A^\dagger]e^{-2i\omega_p t}) + Ct + D, \quad (5.72)$$

$$\phi = \phi_h + \phi_s = Be^{i\omega_p t} + B^\dagger e^{-i\omega_p t}, \quad (5.73)$$

$$v_{1\pm} = -\frac{i\omega_p^2}{4} ([kA, A^\dagger] + [kA^\dagger, A]) t \mp \frac{\omega_p}{k} (Be^{i\omega_p t} - B^\dagger e^{-i\omega_p t}) + \frac{\omega_p}{8} ([kA, A]e^{2i\omega_p t} + [kA^\dagger, A^\dagger]e^{-2i\omega_p t}) + D', \quad (5.74)$$

$$E_1 = -\frac{i}{k} (B_h e^{i\omega_p t} + B_h^\dagger e^{-i\omega_p t}). \quad (5.75)$$

We have altered the constants of integration suitably and retain the change of density variables.

Comparison of Quasilinear Theory and Numerical Experiment

We have derived the second order behaviour of the plasma and predicted that ψ and $v_{1\pm}$ have secular growth terms. This seems to be intuitively reasonable, given the behaviour of the plasma. However we wish now to compare the quantitative predictions of the theory with the actual values found in the experiment.

As our analysis relied upon the amplitude being small, it makes sense to first compare our results to the case when $\rho = 0.01$. Having applied an initial sinusoidal perturbation our initial amplitudes are $A = 0 \pm 0.005i$ in Fourier components ± 1 . Thus the second order components which are stimulated are ± 2 , and ψ should be real and v_1 imaginary. We shall look at $k = 2$ in particular.

Figure 5.13 shows the theoretical and numerical values of $\Re(\psi)$ on the same graph. The fit is excellent in the early part of the simulation and is fairly close even towards the end. The secular increase at t^2 is found as well as the harmonic component at frequency $2\omega_p$. After 7 plasma periods the actual growth is slightly larger than the predicted value, but this is what we should expect as other Fourier components are stimulated and these start to couple to affect the growth of the $k = 2$ mode.

Figure 5.14 shows $\Im(v_{1-})$ – theoretical and numerical. Again the fit is good – especially early in the simulation. The linear growth is found and so is the harmonic frequency of $2\omega_p$. The experimental growth is, however, slightly faster than the quasilinear theory suggests; again this is due to the stimulation of higher modes.

We now move to the case where the plasma is disturbed by an initial perturbation of 0.1. We should be somewhat suspicious of the assumptions that were made in the derivation of the quasilinear results here – a perturbation of 10% is not really small and certainly not infinitesimal. However examining figure 5.15 (where the theoretical and numerical values of $\Re(\psi)$ are plotted) we see that

even in this case the fit is reasonable. The divergence from theory and experiment is naturally faster as it is easier for the plasma to stimulate higher frequency modes with a large initial perturbation. Figure 5.16 plots the values of $\Im(v_{1-})$ for the 0.1 perturbation. The linear fit is again good close to $t = 0$, but diverges as t increases, and the harmonic component is in this case larger than quasilinear theory would suggest.

5.5 Conclusions

Overall, the quasilinear theory has been a success — as far as it goes. We have been able to predict correctly the form of the secular growth (t^2 for ψ and t for v_1) and find a good quantitative fit with the numerical experiments when the amplitude is low (0.01) and a reasonable fit when the amplitude is higher (0.1). The main problem, though, is that although we can model the behaviour of the components stimulated by the initial linear solutions, the fact that the growth of these components is secular means that they soon become as large as the original perturbation. Then higher and higher components are stimulated (see figure 5.12) and these couple back to affect the growth of the quasilinear components. Unfortunately no better analytic solution has been found and in this region we are forced to rely upon numerical simulation.

The subsequent evolution of the plasma — with the density spikes growing to higher and higher values — will not occur in a real plasma. The reason for this is that there is no pressure term in the cold plasma model which we used in our simulations. Even if the assumption of zero pressure was valid at the beginning of the plasma evolution, eventually the plasma density gradient becomes so high that to continue to ignore pressure is wrong. We shall discuss the extension of the work to warm plasmas in chapter six.

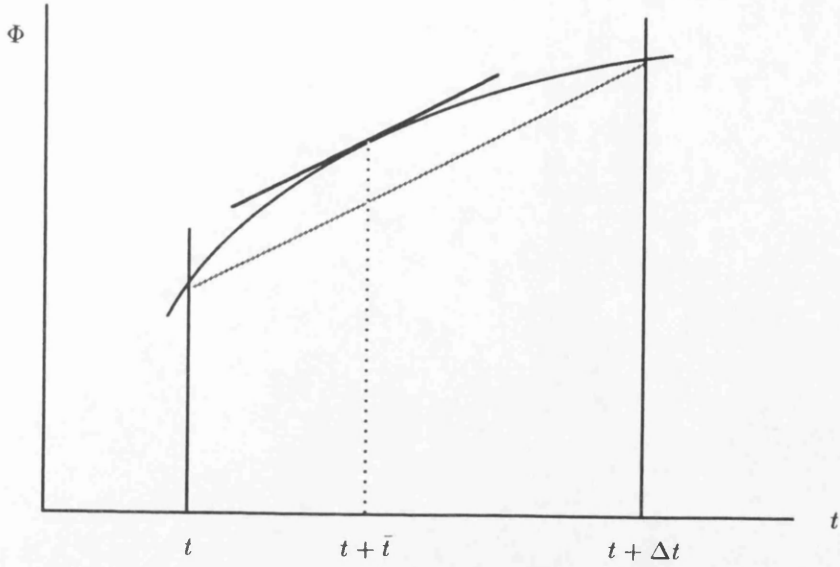


Figure 5.1. The mean value theorem says there is a \bar{t} such that

$$\Phi(t + \Delta t) = \Phi(t) + \Delta t \frac{d\Phi(t + \bar{t})}{dt}.$$

The Euler method uses $\bar{t} = 0$. The predictor-corrector method uses $\bar{t} = \Delta t/2$. If Φ is smooth over Δt this is a very good guess and improves the performance of the integration.

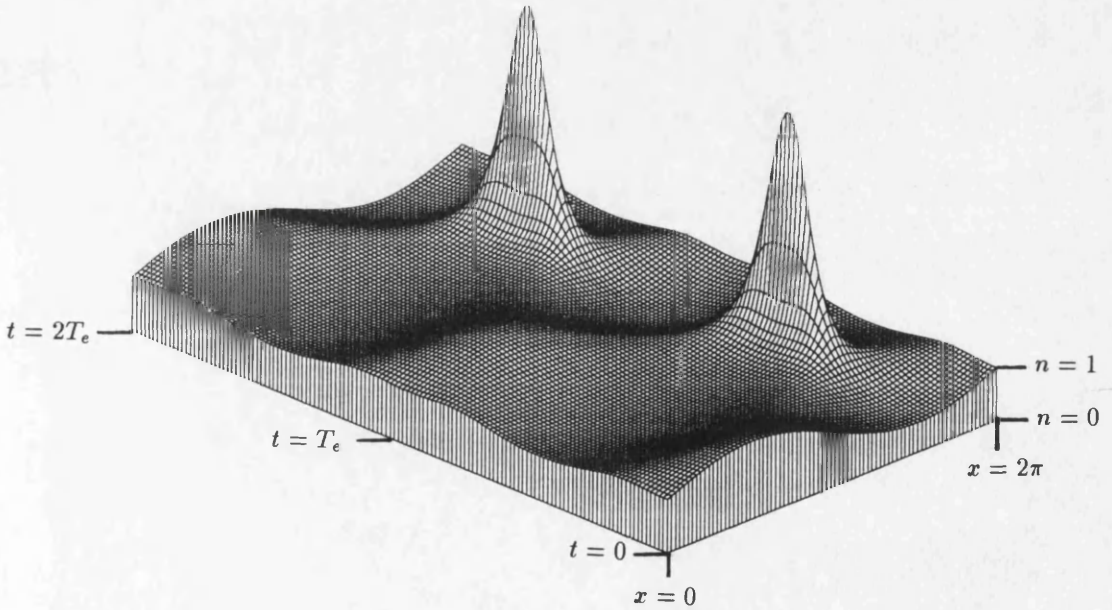


Figure 5.2. Electron density in a plasma with infinitely heavy ions. The initial perturbation is a sinusoid with amplitude $\delta n = 0.45$ and the peak density is 5.5.

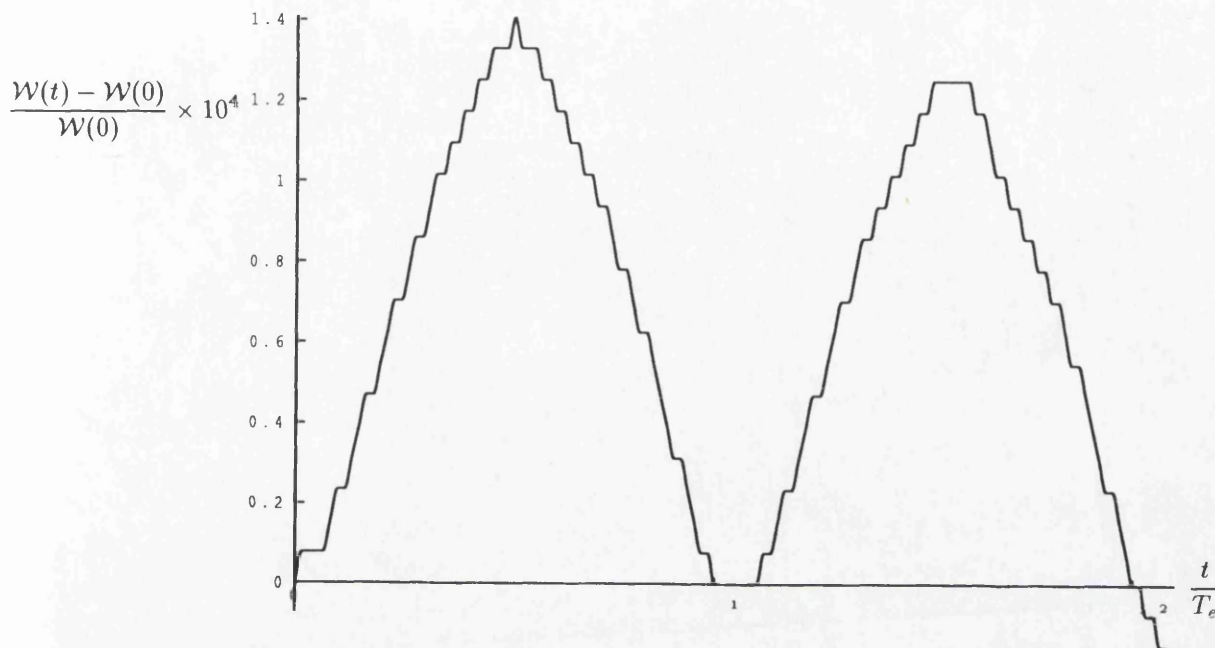


Figure 5.3. The total plasma energy during the simulation shown in figure 5.2.

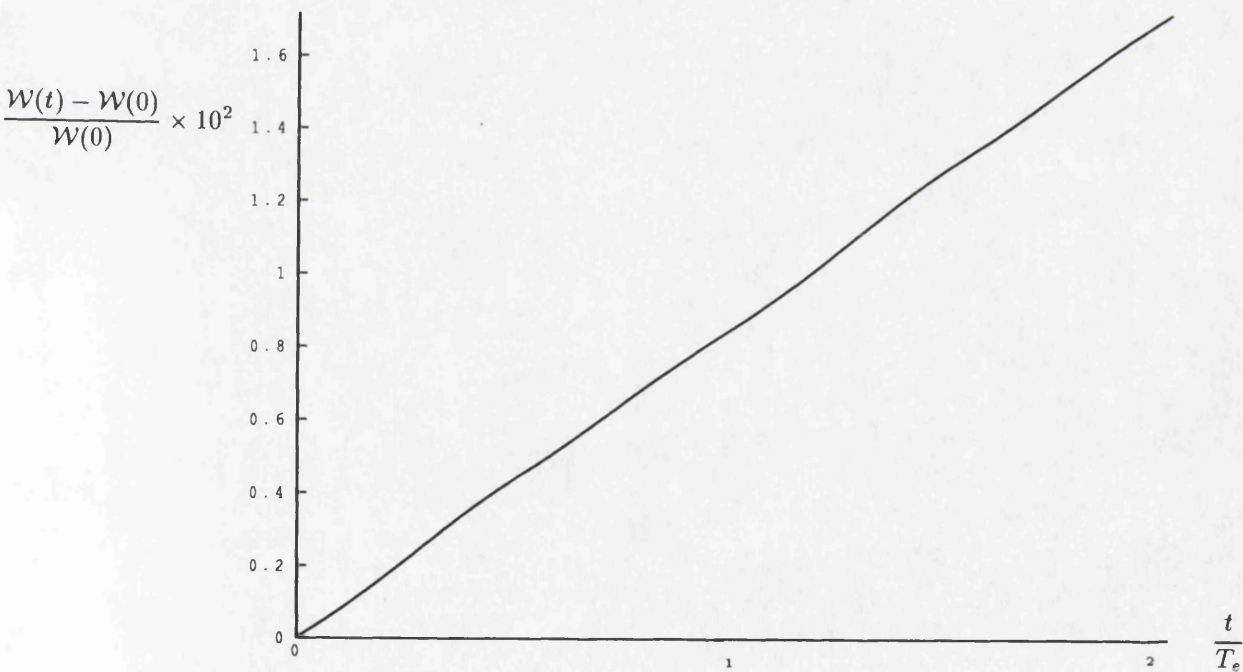


Figure 5.4. The total plasma energy during a similar simulation to figure 5.2 but using the Euler method of integration. Energy is not well conserved with this integration technique.

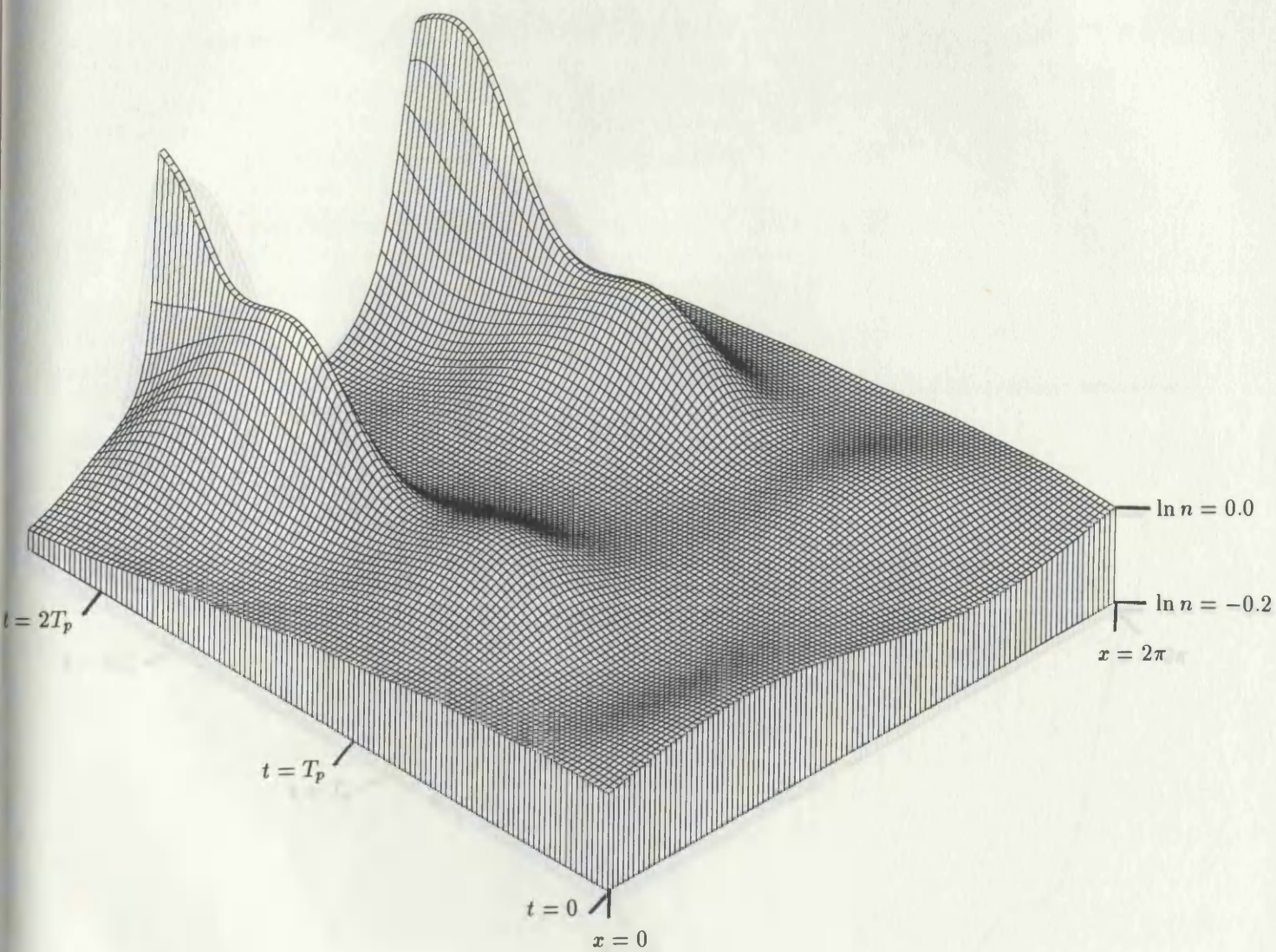


Figure 5.5. Negative component density in a cold equal mass plasma during electrostatic oscillations. Initial conditions were sinusoidal density perturbations of ± 0.1 to each component.

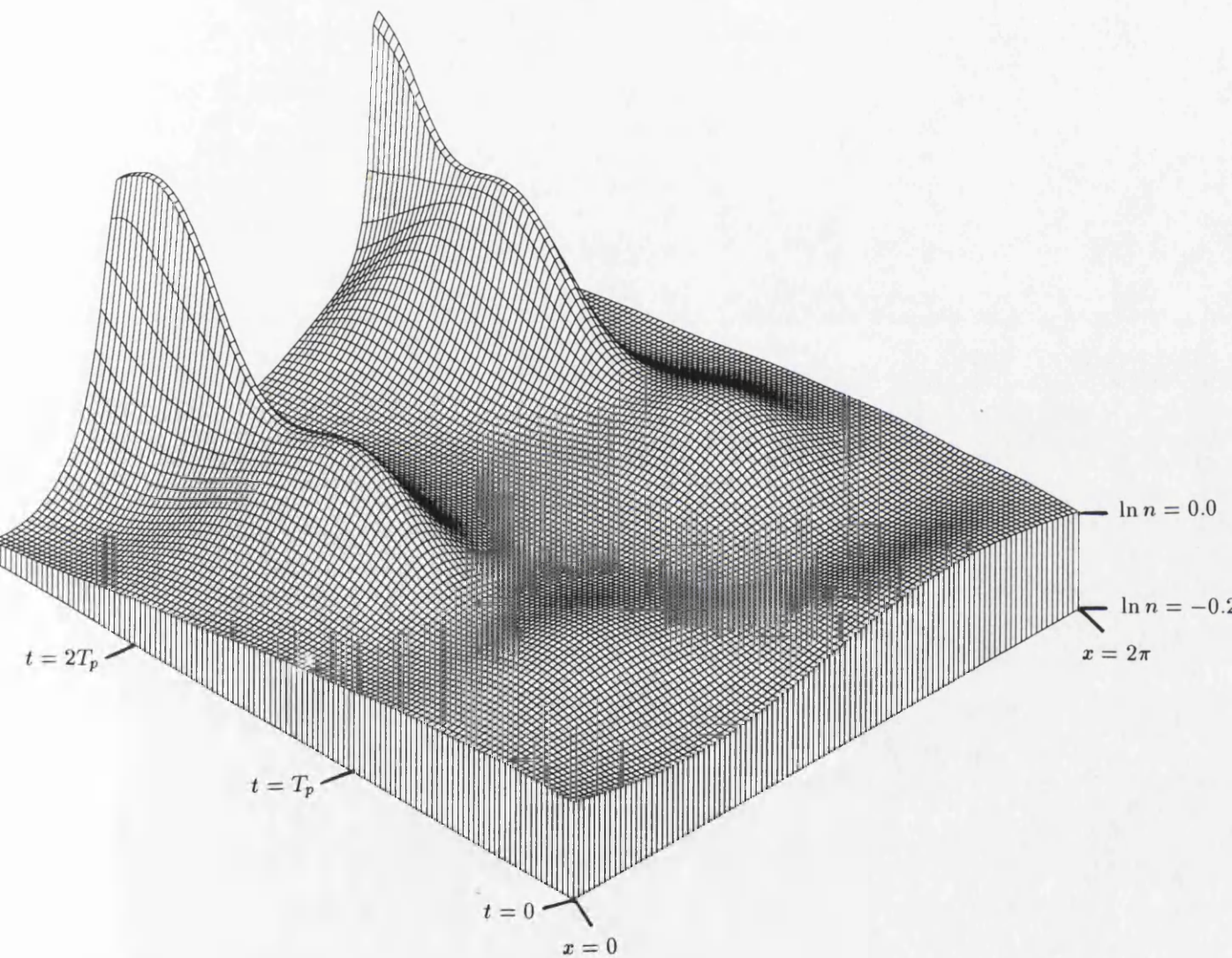


Figure 5.6. Positive component density in the equal mass plasma for the same simulation as figure 5.5.

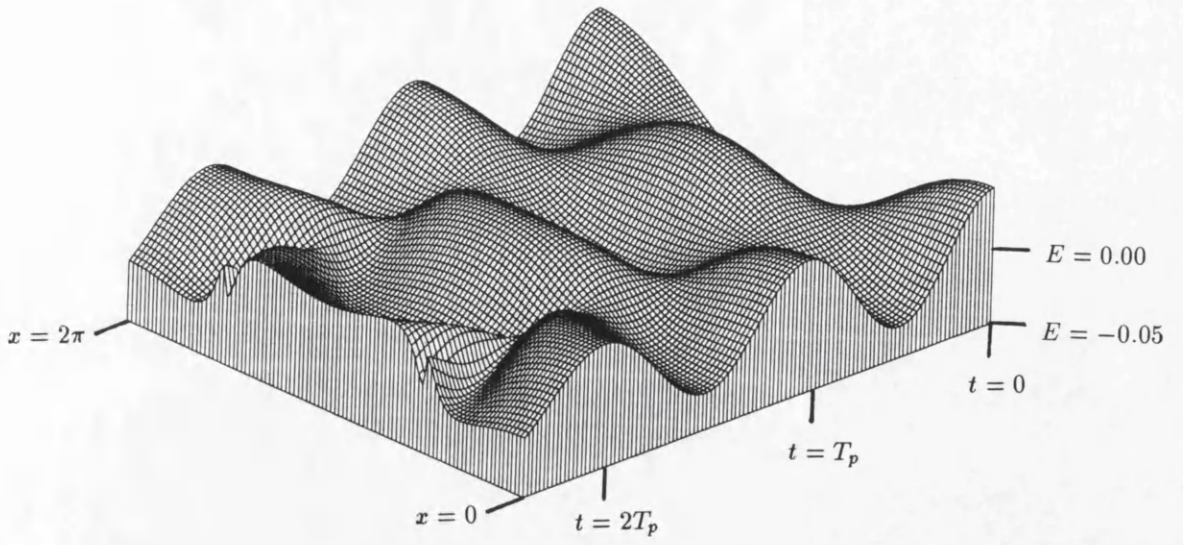


Figure 5.7. Electric field strength in a cold equal mass plasma during electrostatic oscillations. Initial conditions as figure 5.5.

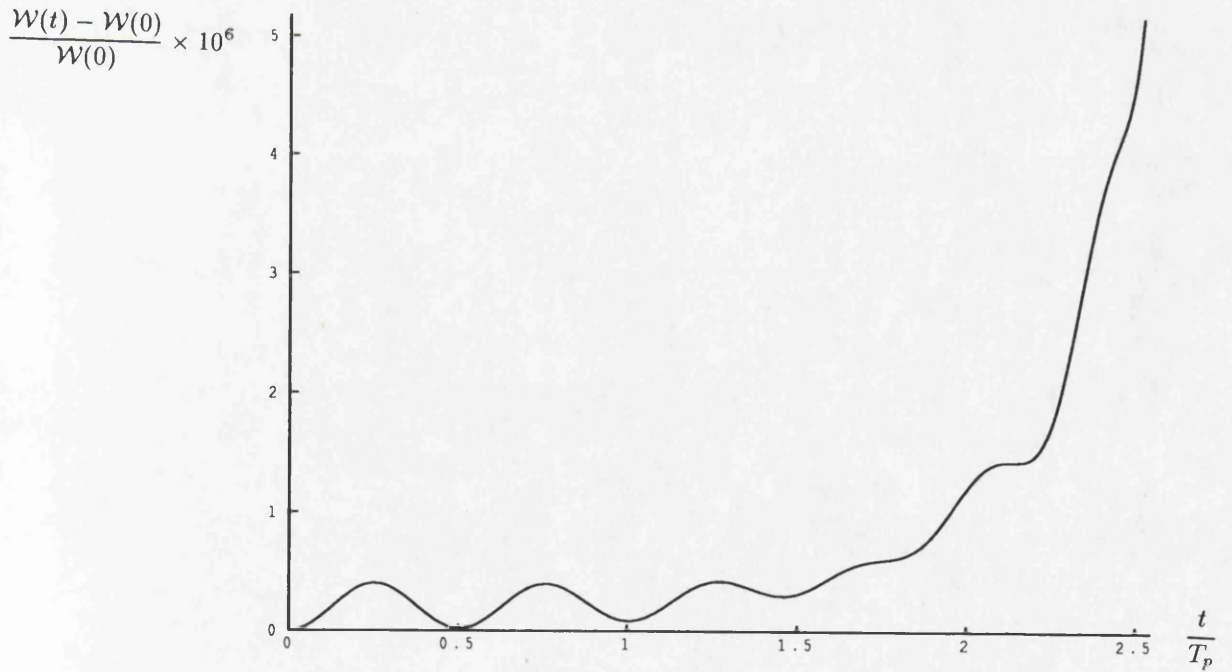


Figure 5.8. Total plasma energy during the simulation shown in figures 5.5-5.7.

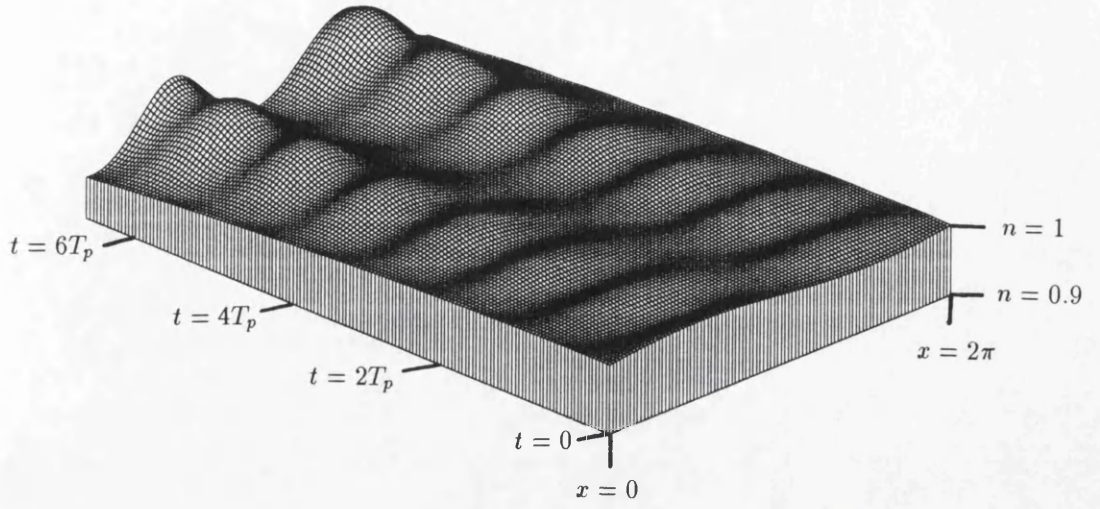


Figure 5.9. Negative component density in a cold equal mass plasma during electrostatic oscillations. Initial conditions were sinusoidal density perturbations of ± 0.01 to each component.

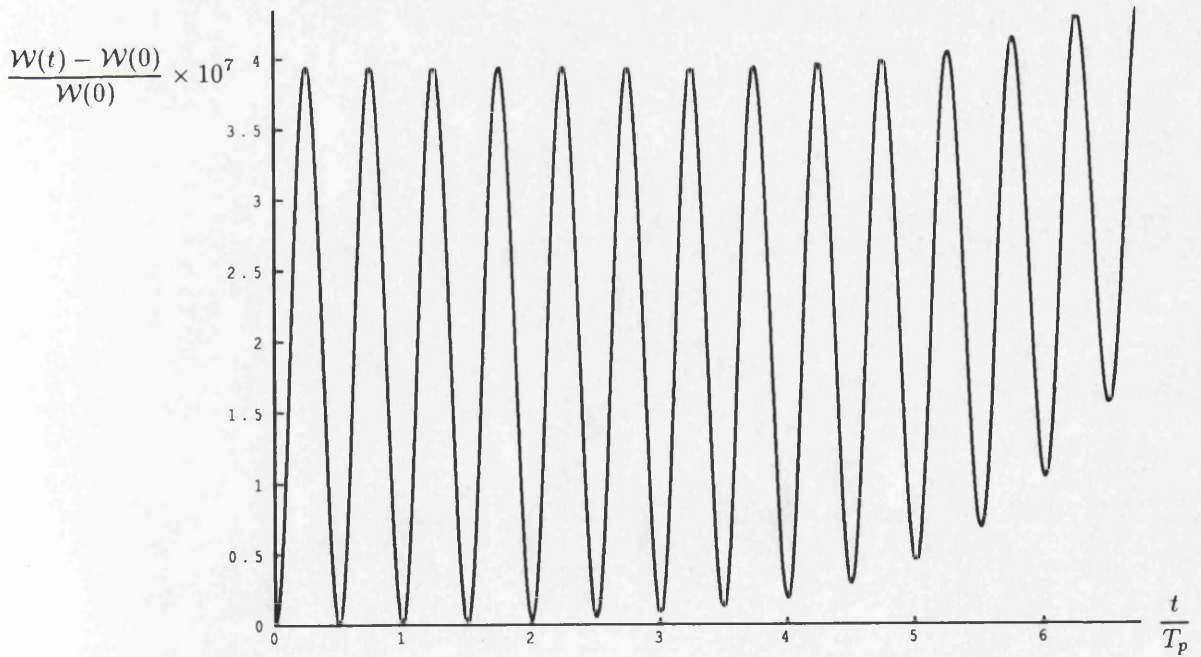


Figure 5.10. Total plasma energy during the simulation shown in figure 5.9.

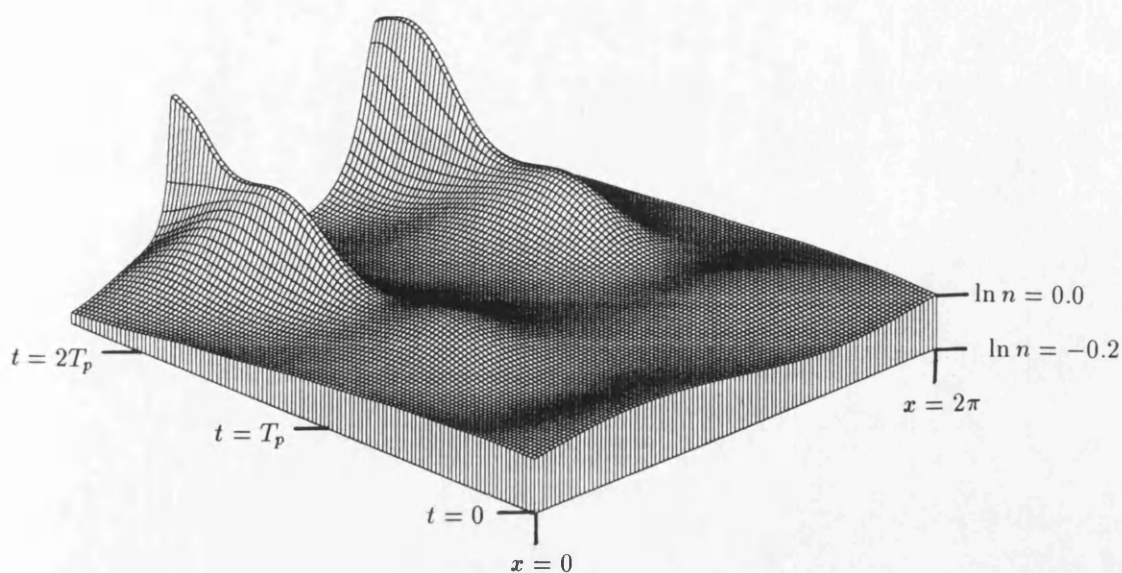


Figure 5.11. Negative component density in a cold equal mass plasma during electrostatic oscillations found from integration of spatially Fourier analysed equations. Initial conditions were sinusoidal density perturbations of ± 0.1 to each component. These results are the same as found in figure 5.5.

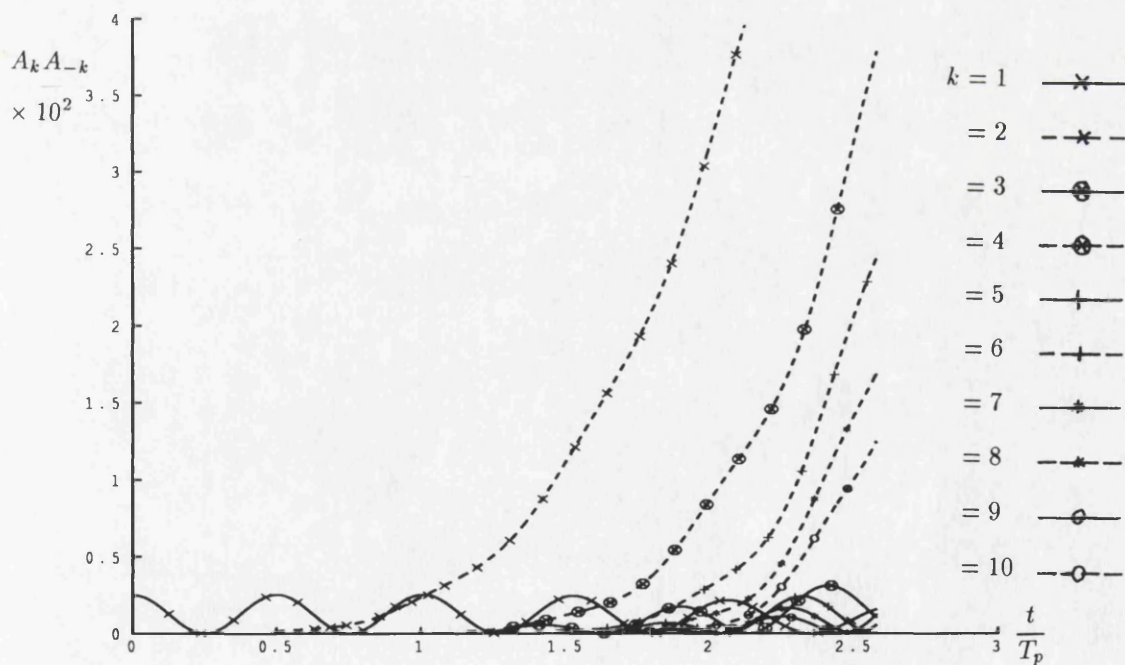


Figure 5.12. First 10 Fourier component amplitudes ($A^k A^{-k}$) of negative density after density perturbation of ± 0.1 to each component.

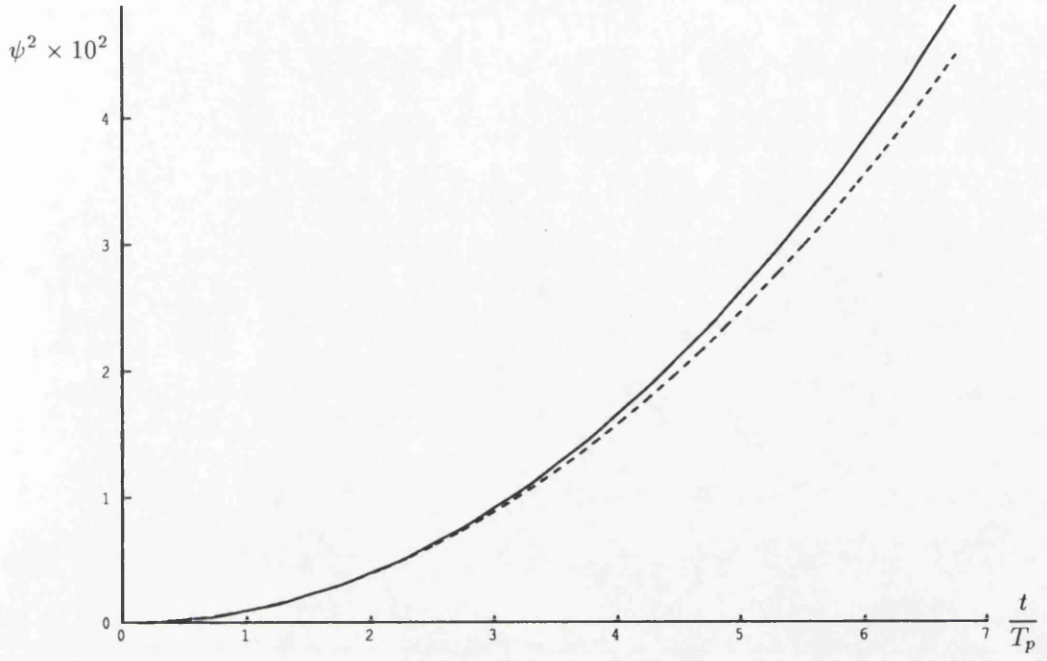


Figure 5.13. ψ^2 (ψ for $k = 2$, **not** ψ squared) when plasma is perturbed by $k = \pm 1$ density perturbations of ± 0.01 :-----, Quasilinear theory;———, numerical experiment.

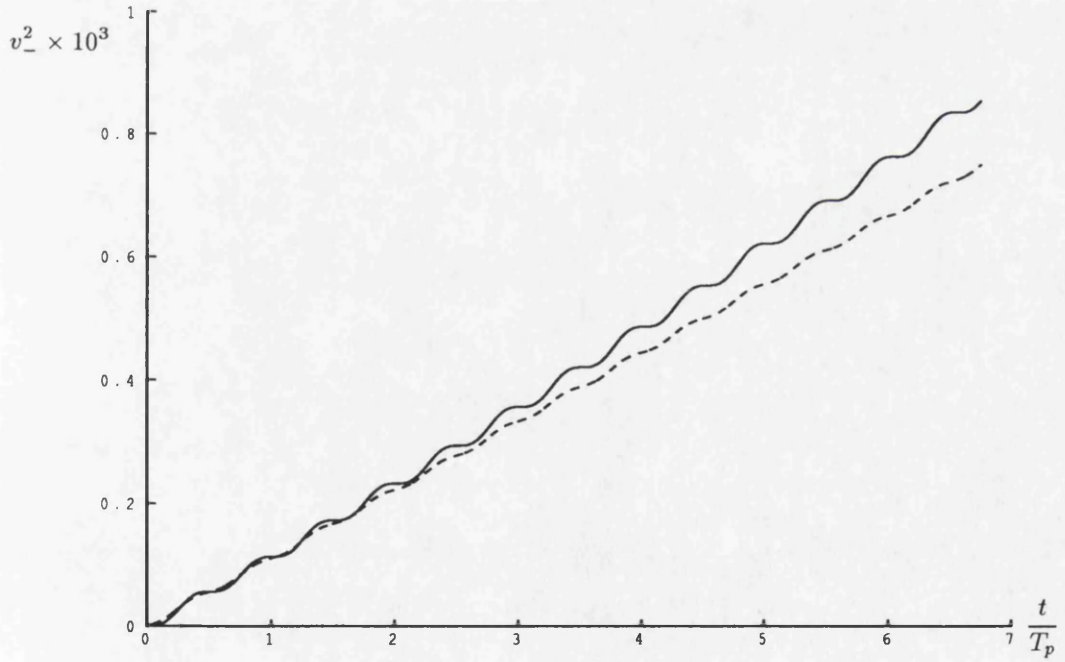


Figure 5.14. v_- (v_- for $k = 2$, **not** v_- squared) when plasma is perturbed by $k = \pm 1$ density perturbations of ± 0.01 :-----, Quasilinear theory;———, numerical experiment.

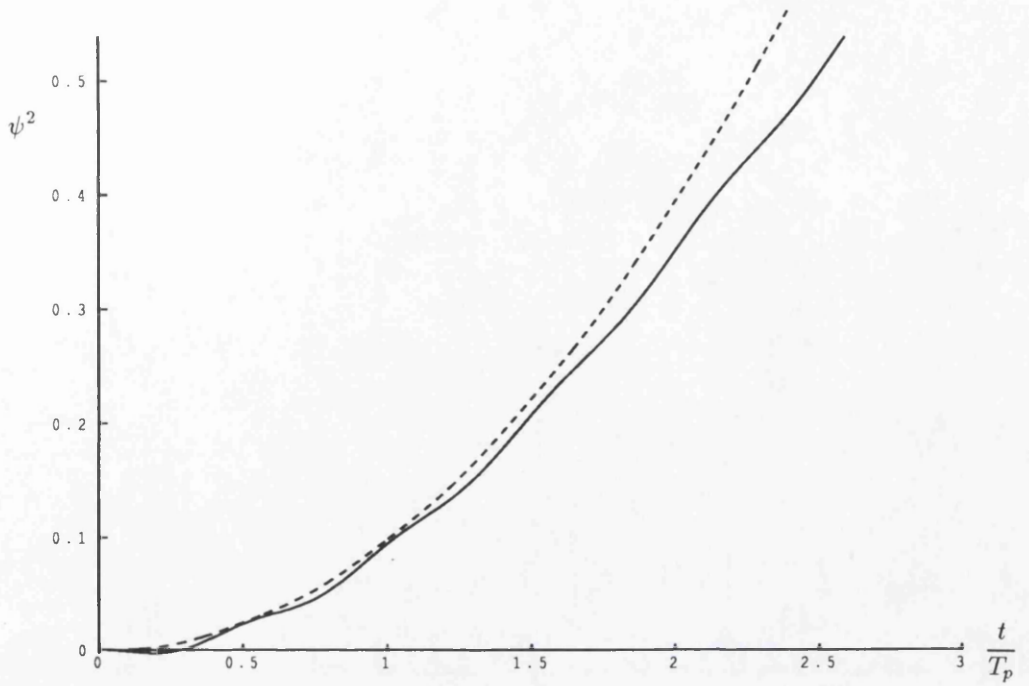


Figure 5.15. ψ^2 (ψ for $k = 2$, not ψ squared) when plasma is perturbed by $k = \pm 1$ density perturbations of ± 0.1 :——, Quasilinear theory;----, numerical experiment.

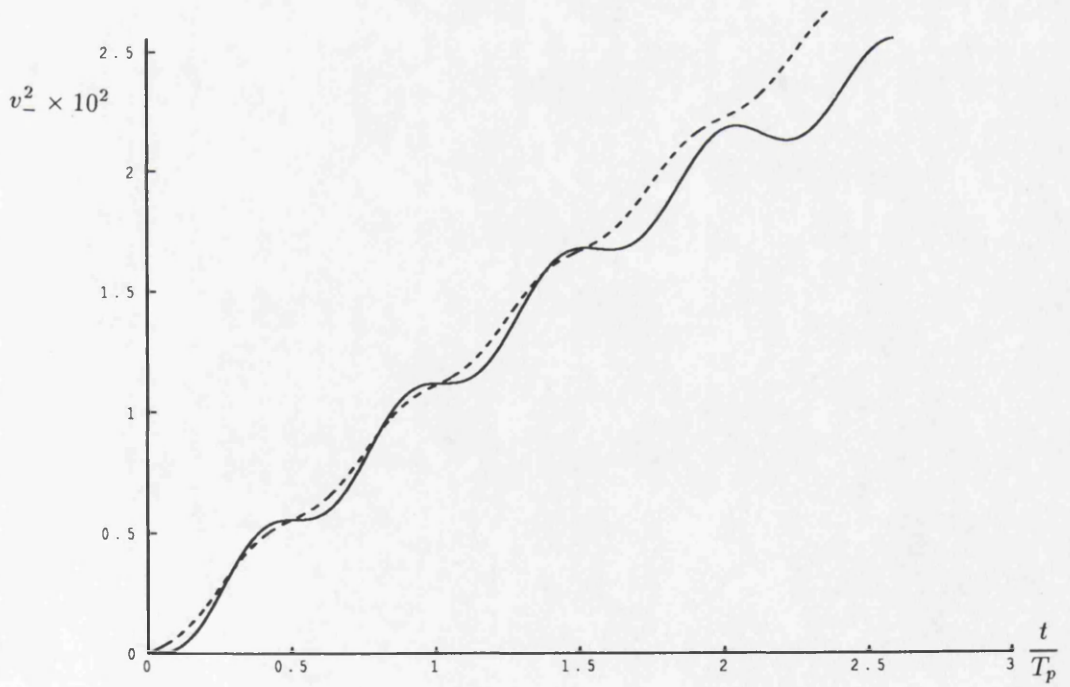


Figure 5.16. v_-^2 (v_- for $k = 2$, not v_- squared) when plasma is perturbed by $k = \pm 1$ density perturbations of ± 0.1 :——, Quasilinear theory;----, numerical experiment.

One thing I have learned in a long life: that all our science, measured against reality, is primitive and childlike – yet it is the most precious thing we have.

Albert Einstein

History itself is an actual part of natural history, of nature's development into man. Natural science will in time include the science of man as the science of man will include natural science: there will be one science.

Karl Marx

Chapter 6

Future Work

6.1 Normal Wave Modes in Inhomogeneous and Hot Plasmas

The aim of this thesis has been to investigate wave propagation in equal mass plasmas. In chapter three we discussed the normal wave modes that exist inside an infinite, homogeneous equal mass plasma. We found that the symmetry of the plasma simplifies the problem immensely and we derived analytic expressions for linear waves in cold and warm plasmas. We also discussed which plasmas with a nonisotropic distribution function would exhibit the same symmetries as the fluid models studied.

As was mentioned in chapter one, we are at the beginning of the study of equal mass plasmas. It was therefore necessary to examine the plasma under the simplifying assumptions of chapter three before proceeding further: however, many of those assumptions can be – indeed should be – relaxed. Real plasmas are not infinite, nor are they homogeneous. One of the most difficult areas of research in plasma physics is to determine *self-consistently* the wave modes of a plasma which is not homogeneous (Diver & Laing 1990; Diver, Laing & Sellar 1990). It would be interesting to see what effect the symmetry of the equal mass plasma has upon this problem. In addition, if the study of molecular equal mass plasma devices is to continue, then a study of the edge effects of such plasmas should be made.

The studies which we undertook also concentrated upon fluid models of the plasma. This is clearly a limitation, as many interesting plasma effects only happen when the velocity space structure of a plasma is accounted for by using kinetic theory (e.g. Landau damping). As the general theory of kinetic wave propagation is very difficult, the symmetry of the equal mass plasma can be expected to provide some help in making analytic progress.

In chapter four we studied linear waves in electron-positron plasmas, under much the same strictures as chapter three. Faraday rotation was seen to be absent in the models we studied, which incorporated relativistic effects and simplistic annihilation and creation. One thing which remained to be done was to investigate the physicality of one of the waves found when annihilation and creation were incorporated into the model.

All the extensions mentioned above apply both to the study of equal mass plasmas and to electron-positron (and other particle-anti-particle) plasmas. The study of the kinetic theory of waves would seem to be particularly appropriate to these plasmas, which are of course at relativistic temperatures and which are unlikely to have distribution functions which are in thermal equilibrium. In this case we might wish to build upon the work of Gould (1980), who studied a kinetic theory of relativistic plasmas to derive relaxation times but who did not really consider plasma phenomena. We might also hope to start to use some of the electron-positron plasma equilibria found by many authors (see §1.3) as a starting point for really starting to tackle plasma physics problems in astrophysical objects.

An additional, and very important piece of physics, to be included in the proper study of the electron-positron plasma is that of the interaction of the plasma with radiation. In chapter four we ignored radiation, and this is clearly incorrect. In a relativistic plasma there are photons with as much energy and momentum as the electrons and positrons, so they must be very important. Tajima & Taniuti (1990) cope with this by coupling the equation of state of the fluid to the radiation field – perhaps in their early universe scenario when everything is in equilibrium this is valid, but further examination is needed of the ‘thin’ equilibria present in astrophysical situations, and proper account must be taken of the actual radiation spectrum inside the plasma.

Of course, wave propagation is not the be all and end all of plasma physics and there are many interesting phenomena which should be investigated for equal mass plasmas. Transport theory is just one area where the symmetry of the equal mass plasma is important (Abdul-Russak & Laing 1992) and the derivation of transport coefficients is essential if full studies of inhomogeneous, confined equal mass plasmas is to be undertaken.

6.2 Nonlinear Waves

For the author, it is in the area of nonlinear dynamics that the most interesting work is being done in physics today, and it is here that he expects the unique properties of the equal mass plasma to show themselves most vividly. In chapter five we started the study of nonlinear waves in equal mass plasmas by looking at nonlinear electrostatic waves. We found a fundamental instability in the case of the cold plasma, with a simple sinusoidal perturbation developing into a highly peaked distribution. This result was strikingly different from the electron-ion plasma and demonstrated

that there are rich possibilities for the study of nonlinear waves in such plasmas. There is a simple question to be asked of the work in chapter five: what happens to electrostatic plasma oscillations when pressure is included in the dynamics? If our results are to have any relevance to electron-positron plasmas then it is vital to answer this question, and the author is presently studying the effects of pressure upon these plasma waves. The problem becomes much harder in this case, as the waves now travel (they are nonlinear Langmuir waves) but a simple argument can be made to show that they could be important, even in a hot plasma.

The energy contained in an electrostatic wave is

$$\mathcal{W}_E = \int \frac{1}{2} \epsilon_0 E^2 dx, \quad (6.1)$$

and the increase in thermal energy in a pressure wave is

$$\mathcal{W}_T = \int k_B (nT - n_0 T_0) dx = \int (n^\gamma n_0^{-\gamma} - 1) n_0 k_B T_0 dx. \quad (6.2)$$

We have assumed adiabatic compression when calculating the thermal energy in the second expression. Now let us consider a perturbation which has a spatial extent Δl and involves an average density difference between the plasma components of $n_0 \delta$. The electric field is approximately $q n_0 \delta \Delta l / \epsilon_0$ so that the electrostatic and thermal energies are roughly

$$\mathcal{W}_E \approx \frac{\Delta l^3 \delta^2 q^2 n_0^2}{2 \epsilon_0}, \quad (6.3)$$

$$\mathcal{W}_T \approx \left(\frac{n^\gamma}{n_0^\gamma} - 1 \right) n_0 k_B T_0 \Delta l. \quad (6.4)$$

After a time the plasma will try to equipartition its energy between the two forms, so that equating \mathcal{W}_E with \mathcal{W}_T we find

$$\left(\frac{n^\gamma}{n_0^\gamma} - 1 \right) = \frac{\delta l^2 \delta^2 n_0 q^2}{2 \epsilon_0 k_B T_0} \approx 10^{-4} \Delta l^2 \delta^2 \frac{n_0}{T_0}. \quad (6.5)$$

In the last step we substituted $q = e$. Notice that this ratio scales with the plasma parameters as n_0/T_0 – so that a cold dense plasma is more likely to exhibit density enhancement than a hot diffuse one.

The big unknown in the equations (6.5) is the scale length of the perturbation Δl . A reasonable guess might be the vacuum wavelength of light at the plasma frequency – certainly acoustic waves are unlikely to have a shorter wavelength than this. This would give Δl as

$$\Delta l^2 = \frac{4 \pi^2 c^2 m \epsilon_0}{2 n_0 q^2}, \quad (6.6)$$

so that

$$\left(\frac{n^\gamma}{n_0^\gamma} - 1\right) = \frac{4\pi^2 c^2 \delta^2 m}{k_B T_0}. \quad (6.7)$$

If we put in numbers appropriate to an electron-positron plasma then this becomes

$$\left(\frac{n^\gamma}{n_0^\gamma} - 1\right) = \frac{10^{11} \delta^2}{T_0}. \quad (6.8)$$

We have taken $m = m_e$ (relativistic mass increase would help the density perturbation, so we are being conservative here). This means that for density perturbations of 0.1 we would expect the density enhancement to be important for $T_0 O(10^9)$ – just the temperature of a relativistic electron-positron plasma.

There are a number of comments to be made. Our criterion has no density dependence: however, more energy is required to perturb a high density plasma than a low density one so perhaps δ might depend upon n_0 . We ignored relativistic mass increase and probably underestimated the scale of the perturbation, and both these factors might allow a higher temperature threshold for the demonstration of enhancements of density. However, we have made no allowance for the fact that these waves will travel, which might smooth out the density perturbation, leading to a lowering of the temperature threshold.

Whatever, it would seem that further work should be undertaken towards understanding these waves and seeing where they might be relevant in astrophysics.

The above is of course just one small corner of the field of nonlinear waves and there are many other possibilities for study. Recall that it was when studying nonlinear waves in electron-positron plasmas that Tajima & Taniuti (1990) discovered new wave modes not present in electron-ion plasmas. There may be other nonlinear wave modes which are also present in equal mass plasmas which are not found in electron-ion plasmas. This of course also applies to nonlinear modes from kinetic theory – BGK modes for example. It is easy to construct these modes but what impact an equal mass plasma might have upon their stability is an important question.

Finally, there is the extremely difficult project of unifying the approaches of those studying the equilibria of electron-positron plasmas and the study of the plasma physics of these plasmas. We should remember that the collective effects exhibited by a plasma have a profound impact upon its global structures and equilibrium. Therefore, to try to construct equilibria for a plasma yet to ignore the fact that it is a plasma is to miss out the essential physics of the situation. (The control of instabilities in tokamaks can be seen as a case in point here.) However, despite the enormous difficulties of this approach, the continuing development of computer power and advances in nonlinear plasma physics should let us attempt this project in the not too distant future.

References

- S. Abdul-Russak & E.W. Laing 1992 *Transport Properties of Equal Mass Plasmas* In preparation.
- H.O.G. Alfvén 1990 *IEEE Transactions on Plasma Science* **18**, 5.
- G.L. Baker & J.P. Gollub 1990 *Chaotic Dynamics* Cambridge University Press.
- M.C. Begelman, R.D. Blandford & M.J. Rees 1984 *Rev. Mod. Phys.* **56**, 255.
- K. Boyer, T.S. Luk & C.K. Rhodes 1988 *Phys. Rev. Letters* **60**, 557.
- R.N. Bracewell 1986 *The Fourier Transform and its Applications* McGraw-Hill.
- M.L. Burns & R.V.E. Lovelace 1982 *Ap. J.* **262**, 87.
- P.C. Clemmow & J.P. Dougherty 1969 *Electrodynamics of Particles and Plasmas* Addison-Wesley.
- J.M. Cordes 1983 In *Positron-Electron Pairs in Astrophysics* (ed. M.L. Burns, A.K. Harding & R. Ramaty), pp98 American Institute of Physics.
- R.C. Davidson 1972 *Methods in Nonlinear Plasma Theory* Academic Press.
- R.C. Davidson & P.P. Schram 1968 *Nucl. Fusion* **8**, 183.
- D.A. Diver & E.W. Laing 1990 *J. Plasma Physics* **43**, 107.
- D.A. Diver, E.W. Laing & C.C. Sellar 1990 *J. Plasma Physics* **43**, 101.
- M.J. Feigenbaum 1980 *Los Alamos Science* **1**, 4.
- D.J. Forrest 1983 In *Positron-Electron Pairs in Astrophysics* (ed. M.L. Burns, A.K. Harding & R. Ramaty), pp3 American Institute of Physics.
- R.H. Fowler 1936 *Statistical Mechanics* Cambridge University Press.
- R.J. Gould 1980 *Phys. Fluids* **24**, 102.
- M. Heñon 1976 *Commun. Math. Phys.* **50**, 69.
- K.A. Holcomb & T. Tajima 1989 *Phys. Rev. D* **40**, 3809.
- E. Infeld & G. Rowlands 1990 *Nonlinear Waves, Solitons and Chaos* Cambridge University Press.
- R. Itatani 1992 *Private Communication*
- T.W. Jones & L. O'Dell 1977 *Astron. Astrophys* **61**, 291.
- G. Kalman 1960 *Annals of Physics (New York)* **10**, 29.
- M.V. Konyukov 1960 *Soviet Physics JETP* **37**, 570.
- W. Kundt & Gopal-Krishna 1980 *Nature* **288**, 149.
- E.P.T. Laing 1979 *Ap. J.* **234**, 1105.
- E.W. Laing 1981 In *Plasma Physics and Nuclear Fusion Research* (ed. R.D. Gill), pp155 Academic Press.
- I. Langmuir & L. Tonks 1929 *Physics Review* **33**, 195.

- A.P. Lightman 1982 *Ap. J.* **253**, 842.
- A.P. Lightman 1983 In *Positron-Electron Pairs in Astrophysics* (ed. M.L. Burns, A.K. Harding & R. Ramaty), pp359 American Institute of Physics.
- A.P. Lightman & D.L. Band 1981 *Ap. J.* **251**, 713.
- A.P. Lightman, A.A. Zdziarski & M.J. Rees 1987 *Ap. J. Letters* **315**, 113.
- R.E. Lingfelter & R. Ramaty 1983 In *Positron-Electron Pairs in Astrophysics* (ed. M.L. Burns, A.K. Harding & R. Ramaty), pp267 American Institute of Physics.
- E.N. Lorenz 1963 *J. of the Atmospheric Sciences* **20**, 130.
- E.J. Lerner 1992 *Sky & Telescope* **1984**, 124.
- C.J. MacCallum & M. Leventhal 1983 In *Positron-Electron Pairs in Astrophysics* (ed. M.L. Burns, A.K. Harding & R. Ramaty), pp211 American Institute of Physics.
- R.M. May 1976 *Nature* **261**, 459.
- M.M. Murnane, H.C. Kapteyen & R.W. Falcone 1989 *Phys. Rev. Letters* **62**, 155.
- D.R. Nicholson 1983 *Introduction to Plasma Theory* John Wiley & Sons.
- P.D. Nordelinger 1978 *Phys. Rev. Letters* **41**, 135.
- A.J. Peratt 1986 *IEEE Transactions on Plasma Science* **14**, 639.
- A.J. Peratt 1992 *The Physics of The Plasma Universe* Springer Verlag.
- E.S. Phinney 1988 In *The Centre of the Galaxy* (ed. M. Morris), pp543 International Astronomical Union.
- G.A. Stewart & E.W. Laing 1992 *J. Plasma Phys.* **47**, 295.
- P.A. Sturrock 1971 *Ap. J.* **164**, 529.
- F. Takahara & M. Kusunose 1983 In *Positron-Electron Pairs in Astrophysics* (ed. M.L. Burns, A.K. Harding & R. Ramaty), pp400 American Institute of Physics.
- T. Tajima 1989 *Computational Plasma Physics: With Applications to Fusion and Astrophysics* Addison-Wesley.
- T. Tajima & T. Taniuti 1990 *Phys. Rev. A* **42**, 3587.
- R.Z. Sagdeev, D.A. Usikov & G.M. Zaslavsky 1988 *Nonlinear Physics : From the Pendulum to Turbulence and Chaos* Harwood.
- T.H. Stix 1962 *The Theory of Plasma Waves* McGraw-Hill.
- P.A. Sturrock 1957 *Proc. Roy. Soc. Series A* **242**, 277.
- A.D.M. Walker 1977 *J. Plasma Physics* **17**, part 3, 467.
- J.F.C. Wardle 1977 *Nature* **269**, 563.
- A.A. Zdziarski 1988 *Ap. J.* **335**, 786.

I'm closin' the book
On the pages of the text
And I don't really care
What happens next
I'm just going
I'm going
I'm gone

Bob Dylan, *Going, Going, Gone*